UNIVERSIDAD AUTÓNOMA DE MADRID

Departamento de Bioquímica

microRNA regulation in the Immune Response: Intercellular transfer at the Immune Synapse and post-transcriptional modifications

Cristina Gutiérrez Vázquez

Madrid, 2015

Departamento de Bioquímica

Facultad de Medicina

Universidad Autónoma de Madrid

microRNA regulation in the Immune Response: Intercellular transfer at the Immune Synapse and post-transcriptional modifications

Memoria presentada por la licenciada en Bioquímica:

Cristina Gutiérrez Vázquez

para optar al título de Doctor por la Universidad Autónoma de Madrid

Director de tesis:

Dr. Francisco Sánchez Madrid

Este trabajo ha sido realizado en el laboratorio de Comunicación Intercelular, en el Centro Nacional de Investigaciones Cardiovasculares (CNIC)

Madrid, 2015

A mi Familia:

Mis padres,
mis hermanas,
y Julio.

Croyez ceux qui cherchent la vérité, doutez de ceux qui la trouvent

(Cree a aquellos que buscan la verdad, duda de los que la encuentran)

André Gide

AGRADECIMIENTOS

AGRADECIMIENTOS

Esta tesis doctoral no es solo el resumen del trabajo de 6 años en el laboratorio, sino que supone el final la etapa más bonita y enriquecedora de mi vida, tanto profesional como personalmente, y quiero dar gracias a todas y cada una de las personas que, de un modo u otro, la han compartido conmigo.

En primera lugar, quiero dar gracias a **Paco**, por escogerme de entre tantos buenos estudiantes de Bioquímica, por confiar en mí desde el primer momento y por traerme a trabajar al CNIC. Ni que decir tiene que sin él nada de esto habría sido posible. Gracias, Paco, por darme alas, y a la vez acogerme bajo la tuya entre tus polluelos.

Tampoco esto habría sido posible sin mi familia. Sin mis padres, que tan bien nos inculcaron desde pequeñas el ambiente de estudio, a la vez que, entre uno y otro, despertaron en mí esa curiosidad tan imprescindible en la Ciencia. Nunca olvidaré la cara (de cabreo) de mi padre cuando con 8 años volví a casa muy orgullosa de haber comprendido por fin cómo funcionaban las fases lunares, cuando en realidad lo que nos había explicado el profesor, equivocando terriblemente los conceptos, había sido el fenómeno del eclipse lunar. Gracias, **Papá,** porque entonces empecé a comprender la necesitad del rigor en la Ciencia. Recuerdo muy bien también haberme preguntado cómo funciona nuestro cuerpo por dentro mirando aquella tétrica calavera que tenía mi madre en su consulta de Medicina, y escuchar sus explicaciones con ayuda de aquel modelo anatómico de plástico de mi hermana mayor. Cómo pasar por alto, además, esa vocación tuya, **Mamá,** de ayuda desinteresada a los demás, que va más allá de la práctica de la Medicina.

Quiero dar las gracias también a mis tres hermanas: **Celia, Marina y Lucía**. Para empezar, porque sin vosotras mi vida habría sido tan diferente que es imposible de imaginar; para seguir, por aguantarme, y para terminar, por haber ocupado todas las facetas posibles del Arte para dejarme a mí la Ciencia ☺. Como dijo alguien una vez, sois las hijas que todo padre desearía tener, pero también sois las hermanas con que toda hermana desea compartir experiencias, juegos, aquelarres... También quiero dar gracias al resto de mi familia, a los **Gutiérrez** y a los **Vázquez**, en especial a mis **tíos doctores**, porque ahora sé por lo que habéis pasado y dentro de nada voy a ser una de vosotros. Suerte que ahora la tesis no es una única copia que se pueda volar del trasportín de una vespino.

Quiero agradecer también a todos mis buenos profesores, que han sido muchos desde el colegio. Especialmente a **Susana Bronchalo**, **Jose Luis Bilbao** y **José Luis de los Ríos**. También debo mucho a mis profesores de la **Universidad Autónoma de Madrid** con los que tanto he aprendido, especialmente a **Ángeles Villanueva** (mi primera mentora) y a **José Fernandez Piqueras,** por dejarme ir a cotillear en sus laboratorios y despertar mi ilusión por la Ciencia. Agradezco especialmente a **Mercedes Rincón** que me acogiera en

su laboratorio de Vermont y me diera la oportunidad de aprender otras formas de trabajar, que me llevara a las montañas y, sobre todo, que siga disponible después de tanto tiempo.

Haber pasado tanto tiempo en un laboratorio puede que no haga más largos los resultados de una tesis, pero, al menos en mi caso, hace muy muy larga la lista de gente con la que he tenido el privilegio trabajar. Gracias a los que me recibieron en el CNIC: **Pilar Martín,** con la que di los primeros pasos y sacrifiqué los primeros ratones; **Sales**; **Juan**; **Marta** (mucho más que apoyo en el laboratorio, eres la mente práctica y clarividente, mil gracias por toda tu ayuda y comprensión en estos años); **Olga Barreiro,** con su farándula y su genio; **Gloria**; **Emilio,** con sus historias y sabidurías siempre preparadas, además de su hombro para apoyarme cuando lo he necesitado; **María Yañez,** por enseñarme la flexibilidad y el sentido común del protocolo y tantas otras cosas. Mucho más que una mención especial necesitaría para **Mónica Sala**, con todo lo que hemos pasado juntas y separadas, sé que siempre estaremos ahí la una para la otra y me siento muy orgullosa de ello. Gracias a **Arantxa,** por tener siempre la sonrisa preparada ante cualquier circunstancia, por ayudarme y escucharme. Otra sonrisa que no se puede pasar por alto es la de **María Mittelbrunn**. ¿Qué puedo decir? Muchas gracias por todos estos años compartidos, especialmente los primeros, donde me enseñaste todo cuanto pude necesitar, confiaste en mí y me diste la oportunidad de trabajar contigo.

No puedo olvidar tampoco a los que fueron llegando poco a poco al CNIC, **Fran**, con su maestría en el tomar prestado; **Norman**, el sigilo personificado; **Almudena**; **Adela**; **Carol** que tan bien recogió el testigo de becaria de exosomas y que tanto me ha ayudado y me sigue ayudando; **Danay,** siempre con alguna idea, opinión o reactivo interesante que compartir; **María (Laura),** por su buena disposición y esos paseos en coche que tan feliz me hacen; **MJ,** por su paciencia; **Ángel Jaso** y **Daniel Torralba,** por su motivación e ilusión, en algunas ocasiones contagiosas, y en otras taaan divertidas. Un agradecimiento particular merecen **Marcos y Ana (ARG)**, mis dos pupilos a los cuales espero haber enseñado algo en el tiempo que hemos trabajado juntos. Un placer aprender enseñándoos.

Resulta más que obligatorio hacer una especialísima mención a dos personitas que vinieron al laboratorio del extranjero para convertirse casi en mi familia: ¿qué puedo decir de **Giulia Morlino**? Mi incondicional amiga, compañera de aventuras, disgustos y también muchas alegrías. Mi estancia en el laboratorio de FSM no habría sido ni medio parecida sin ti y tu amistad es una de las cosas más grandes que me llevo de esta etapa. ¿Y la **Doctora Vera**? Desde luego más de una úlcera nos habría dado si no fuera porque llegaste para enseñarnos a respirar hondo tres veces (o si hacía falta, más). Muchas gracias por toda tu ayuda tanto en lo profesional como en lo personal.

Gracias también a **Noelia**, mi galleguiña preferida, y a **David** y a toooda la ristra de Davides que han ido formando vuestro grupo y con los que tanto me he reído, **María,**

Rut, Carlos, Salva (Salvador), **Laura** (Consejero), **Carlos**, **Johan** (esa mirada tuya…), **Helena**, **Michel, Sarai**. Desde que os mudasteis del Norte al Sur ya nada es igual. Gracias también al resto de grupos que fueron poblando la 2N, los **Guadalupos**, y **Almudena Ramiro,** en especial a **Virginia** y la propia **Almudena**. Gracias también al resto del CNIC, tanto de dentro como de fuera del departamento; a **las unidades**: Animalario, Genómica, Microscopía y, en especial, Citómetría, con **Ligos, Mariano y Raquel,** donde he aprendido y me he reído tanto. También debo mucho a la gestión de **Almudena Fernández** y **Antonio Quesada**, haciéndonos siempre dentro de lo posible la vida más fácil; así como a **Simon Barlett**, por tu eficiencia dejando nuestros manuscritillos convertidos en "Real Manuscripts".

No quiero dejar de mencionar aquí a los compañeros de los Pacos de la Princesa, los clásicos para mí: **Manolo, Ana, Hortensia, Manu, Marta Barrero, Román, Mónica Gordón, Noa, Ángeles Ursa, Amalia, Javi**, y por supuesto **Mari Ángeles,** engranaje principal e imprescindible que hace inigualable el servicio de Inmunología. Ni de los actuales, el grupo de **Miguel Vicente**, **Noelia, Rafa, Eugenio, Lola, María Navarro**...

No pueden quedarse fuera tampoco los del Holy. Gracias a todos por estar ahí, especialmente a **Inés, Edu, Angel, Soraya, MYMó** de nuevo, el grupo de **Esteban Veiga** al completo, pero muy especialmente a **mi Primo**. Los "**Moles**" y los del **fútbol**, gracias por dejarme jugar a pesar del evidente desastre que era en el campo.

Un pilar muy importante durante todo este tiempo predoctoral y sin quienes, sin duda, no habría llegado hasta aquí, es el que forman **mis amigos**. No solo los que traía de antes, sino también los que he ido haciendo, tanto dentro como fuera del laboratorio, y que me han dado toda su compresión y apoyo.

¿Qué puedo decir de mis amigos de la carrera?, compañeros de fatigas, colegas, confesores, un apoyo enorme cuando los he necesitado y una gran diversión siempre que nos hemos juntado. Cómo os echo de menos y cómo me gustaría volver atrás, aunque solo fuera para ver por un agujerito aquellas tardes con **Lara, Jaime y Maribel**, mi trío inseparable de Biología, siempre estaréis en mi corazón. Cómo olvidar al grupo de Bioquímica y del máster, porque sois grandes y llegaréis lejos, pero cuando estuvimos cerca os disfruté como una enana: **Alex, Jara, Elisa, Irene, Piñero, Marta, David, Alfonso, Lucía, Miguel, Alejo, Edu, Dani, Lara y Jaime** otra vez. Una mención especial a **Pilar e Inés**, mis queridas "write or die", ¡ya casi lo tenemos! Gracias también a **Flo**, ahora una más entre nosotros, incluso sin dedicarse a esto de la Ciencia, ¡eso sí que es dedicación!

Quiero agradecer a también a mis "Vidas Cotidianas": **Javi**, otra vez, gracias por seguir tan cerca aun estando en Salamanca y hacer que cada vez que nos veamos sea como si no hubiera pasado el tiempo; **Rubén,** con esa curiosidad por todo lo que hacemos; **Pablo,** por tu incondicional ayuda gráfica y tantas cosas más; **Alberto,** con su título nobiliario; **Natalia,** y **Adrián**. También estoy muy agradecida a "Juntos y Revueltos"aka "Baselga"

porque las carcajadas que he pasado con vosotros han sido capaces de borrar cualquier problema viniera de donde viniera. Estos son **Dani, Chechu, Gloria, Africa,** y mi querida **Virginia Cristina,** que realmente la podemos contar en los dos grupos.

Por supuesto, también debo tanto a los amigos que he hecho en el CNIC, especialmente a los que conocí gracias a uno de mis **Dani**, el inigualable **Mateos** master del ilustrator, compañero, celestino y mucho más. Estos son: **Aurora; Susana,** la cheer leader del grupo**; Héctor** y su encantadora manera de retomar conversaciones de hace horas**; Rocío**, los Manzanares: **Teresa,** esos viajes en bus; **Melisa; Sergio y Jesú**. Gracias por acogerme como uno más en vuestros desayunos, meriendas, prestarme justo el reactivo necesario en el momento idóneo, por enseñarme otro ángulo de visión de lo biología y mucho más. Hemos pasado grandes momentos y estoy segura de que pasaremos muchos más.

Y hablando de Manzanares llegamos al "last but not least". ¿Qué puedo decir, **Julio**, que ya no sepas? Haberte conocido es lo más bonito e intenso que me ha pasado en el doctorado. Si hace 6 años me hubieran contando que iba a conocer a alguien como tú y que ese "alguien como tú" se convertiría además en mí compañero de vida, nunca lo hubiera creído. Tu potencial científico, tu ilusión y tu constante avidez por el saber contagian a cualquiera. Mil gracias por estar ahí siempre que te necesito, por apoyarme, animarme, inspirarme y comprenderme. Pero sobre todo, por tu paciencia infinita, como infinito es el misterio de la Ciencia.

RESUMEN

RESUMEN

Los MicroARNs (miARNs) son pequeñas moléculas de ARN que regulan la expresión génica en diversos procesos biológicos incluida la respuesta inmunitaria. Se ha descrito que los miARNs pueden transferirse entre células a través de exosomas. La sinapsis inmune (SI) es una estructura muy organizada de comunicación entre los linfocitos T y las células presentadoras de antígeno (CPA) que se forma durante el reconocimiento de antígeno. En esta tesis se ha estudiado en primer lugar la comunicación intercelular entre los linfocitos T y las CPAs a través de la SI, mediada por el intercambio de exosomas que contienen miARNs. En los siguientes objetivos se analizaron los patrones de expresión de los miARNs durante la activación de los linfocitos T incluyendo el estudio de sus dianas de mRNA así como su regulación por modificaciones post-transcripcionales.

Los datos presentados en esta tesis muestran que los exosomas de las células T, B y células dendríticas (CDs) contienen miRNAs específicos que difieren de los de la célula productora. Tras la formación de la SI, encontramos una transferencia unidireccional de miARNs desde la célula T a la CPA mediada por la transmisión de exosomas. Los miARNs transferidos durante la SI son capaces de alterar la expresión génica de la célula receptora.

En el segundo objetivo, analizamos cómo cambia el patrón de miARNs de la célula T después de ser activada por distintos tipos de CDs. También estudiamos las dianas de mRNA comunes a los miARNs que se modulan durante la activación T y validamos la relación entre uno de los miARN que más se inducen, miR-132-3p, y el gen *pik3r1* que se predijo como diana común de los miARNs aumentados en activación.

Finalmente, en el tercer objetivo de esta tesis, nos centramos en la regulación de miARNs durante la activación de los linfocitos T mediante la adición de nucleótidos no codificados en 3' (3'ANC). Detectamos que tras la activación, la adición de uracilos disminuye específicamente, acompañada por una disminución de los niveles de las enzimas uracil transferasas TUT4 y TUT7. La adición en 3' de uracilos, además, promueve la degradación de miARNs específicamente durante la activación del linfocito T.

Los resultados presentados en esta tesis apoyan un nuevo mecanismo de comunicación intercelular que consiste en la transferencia de miRNAs mediante exosomas durante la SI. Además se ha analizado el perfil de miARNs durante la activación T y se ha descrito que la uridilación modula los niveles de miARNs durante este proceso.

SUMMARY

SUMMARY

microRNAs (miRNAs) are small regulatory RNA molecules that control gene expression in many biological processes including immune response. Moreover, it has been described that miRNAs can be transferred between cells via exosomes. The Immune Synapse (IS) is a very well organized structure of communication between T cells and antigen presenting cells (APC) formed during antigen recognition. This thesis addresses firstly the intercellular communication between T cells and APCs at the IS mediated by the exchange of exosomes bearing miRNAs. Our next objectives were to analyze the changes on T cell miRNA profile during T cell activation including the mRNA targets and post-transcriptional modification of the miRNAs.

Our data showed that exosomes of T, B and dendritic cells (DCs) contain specific miRNAs repertories different from those of their cellular counterpart. We found that upon IS formation there is a unidirectional transfer of miRNAs from the T cell to the APC, mediated by the delivery of exosomes. Moreover, miRNAs transferred during IS were able to modulate gene expression in recipient cells.

In the second objective we analyzed how the miRNA profile of T cells changes after activation by different DCs subsets. We also studied the mRNA targets common to miRNAs regulated in T cell activation and validated the inhibitory relationship between the upregulated miR-132-3p and *pik3r1* gene, which is a target for the miRNAs upregulated after T cell activation.

Finally, as a third objective we focused on the regulation of miRNAs during T cell activation by 3' non-templated nucleotide addition (3'NTA). We detected that upon T cell activation, uracyl addition is specifically decreased, concomitantly with downregulation of TUT4 and TUT7 enzymes. We found that 3' addition of uridine promotes degradation of miRNAs after T cell activation.

The results presented in this thesis support a novel mechanism of cellular communication involving antigen-dependent, unidirectional intercellular transfer of miRNAs by exosomes during immune synapsis. Moreover, we have addressed the activation-driven changes on T cell miRNAs profile and we uncover post-transcriptional uridylation as a mechanism to fine tune miRNA levels during T cell activation.

INDEX

INDEX

LIST OF ACRONYMS

LIST OF ACRONYMS

3′ UTR	3′ Untranslated Region
AGO	Argonaute proteins
APC	Antigen Presenting Cell
BCR	B cell receptor
cDC	conventional Dendritic Cell
ConA	Concanavalin A
cSMAC	central supramolecular activation cluster
CTLs	Cytotoxic T Lymphocytes
DCs	Dendritic Cells
DGCR8	DiGeorge syndrome critical region 8
dsRNA	double strand RNA
EAE	Experimental Autoimmune Encephalomyelitis
Eri1	exoribonuclease 1
ERMs	Ezrin, Radixin and Moesin proteins
EVs	Extracellular Vesicles
GW182	glycine-tryptophan protein of 182 kDa
HA	influenza hemagglutinin
IL-2	Interleukin 2
ILVs	intraluminal vesicles
Iono	Ionomycin
IS	Immunological Synapse
LPS	lipopolysaccharide
MHC	Major Histocompatibility Complex
miRNA	microRNA
mRNA	messenger RNA
MTOC	Microtubule organizing center
MVB	Multivesicular bodies
nSMase2	sphingomyelinase-2
NTA	non-templated nucleotide additions
OVA	Ovoalbumin
PABP	poly(A) binding protein (PABP)
PAP	polyA polymerase
PARN	poly(A)-specific ribonuclease
PCA	Principal component analysis
pDC	plasmacytoid Dendritic Cell
PHA	phytohemagglutinin
PI3K	phosphatidylinositol 3-kinases

Pik3r1	Phosphoinositide-3-Kinase, Regulatory Subunit 1 Alpha
PIP2	phosphatidylinositol-4,5-bisphosphate
PIP3	phosphatidylinositol-3,4,5-trisphosphate
piRNA	piwi interacting RNA
PLD2	phospholipase D
PMA	Phorbol Myristate Acetate
pre-miRNA	precursor harpin microRNA
pri-miRNA	primary microRNA
pSMAC	peripheral supramolecular activation cluster
RISC	RNA-induced silencing complex
RNA	Ribonucleic acid
RNAi	RNA interference
SEE	Staphylococcus enterotoxin superantigen-E
siRNA	small interfering RNA
TCR	T Cell Receptor
Th	T helper
TUTases	terminal uridyl transferases

LIST OF FIGURES

LIST OF FIGURES

INTRODUCTION

1 INTRODUCTION

1.1 The T cell Response

Adaptive immune response is a form of immunity that, in contrast to innate immunity, adapts to develop a specific response to a particular antigen. For that reason it can also be called specific or acquired immunity. The main components of adaptive immune system are lymphocytes and their secreted products. While B lymphocytes are the central mediators of humoral immunity (mediated by their secreted antibodies against extracellular microbes and their toxins), T cells are the mediators of cellular immunity. This type of immunity promotes the elimination of intracellular microbes and either help the phagocytes to destroy these microbes or directly kill the infected cells. Thanks to their highly evolved T cell Receptors (TCR), T cells recognized only and specifically peptides derived from foreign proteins that are bound to host proteins called major histocompatibility complex (MHC) molecules, which are expressed on the surface of other cells. T lymphocytes consist of functionally distinct populations, cytotoxic (CTLs or CD8+) and helper T cells (Th or CD4+). In response to antigenic stimulation, CD4 Th cells secrete cytokines that will stimulate the proliferation and differentiation of the T cells themselves and activate other cells, including B cells, macrophages and other leukocytes.

1.1.1 The Immune Synapse

As mentioned above, T cells need to recognize a specific antigen in the context of MHC molecule on the surface of another cell. Professional antigen presenting cells (APC), such as dendritic cells, B cells and mononuclear phagocytes, bear MHC-II molecules and are able to engage CD4 T cells; while every cell of the organism bears MHC-I molecules able to engage CD8 T cells. Thus, the contact between these cells is required for the development and maintenance of the immune response. This highly evolved cognate interaction that is named Immunological or Immune Synapse (IS), consists of a long lasting and tight spatial reorganization of the surface receptors and cytoplasmic molecules at the interface between the two interacting cells (Dustin, 1998; Monks et al., 1998). The TCR and peptide–MHC complexes are clustered together with costimulatory molecules (CD4, CD2, and CD28) at the center of the contact zone, the central supramolecular

activating complex (cSMAC) (Monks et al., 1998). The intracellular signaling molecules associated to the TCR -PKC-θ, lck, Fyn, and ζ-associated proteins of 70 kDa (Zap70)- are

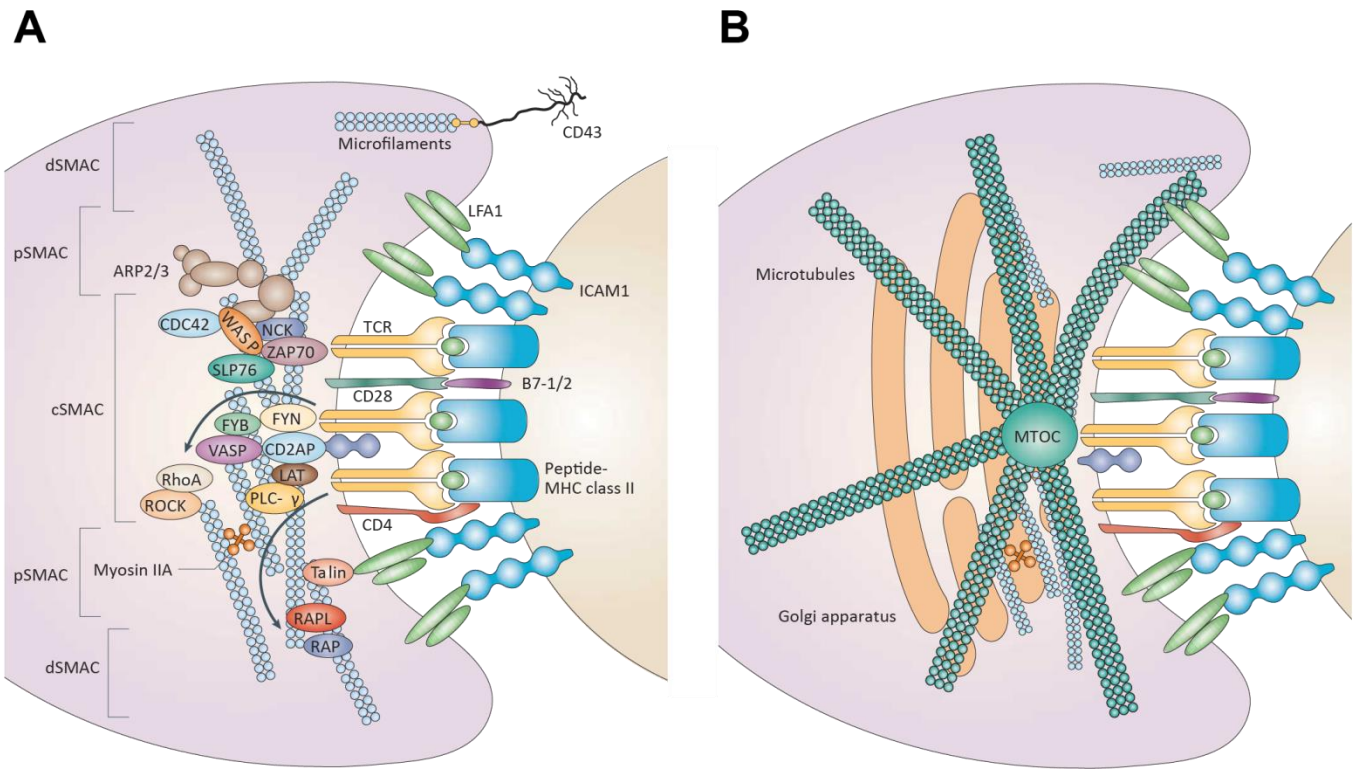

Figure 1.1 The Immunological Synapse between a T cell and an APC
(A) Supramolecular activation clusters (SMACs), signaling downstream the TCR and actin polymerization at the immunological synapse. The central SMAC cointains the TCR and coestimulatory molecules that interact with MHCII and their counterparts at the APC side. The peripheral SMAC is composed among others by LFA1 interacting with ICAM1. The distal SMAC finally is enriched in actin microfilaments. (B) Cytoskeletal distribution on a immunological synapse. MTOC is reoriented and the Golgi apparatus is relocated with it. Figure modified from (Vicente-Manzanares and Sanchez-Madrid, 2004).

also localized at the cSMAC in the inner side of the T-cell membrane. This cSMAC is surrounded by the peripheral SMAC (pSMAC), a ring of leukocyte function-associated antigen 1 (LFA1) that interacts with intercellular adhesion molecule 1 (ICAM1) as well as other integrins that are linked to actin cytoskeletal protein Talin and other intracellular molecules that regulate integrin function (Barreiro et al., 2007). More recently, an additional SMAC has been described as distal SMAC (dSMAC), an actin-rich region containing the actin that has been firstly accumulated at cell-cell contact and subsequently cleared to this outer ring (Bunnell, 2010). The microtubule-organizing center (MTOC) translocates toward the IS (Martin-Cofreces et al., 2014; Sancho et al., 2002; Stinchcombe et

al., 2006) bringing the secretory compartments, and providing the basis for polarized secretion of cytokines (Huse et al., 2006; Kupfer and Dennert, 1984) and the exocytosis of lytic granules by cytotoxic T cells (Griffiths et al., 2010). Endocytic trafficking of the TCR (Das et al., 2004) and lymphocyte specific tyrosine kinase (lck) (Gorska et al., 2009) to the IS has been reported to be essential both to target TCRs and other molecules to the APC contact site and for signal downmodulation by controlling TCR endocytosis. Finally, lysobisphosphatidic acid, a marker of late endosomes (multivesicular bodies; MVBs), localizes very close to the center of the IS of helper T cells (Varma et al., 2006), suggesting that MVBs also polarize to the IS. The IS may thus serve as a focus for both exocytosis and endocytosis (Alcover and Thoulouze, 2009; Griffiths et al., 2010).

1.1.2 CD4 T cell activation and polarization

The initial activation of naïve T cells occurs mainly in secondary lymphoid organs where they can encounter antigens presented by APCs with the subsequent formation of the above explained immune synapse. As mentioned, antigen will be recognized in a specific context of the MHC, and only with additional stimuli coming from the co-stimulatory molecules (mainly CD28 and CD40L) and soluble cytokines will be the cell correctly activated. Once activated, antigen-specific T lymphocytes secrete cytokines, proliferate and differentiate into effector and memory lymphocytes. Memory cells are long-lived cells with an enhanced ability to react against antigen that will recirculate through the lymphoid organs, tissue and skin and in case of reappearance of their specific antigen will respond rapidly and generate new effector cells.

CD4 T helper cells can differentiate into distinct subsets of effector cells: Th1, Th2, Th17, Th9, Th22, follicular helper T cells (T_{FH}) and induced regulatory T (iTreg) cells. Th1 and Th2 subsets were initially described in 1986 (Mosmann et al., 1986). Th1 cells mediate immune responses against intracellular pathogens but they are also responsible for the induction of some autoimmune diseases. Th2 cells are recognized for their role in host defense against multi-cellular parasites and their involvement in allergies, asthma and atopic illnesses. Th17 cells mediate immune responses against extracellular bacteria and fungi but also participate in the induction of many autoimmune diseases. Recently, new subsets of CD4 T cells have been described like peripherally derived regulatory T cells, T

T_{FH} cells, Th9 and Th22. These new subsets have initiated some reconsideration in the field regarding the plasticity of Th cells that used to be thought to be much more static (Raphael et al., 2015; Sun and Zhang, 2014). For a scheme of the properties and known driven- and secreted factors of the different Th subsets see *Figure 1.2*.

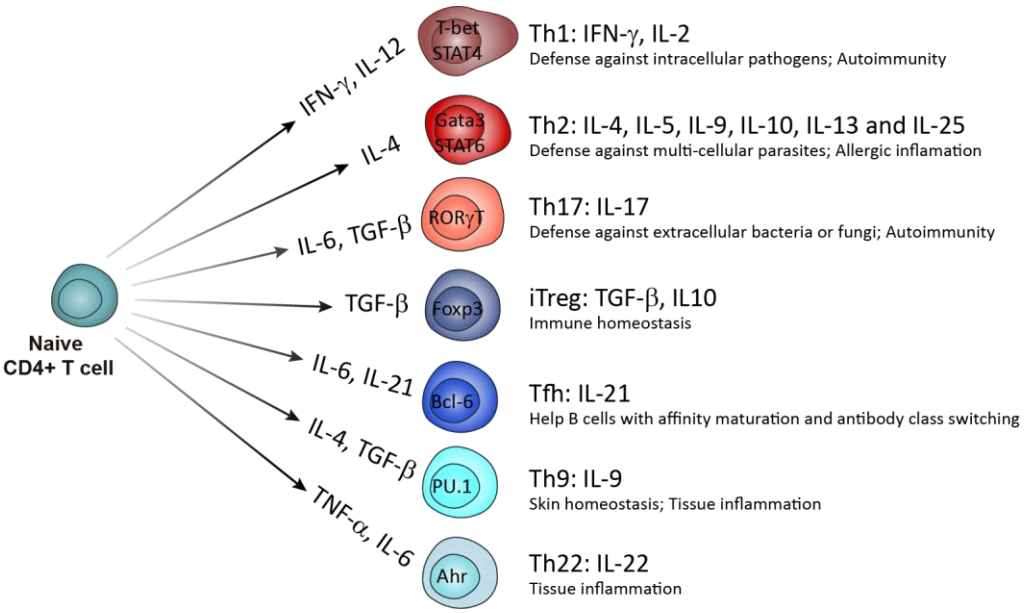

Figure 1.2 The CD4 T cell differentiation
The differentiation of naive CD4+ T cells into different T helper cell subsets is dependent on factors present in the local environment, mostly cytokines (arrows). Differential transcription factors are expressed by each subset (written inside the cells), determining in turn the cytokines produced and their function (listed on the right). Figure based on (Sun and Zhang, 2014)

1.2 Extracellular Vesicles and Exosomes

1.2.1 Biogenesis of extracellular vesicles

There is yet no consensus on the nomenclature of EVs, although the term exosome is generally restricted to vesicles derived from endosomal compartments. *Figure 1.3* represents the different origins of EVs. They can thus be classified according to their subcellular origin (Thery et al., 2009):

a) ECTOSOMES: EVs that bud directly from the plasma membrane have been termed microparticles, shedding vesicles, ectosomes, or arrestin domain-containing protein 1-mediated microvesicles (ARMMs) (Cocucci et al., 2009).

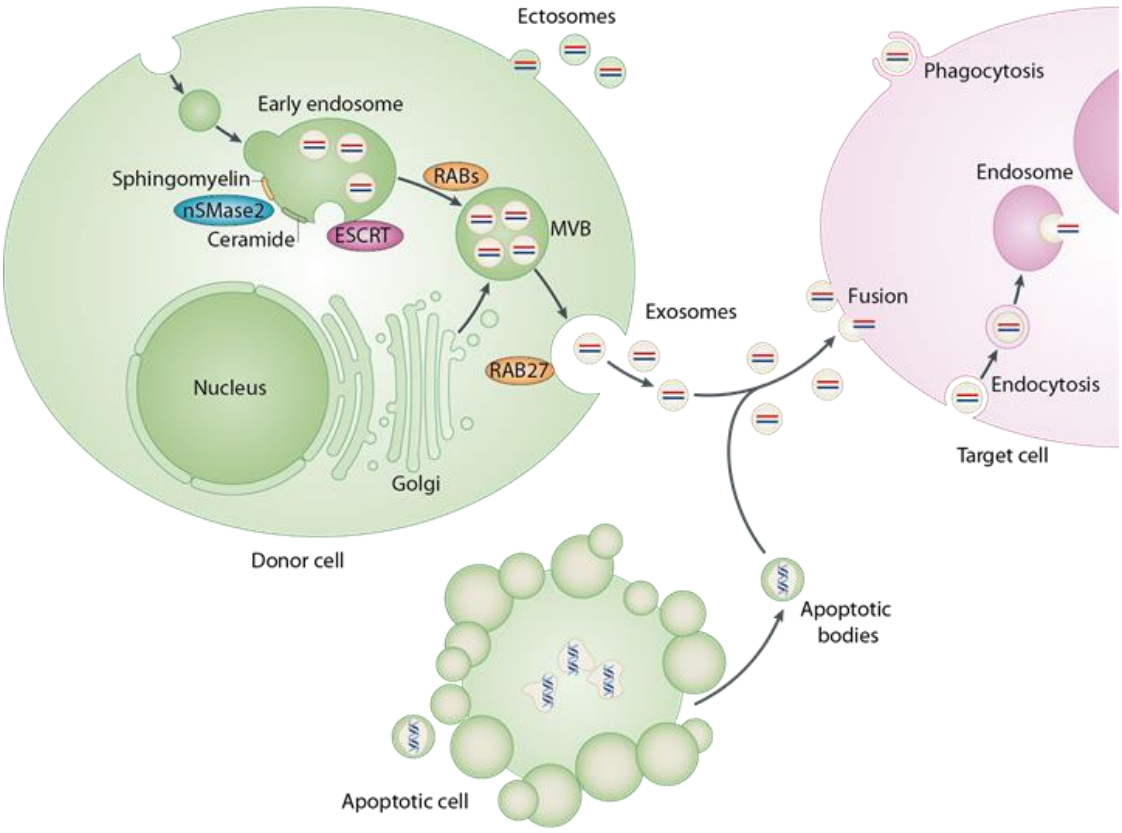

Figure 1.3 Mechanisms of Extracellular vesicles biogenesis
Exosomes are generated by the fusion of multivesicular bodies (MVBs) with the plasma membrane and the release of their intraluminal vesicles (ILVs) as exosomes. Molecules described to be regulating exosome release are highlighted. Neutral sphingomyelinase 2 (nSMase2), ESCRT (endosomal sorting complex required for transport), RAB proteins such as RAB11, RAB27 and RAB35. Ectosomes are originated by blebbing of the cellular plasma membrane. Apoptotic bodies are generated after the breakdown of dying cells. When extracellular vesicles are secreted into the extracellular milieu they can be taken up by recipient cells through mechanisms including fusion with the plasma membrane, phagocytosis and endocytosis. Figure modified from (Mittelbrunn and Sanchez-Madrid, 2012)

They are heterogeneous in size and can be bigger than exosomes (up to 1 micron).

b) EXOSOMES: The origin of exosomes are intracellular vesicles formed by inward budding of the limiting membrane of late endosomes or multivesicular bodies (MVB) of the endocytic compartment. These intraluminal vesicles (ILV) can be released after fusion of the MVB limiting membrane with the plasma membrane so they will start being called exosomes. Lipids play an important role in the formation of ILVs, and blockade of ceramide production by suppressing neutral sphingomyelinase activity inhibits exosome production

(Trajkovic et al., 2008) *Figure 1.3*. Exosome secretion is also promoted by DGKα kinase and phospholipase D (PLD2) activities (Alonso et al., 2011; Alonso et al., 2005; Laulagnier et al., 2004a). In addition, depletion of components of the ESCRT machinery results in fewer ILVs *Figure 1.3*. Of the ESCRT complexes, TSG101 plays a major role in the biogenesis of MVBs. Alix, a protein that interacts with several ESCRT proteins, regulates the biogenesis of exosomes through its interaction with syndecan and syntenin (Baietti et al., 2012). Moreover, small Rab GTPases such as Rab4, Rab11, Rab27A, Rab27 and Rab35 regulate various steps of exosome release, being implicated in cargo sequestration, ILV budding, and the transport and docking of MVBs at the plasma membrane (Hsu et al., 2010; Ostrowski et al., 2010; Savina et al., 2002; Vidal and Stahl, 1993) *Figure 1.3*.

c) APOPTOTIC BODIES are larger than ectosomes or exosomes (>1μm in diameter). These vesicles originate from apoptotic cells, and contain genomic DNA *Figure 1.3*.

1.2.2 Exosome composition

Exosome composition comprises some common proteins and lipids independently of their cellular origin as well as specific molecules that depend on the nature of the producer cell. For example, exosomes from T cells contain T cell receptor (TCR) and costimulatory molecules, while those from B cells contain B cell receptor (BCR) and so on.

The typical composition of a T cell exosome is shown in *Figure 1.4*. The exosome membrane is a lipid bilayer in which integral membrane proteins maintain the same orientation as in the donor-cell plasma membrane. Exosomes are enriched in sphingomyelin, phosphatidilserine, glycolipid GM3 and phosphatidethanolamines (Laulagnier et al., 2004b). Exosomes are specially enriched in Tetraspanins (Yanez-Mo et al., 2009) and their associated proteins. They also contain GPI-anchored proteins, complement regulators, transmembrane receptors like class I and II MHC molecules, co-stimulatory molecules, BCR (B-cell-derived exosomes), TCR (T cells), and FceRI (Mast cells) and growth-factor receptors, as well as cytokines and their receptors. Death receptors ligands and components of signaling cascades, like Wnt and Ras, can also be

found in exosome membranes. Moreover, exosomes carry molecules in their interior, like cytoskeletal components (actin, tubulin), cytosolic proteins involved in signal transduction, protein translation, metabolic enzymes, as well as proteins related to apoptosis. The endosomal origin of exosomes is reflected in the presence of components of the ESCRT complex and intracellular vesicle trafficking. For an extensive review on exosomes composition see (Gutierrez-Vazquez et al., 2013).

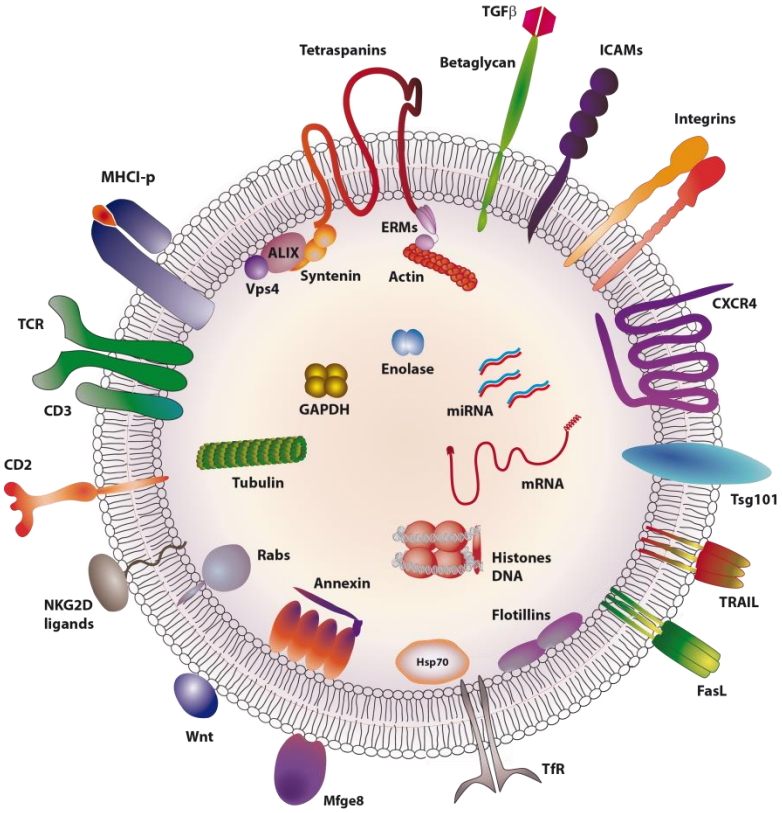

Figure 1.4 Molecular composition of T-cell exosomes Membrane and luminal distribution of molecules predicted to be found in a typical exosome produced by a T lymphocyte. TCR: T-cell receptor; TGFβ: transforming growth factor beta; ICAMs: intercellular adhesion molecule family; CXCR4: C-X-C chemokine receptor type 4 or CD184; Tsg101: tumor susceptibility gene 101; TRAIL: TNF-related apoptosis-inducing ligand; FasL: Fas ligand or CD95L; TfR: transferrin receptor; Mfge8: milk-fat globule-EGF factor 8; ALIX: ALG-2-interacting protein X; GAPDH: glyceraldehyde 3-phosphate dehydrogenase; ERMs: ezrin, radixin and moesin proteins. Figure from (Gutierrez-Vazquez et al., 2013).

An unexpected finding was that EVs contain DNA and RNA. EVs derived from embryonic stem or tumor cells contain messenger RNAs (mRNAs) (Baj-Krzyworzeka et al., 2006; Skog et al., 2008). EVs also contain microRNA (Valadi et al., 2007). The mRNAs and miRNAs of EVs differ from the miRNA and mRNA repertoire of the parent cell, indicating the existence of a mechanism for sorting specific RNAs into EVs (*Figure 1.4*). An updated repertoire of miRNAs and mRNAs as well as lipids and proteins found in exosomes is available at Exocarta (http://exocarta.org/index.html).

1.2.3 Exosomes in immune cell communication

Exosomes have been reported to be involved in important processes such as antigen presentation, tumor immunity and the transmission of infectious agents. Moreover, they are increasingly recognized as significant vehicles for intercellular communication (Simons and Raposo, 2009; Thery et al., 2009). The number of works analyzing their role in diverse physiological and pathological settings has increased enormously in the last few years. As mentioned, exosomes express cell recognition molecules on their surface that facilitate their selective targeting of and uptake by recipient cells. Recent reports indicate that exosomes also harbor a variety of mRNAs and microRNAs (Skog et al., 2008; Valadi et al., 2007), which can be transferred to recipient cells and modulate their function (Deregibus et al., 2007; Pegtel et al., 2010; Ratajczak et al., 2006a; Skog et al., 2008; Valadi et al., 2007; Zernecke et al., 2009). These findings have increased the interest in the role of exosomes in cell-to-cell communication, and support the notion that exosomes might constitute an exquisite mechanism for local and systemic intercellular transfer not only of proteins but also of genetic information in the form of RNA (Ratajczak et al., 2006b; Simons and Raposo, 2009; Thery et al., 2009)

1.3 microRNAs

microRNAs (miRNAs) are a large family of small (22-24 nucleotides long), non-coding RNAs that down-regulate gene expression by preventing the translation of specific mRNAs into proteins (Carthew and Sontheimer, 2009). The emergence of miRNAs as potent post-transcriptional regulators of gene expression has broad implications in all areas of cell biology, including the immune system (Lodish et al., 2008; O'Connell et al., 2010; Sonkoly et al., 2008). One miRNA can regulate hundreds of different mRNAs while the same mRNA can be regulated by many different miRNAs.

1.3.1 The awakening of RNA interference and small silencing RNAs

RNA interference (RNAi) discovery was preceded by observations in the 80's of transcriptional inhibition by antisense RNA expressed in transgenic plants (Ecker and Davis, 1986). However it was not until 1998, that Fire and Mello established that double

strand RNA (dsRNA) was the key silencing molecule in *Caenorhabditis elegans* (Fire et al., 1998). RNAi resulted to be systemic in plants and nematodes, and in the case of *C. elegans* it was also heritable. dsRNA is converted into small interfering RNA (siRNA), which were firstly discovered in plants (Hamilton and Baulcombe, 1999). Later their mechanism was described in animals being the guides for endonucleolytic cleavage of RNA targets (Hammond et al., 2000; Zamore et al., 2000). Nowadays, siRNAs are categorized in many different types depending on the organism, the origin, their regulation or the proteins involved in their biogenesis. In animals there are three major types of small silencing RNAs: microRNAs (miRNAs), siRNAs and PIWI-interacting RNAs (piRNAs). miRNAs are generated from short hairpin RNAs and depend on RNAaseIII enzyme Dicer processing. siRNAs (~21 nucleotides long) are derived from long double-stranded RNAs or long stem–loop structures through Dicer processing. They mediate the post-transcriptional suppression of transcripts and transposons, and contribute to antiviral defense. piRNAs (24–33 nucleotides long) are not dependent on Dicer and are produced from single-stranded precursors. The main function of piRNAs is to silence transposable elements in germline cells, although there is room for some still enigmatic roles of some piRNAs outside the germline. Of the two subclades of Argonaute proteins (AGO and PIWI), miRNAs and siRNAs are associated with the AGO proteins, whereas piRNAs bind to PIWI proteins (Ghildiyal and Zamore, 2009).

1.3.2 microRNAs overview

The first miRNA to be discovered, lin-4, was identified in *C. elegans* in a screen for essential genes in post-embryonic development. The lin-4 locus produced a non-coding 22-nucleotide RNA that was partially complementary to sequences in the 3'UTR of lin-14 mRNA and had opposite phenotype to it. Moreover, the negative regulation of lin-14 required an intact 3'UTR of its mRNA as well as a functional lin-4 gene (Lee et al., 1993; Wightman et al., 1993). Seven years later, tens of miRNAs were identified in humans, flies and worms establishing miRNAs as a new class of small silencing RNAs (Lagos-Quintana et al., 2001; Lau et al., 2001; Lee and Ambros, 2001). At present, miRBase (Release 21: June 2014; http://www.mirbase.org/) (Griffiths-Jones, 2004) contains 28645 entries representing hairpin precursor miRNAs, expressing 35828 mature miRNA products, in

223 species. Only in humans, 1881 precursors, which code for 2588 mature miRNAs, have been described to date.

In many species, there are multiple miRNA loci with related sequences that arose mainly from gene duplication. miRNAs with identical sequences at nucleotides 2-8 of the mature miRNAs are considered to be of the same miRNA family. miRNAs are highly phylogenetically conserved; so that among mammals 196 families are conserved. miRNA sisters generally act redundantly on target mRNAs, but distinct roles have also been suggested (Ventura et al., 2008).

The nomenclature of miRNA genes is now reaching a consensus. However, those found in early genetic studies were named after their phenotypes (for example, lin-4, let-7 and lsy-6), whereas most miRNAs found from cloning or sequencing received numerical names (for example, miR-125 that actually is the homologue in other species of lin-4). Genes encoding miRNA sisters are indicated with lettered suffixes (for example, miR-26a and miR-26b). If the same mature miRNA is generated from multiple separate loci, numeric suffixes are added (for example, miR-26b-1 and miR-26b-2). Each locus produces two mature miRNAs: one from the 5′ strand and one from the 3′ strand of the precursor (for example, miR-125a-5p and miR-125a-3p). However, one arm (the "guide" strand) is usually much more prevalent and biologically active than the other (the "passenger" strand) (Ha and Kim, 2014) (*Figure 1.5*).

1.3.3 Biogenesis of microRNAs

miRNAs are generally transcribed by RNA polymerase II (Pol II) but RNA Pol III has also been shown to transcribe some viral miRNAs and some endogenous miRNA-like small RNAs derived from tRNAs. miRNA can be transcribed from independent genomic transcription units or from the introns of noncoding or coding transcripts or even from exonic regions. When several miRNA loci are in close proximity to each other, they constitute a polycistronic transcription unit and are generally co-transcribed. The miRNAs that come from introns of protein-coding genes can share the promoter of the host gene but often have distinct transcription start site. The product of the transcription is a primary miRNA (pri-miRNA) over 1kb in length that consists of a stem of 33–35 bp, a

terminal loop and single-stranded RNA segments at both the 5′ and 3′ sides (*Figure 1.5*) (Carthew and Sontheimer, 2009; Kim et al., 2009).

In the canonical pathway the processing is started by the nuclear RNase III Drosha that crops the stem–loop to release the precursor harpin (pre-miRNA) of ~65 nucleotides in length. Drosha forms a complex called microprocessor together with its essential cofactor DGCR8 (DiGeorge syndrome critical region 8, also known as Pasha in *D. melanogaster* and as PASH-1 in *C. elegans*). Drosha and DGCR8 are conserved in animals and their deficiency causes lethality early in embryogenesis.

Pre-miRNAs are subsequently exported by Exportin 5 from the nucleus to the cytoplasm where they are processed by the next RNAaseIII enzyme Dicer in complex with TRBP producing a ~20-bp miRNA duplex. Dicer binds the pre-miRNA simultaneously at its 5′ end and 3′ end with preference for those miRNAs with two-nucleotide-long 3′ overhang previously generated by Drosha. TRBP acts modulating the processing efficiency and tuning the length of mature miRNAs, but in mammals, unlike its Drosophila homologues Loqs, it does not seem to be essential for Dicer-mediated pre-miRNA processing. Dicer1 deletion in mouse results in early embryonic lethality and Dicer1-knockout embryonic stem cells show strong defects in cell proliferation and differentiation.

The resulting double-stranded RNA molecule is loaded onto the RNA-induced silencing complex (RISC) that consists of the small RNA guide strand bound to an Argonaute molecule as well as to auxiliary proteins. In flies, miRNA duplexes and siRNA duplexes are preferentially loaded onto AGO1 and AGO2, respectively. However, in humans, there are no such restrictions and the four AGO proteins (AGO1–4) are associated with almost indistinguishable sets of miRNAs. All four human AGO proteins are capable of inducing translational repression and decay of target mRNAs through interaction with the translation machinery and mRNA decay factors. However, only AGO2 can slice perfectly matched target mRNA. RISC complex assembly involves two steps: the loading of the RNA duplex and its subsequent unwinding accompanied by the passenger strand release or less likely its direct cleavage by AGO2. AGO loading step is the moment when the selection of the "guide" strand is determined, being typically selected the one with relatively unstable terminus at the 5′ side. The released passenger strand is quickly

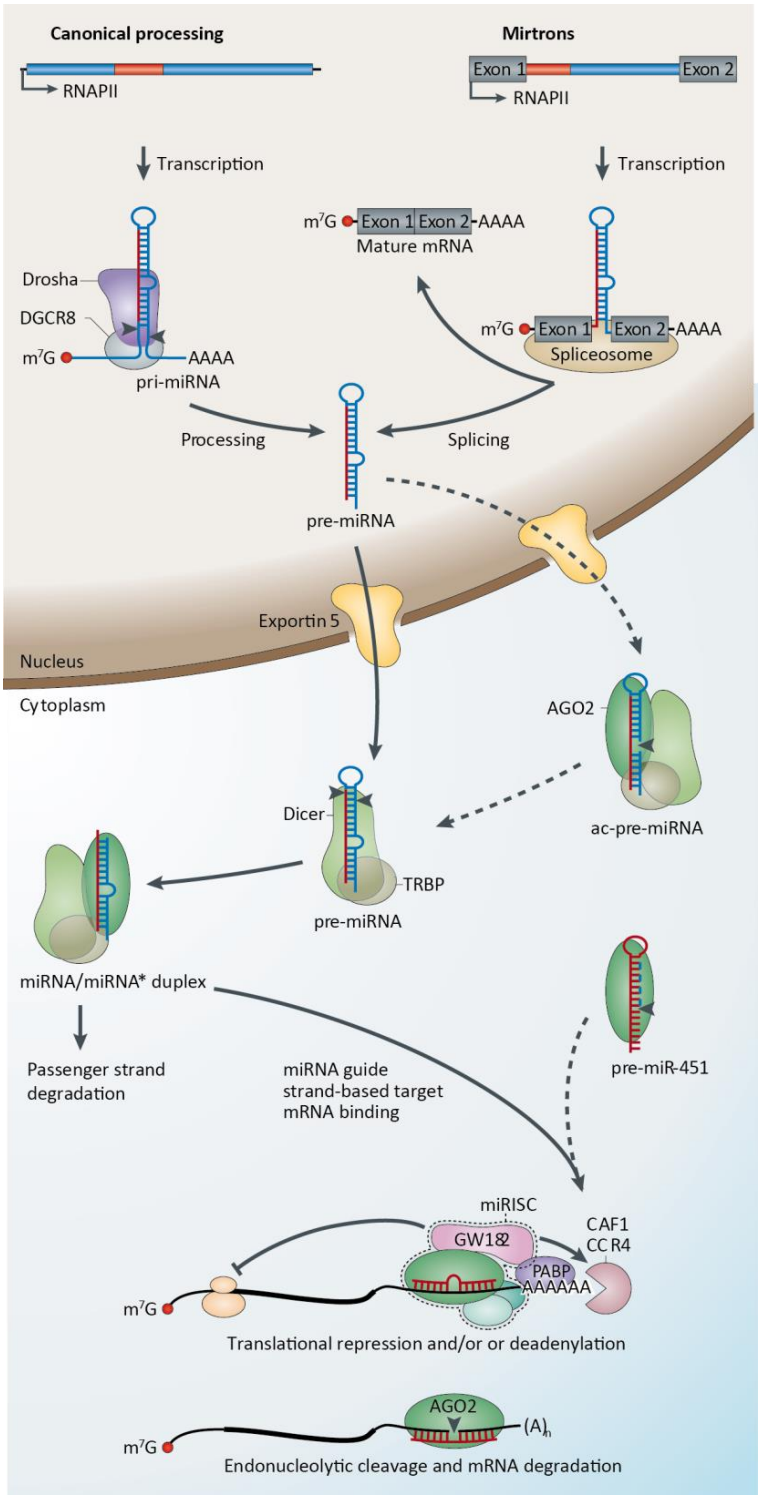

Figure 1.5 Biogenesis and Function of microRNAs
Canonical and alternative pathways of miRNAs production are depicted. Pri-miRNAs are transcribed from cell genome, cropped by microprocessor and exported to the cytoplasm where it will be further processed by Dicer complex into a mature miRNA duplex. Only one strand will be selected and assembled with the RISC complex to prevent mRNA translation and/or to promote its degradation. Figure Modified from (Krol et al., 2010)

degraded resulting in a strong bias towards the guide in the mature miRNA pool. The full mature RISC complex will be now formed and ready to exert its function (Ha and Kim, 2014; Krol et al., 2010).

Some alternative pathways or steps have been described for miRNA biogenesis: Some pre-miRNAs are produced directly from very short introns (mirtrons) as a result of splicing and debranching, bypassing Drosha-DGCR8 step (Ruby et al., 2007). Also, an alternative pathway for some pre-miRNAs consists of an additional processing intermediate resulting from the cleavage of their 3' arm by AGO2 previous to Dicer slicing (Diederichs and Haber, 2007). Moreover, processing of pre-miR-451 at least, also requires AGO2 cleavage, but is completely independent of Dicer. An additional trimming step of the 3' end is in this case required to finish its maturation and ensure RISC complex loading (Cifuentes et al., 2010; Cheloufi et al., 2010). For a schematic representation of miRNA biogenesis and function see ***Figure 1.5.***

1.3.4 Function of microRNAs

Once RISC complex is assembled, the miRNA strand will guide to target partially complementary sites at the 3' untranslated region (3'UTR) of mRNAs, resulting in inhibition of mRNA translation or promotion of mRNA deadenylation and decay. Efficient mRNA targeting requires continuous base-pairing of miRNA nucleotides 2 to 8 (the seed region). Although the mechanistic details of miRNA-mediated translational repression are not well understood, it is well stablished that the deadenylation that leads to decay of mRNAs is mediated by glycine-tryptophan protein of 182 kDa (GW182), a component of the RISC complex. GW182 is able to interact with the poly(A) binding protein (PABP) and to recruit deadenylases. Interestingly, the PABP regions targeted by GW182 are also recognized by many other translational factors, suggesting that these interactions may be subjected to sophisticated regulation. When RISC containing AGO2 encounters a mRNA bearing sites nearly perfectly complementary to miRNA, the mRNA is endonucleolytically cleaved and degraded. Although rare in animals, this is a common mode of miRNA action in plants. Anyhow nowadays it is accepted that most (66–90%) of the miRNA-mediated repression end up with the degradation of the target (Jonas and Izaurralde, 2015).

1.3.5 Isomirs and regulation of microRNA turnover

miRNA levels can be regulated from their biogenesis. Both their own transcription as well as the levels and activity of the proteins involved in their processing are tightly regulated. However, alterations in RNA sequence and/or structure can affect the miRNA turnover and maturation.

Once transcribed miRNAs sequence can vary. In the last few years, next generation sequencing analysis has revealed variability in the individual miRNA sequences derived from the same precursor (pre-miRNA), giving rise to the termed "isomiRs" (Ameres and Zamore, 2013). Sequence heterogeneity in mature miRNAs can be produced through a variety of mechanisms. Several pri-miRNAs have been described to undergo post-transcriptional A-to-I editing mediated by the enzyme ADAR (adenosine deaminase acting on RNA) that involves the conversion of adenosine to inosine and affected their correct processing by Drosha or Dicer (Kawahara et al., 2007; Yang et al., 2006). Moreover, RNA tailing or non-templated nucleotide additions (NTA) has been described for pre-miRNAs and mature miRNAs. Several noncanonical polyA polymerases (PAP) have been shown to add ribonucleotides to the 3′ end of pre-miRNAs and mature miRNAs in a template-independent manner. These enzymes are able to utilize not only adenine triphosphate (ATP) but also uridine triphosphate (UTP), and because of this are also called terminal uridyl transferases (TUTases or TUTs) (Heo et al., 2012; Heo et al., 2009). The identified TUTs are TUT1 (MTPAP), TUT2 (GLD2 or PAPD4), TUT3 (PAPD5), TUT4 (ZCCHC11) and TUT7 (ZCCHC6) (Wyman et al., 2011). Of these enzymes, TUT4 and TUT7 have been shown to preferentially uridylate mature miRNA (Jones et al., 2012; Jones et al., 2009; Minoda et al., 2006; Thornton et al., 2015).

The addition of polyU tails to the 3′ ends of pre-miRNAs has been reported to trigger their degradation in stem cells (Heo et al., 2009), while in somatic cells lacking Lin28, TUT-mediated mono-uridylation of pre-miRNAs facilitates their processing (Heo et al., 2012). The impact of 3′NTA on mature miRNAs varies depending on the organism and the miRNA examined. Adenylation has been reported to increase the stability of certain plant miRNAs (Lu et al., 2009), while in mammals it is not yet established whether adenylation stabilizes the miRNA (Katoh et al., 2009) or interferes with its loading into the

RISC complex, reducing its effectiveness (Burroughs et al., 2010). Uridylation of miRNAs leads to degradation in *Chlamydomonas* (Ibrahim et al., 2010) and plants, where it prevents their methylation (Zhao et al., 2012). In mammals there is no evidence for such an effect of uridylation on mature miRNA, but it has been shown to specifically reduce the function of miR-26a, miR-126-5p and miR-379 (Jones et al., 2012; Jones et al., 2009). Finally it is worth to mention that miRNAs can also be modified by terminal trimming of nucleotides. All these mechanisms increase the repertoire of regulatory miRNAs that can be generated in a cell and therefore amplify the possibilities for miRNA-mediated regulation of gene expression (Ameres and Zamore, 2013).

1.3.6 miRNA in the T cell response

High-throughput miRNA profiling has described specific patterns of miRNAs expression during haematopoiesis as well as immune cells development, activation and function, suggesting a role for microRNAs in cell lineage specification and effector functions (Kuchen et al., 2010; Landgraf et al., 2007; Monticelli et al., 2005). Studies using mice deficient for genes involved in the miRNA biogenesis pathway, such as Dicer and Drosha, provided evidences for the central role of miRNAs in the regulation of both development and homeostasis of the immune system and specifically Th cell differentiation (Cobb et al., 2006; Chong et al., 2008; Muljo et al., 2005). T cell activation promotes the shortening of mRNA 3′ untranslated regions (3′UTR) (Sandberg et al., 2008), which goes in accordance with an apparent global downregulation of miRNAs after T cell activation (Bronevetsky et al., 2013). Additional studies have identified the function of individual miRNAs in Th effector function. For example, miR-181a has been identified as a regulator of T cell development (Li et al., 2007). Some miRNAs, such as miR-29 or miR-146, seem to be important for the differentiation of a particular type of T helper cells (Th1 and Tregs respectively) (Lu et al., 2010; Steiner et al., 2011), while others, such as miR-155 or miR-125, seem to inhibit effector T cell differentiation in general (Rodriguez et al., 2007; Rossi et al., 2011). Moreover, the miR-17~92 cluster regulates several aspects of T cell activation and their overexpression causes lymphoproliferation and autoimmunity (Xiao et al., 2008). miR-17 and miR-92 enhance T cell proliferation while miR-19, another member of the cluster, promotes the survival of activated T cells (Steiner et al., 2011; Xiao et al., 2008). In another study, miR-17 and miR-19b were shown to promote Th1 responses through

multiple processes like promoting proliferation or IFN-γ production, while suppressing iTregs differentiation (Jiang et al., 2011). Finally it is worth to mention that miR-155 is the miRNA most highly induced by TCR stimulation. Its deficiency decreases T cell dependent immune responses and analysis of AGO2 binding sites in mRNA from activated T cells identified more than 300 containing miR-155 seed recognition sequences (Loeb et al., 2012).

OBJECTIVES

2 OBJECTIVES

The general objective of this thesis was focused on the analysis of miRNAs and their regulation during T cell responses. The following specific issues were covered:

1. **Analysis of the miRNA exchange between immune cells during Immune Synapsis**
   - miRNA profile of exosomes produced by immune cells
   - Exosomal secretory machinery during immune synapsis
   - Transfer of exosomes at the immune synapse
   - miRNA transfer at the immune synapse
   - Consequence of miRNA transference in the recipient cell

2. **Study of T lymphocyte miRNA profile regulation during T cell activation**
   - miRNA repertoire of T cells activated by different subsets of Dendritic Cells
   - Common targets of miRNAs regulated after T cell activation
   - *pik3r1* regulation as an example of a target of upregulated miRNAs after T cell activation
   - Validation of miR-132-3p inhibition of *pik3r1.*

3. **Analysis of the post-transcriptional regulation of miRNA after T cell activation**
   - Regulation of Terminal Uridyltransferases during T cell activation
   - 3′ non-templated nucleotide additions to miRNAs during T cell activation
   - Regulation of miRNAs turnover by 3′ non-templated nucleotide additions
   - Impact of TUT4 absence on uridylation of miRNAs

MATERIALS AND METHODS

3 MATERIALS AND METHODS

3.1 MATERIALS

3.1.1 Mice

C57BL/6, OT-II and Zcchc11 deficient mice were bred under specific pathogen-free conditions according to European Commission recommendations at CNIC animal facility.

3.1.2 Cell lines and culture

We used two human Jurkat-derived T-cell lines J77cl20 (TCR Vα1.2 Vβ8) (Niedergang et al., 1995) and CH7C17 (Vβ3 TCR specific for HA peptide) (Hewitt et al., 1992) and tree lymphoblastoid B-cell lines Raji (Burkitt lymphoma), HOM-2 (HLA-DR1 EBV-transformed) and BLS-1 (HLA class II-null B-LCL, generated from cells of patients with type II Bare Lymphocyte Syndrome) (Hume et al., 1989).

Stable cell line clones overexpressing CD63-GFP were generated by transfection and selection with G418 (1 mg ml^{-1}). The CD63-GFP cell lines were subsequently transduced by lentiviral infection (see method) to overexpress miR-335 or miR-101 and selected with blasticidin (5 μg ml^{-1}) and G418 (2 mg ml^{-1}); the resulting cell lines were designated as follows: J77-CD63-GFP-miR335 (J-335), J77-CD63-GFP-miR101 (J-101), CH7C17-CD63-GFP-miR335 (C-335) and CH7C17-CD63-GFP-miR101 (C-101).

Above cells were cultured in RPMI (Sigma) containing 10% fetal bovine serum (Invitrogen) plus the mentioned antibiotics when needed.

3.1.3 Human primary cells

Human peripheral blood mononuclear cells were isolated from buffy coats from healthy donors by separation on a biocoll gradient (Biochrom). After 15 min of adhesion step at 37ºC, no adherent cells were cultured 2 d in the presence of phytohemagglutinin (PHA) (5 μg ml^{-1}) to induce lymphocyte proliferation. To obtain T lymphoblasts IL-2 (50 U ml^{-1}) was added to the medium every 2 d during 8 d. To obtain SEE-specific T lymphoblasts cells were cultured 10 d in the presence of SEE.

After adhesion step, adherent monocytes were cultured in the presence of IL-4 and GMCSF during 6 d to induce their differentiation into DCs. Maturation of DCs was promoted then by adding lipopolysaccharide (LPS) (10ng ml^{-1}).

3.1.4 Mouse primary cells

Mouse naive CD4+ T cells were obtained from cell suspensions of lymph nodes or spleen from C57BL/6 or OT-II transgenic mice. Cell suspensions were incubated with biotinylated antibodies against CD8, CD19, CD25, CD11b, CD11c, CD45R, MHC-II (I-Ab), DX5, IgM, Gr-1 and F4/80 and subsequently with streptavidin microbeads (MACS; Miltenyi Biotec). CD4+ T cells were negatively selected in auto-MACS Pro Separator (Miltenyi Biotec) according to the manufacturer's instructions. The cells were then labeled with antibodies to CD4, CD62L and CD25 (BD Biosciences) and analyzed by flow cytometry to confirm their purity and naive status (data not shown).

Conventional DCs were derived from wild type bone marrow cell suspensions after culture on non-treated 150-mm Petri dishes with 20 ng ml^{-1} recombinant GM-CSF (Peprotech). Cells were passed every 2 d and collected on day 9 and subsequently stimulated with 100 ng ml^{-1} LPS from *Escherichia coli* (Sigma) for their maturation. At this point DC preparations were characterized as CD11c+ MHCII+ Ly6G-. Alternatively, when pDCs and cDCs were required bone marrow cell suspensions were cultured in the same medium but with 100 ng ml^{-1} Flt3-ligand (Preprotech) instead of GM-CSF. After 8 d maturation was induced by overnight incubation with 6 µg ml^{-1} of cytosine-phosphate-guanosine (CpG) oligodeoxynucleotide-1826: TCCATGACGTTCCTGACGTT. pDCs and cDCs were isolated using MACS system B220-labeled beads and auto-MACS Pro Separator (Miltenyi Biotec) being pDCs B220+ fraction and cDCs B220- fraction.

Mouse primary cells were cultured in RPMI 1640 medium supplemented with 10% fetal bovine serum, 100 U ml^{-1} of penicillin and streptomycin, 10 mM Hepes, 50 µM 2-mercaptoethanol and 1mM sodium pyruvate and the corresponding factors mentioned above for each cell type.

3.2 METHODS

3.2.1 Cell transfection

J77 or Raji cells were transfected with CD63-GFP, CD44-GFP, EGFP, LAT-GFP or CD38-GFP plasmids by electroporation as previously described (Robles-Valero et al., 2010). Cells were resuspended in Opti-MEM (GIBCO) ($5 \cdot 10^7$ ml^{-1}) with 20 µgr of DNA plasmid and electroporated with Gene Pulser Xcell (Biorad) at 1200 µFa, 240 mV during 30msec in 4mm Bio-Rad cuvettes. CD63-GFP positive cells were FACS sorted, cloned and cultured in RPMI containing 2 mg ml^{-1}G418 (Invitrogen).

HEK cells were co-transfected with Psicheck2 reporter plasmids for *pik3r1* 3'UTR fragments and control GFP plasmid or a miR-132-3p-GFP plasmid with Lipofectamine-2000 (Invitrogen) according to manufacturer's instructions. GFP+ cells were sorted at FACSAria flow cytometer (BD Biosciences) before downstream analysis.

3.2.2 Lentiviral infection

J77-CD63-GFP cells over-expressing miRNA-355 or miRNA-101 were generated by lentiviral infection. HEK293T cells were cotransfected (Lipofectamine-2000; Invitrogen) with miRVec plasmids encoding the desired microRNA (Geneservice) and pCL-Ampho plasmid (RetroMax). Supernatants were collected after 48-72 h, filtered (0.45 µm), and added to J77-CD63-GFP cells. The mix was centrifuged (1200xg, 2h) and incubated for 4 h at 37ºC. Medium was replaced with RPMI containing blasticidin (5 µg ml^{-1}) and G418 (2 mg ml^{-1}). To silence nSMase2, HEK293T cells were cotransfected with corresponding shRNA pLKO system plasmids (Open biosystems) and pCMV-ΔR8.91-(Delta 8.9) and pMD2.G-VSV-G. Supernatants were added to J77-CD63-GFP-miR-335 (J-335) cells, which were cultured in RPMI containing 4 µg ml^{-1} puromcyin.

3.2.3 Nucleofection of synthetic RNAs

Synthetic RNAs that correspond to canonical or di-uridylated miRNAs (Integrated DNA Technologies) were nucleofected into freshly isolated naive CD4 T cells using Amaxa Mouse T cell Nucleofector Kit and Amaxa Nucleofector II (Lonza) according to the manufacturer's instructions.

3.2.4 Cloning

Two different fragments of the 3'UTR of *pik3r1* containing the two potential binding sites of miR-132-3p were cloned into psiCHECK2 vector (Promega). The first fragment

comprises the sequence from 71 to 362 bp and the second from 2957 to 3162. See ***Figure 4.18A*** for a diagram of the 3'UTR of *pik3r1* cloned. *Gibson Assembly* system (Gibson et al., 2009), which is based on the efficient joining of several overlapping DNA fragments, was used for the cloning process. The desired fragments from 3'UTR of *pik3r1* were amplified from genomic DNA using Q5 High-Fidelity DNA Polymerase (New England BioLabs) and the following primers:

For site 1:
5'-*GCCCGGGAATTCGTTT*CCAGCCCGACCTGTGAAC-3'
5'-*GGCCGCTCTAGGTTT*GGCCTCTTTGTCCCTGCA-3';

For site 2:
5'-*GCCCGGGAATTCGTTT*GGAGGGTTGGGACCTTGTGTT-3'
5'-*GGCCGCTCTAGGTTT*G ACCTGTACTGGACATCTGCTTG.

These primers add an extra sequence of 15 or 16 pb complementary to psiCHECK2 vector in both ends of the fragment. This way, the amplified segment contains overlapping sequences with the vector. psiCHECK2 was linearized by PmeI (0,2 U μl^{-1}, New England BioLabs) restriction enzyme digestion and subsequently dephosphorylated with Antartic Phosphatase (0,25 U/µl New England BioLabs) and purified with QIAquick PCR Purification Kit (Quiagen). The ligation of the vector with each amplified fragment was performed using the Gibson Assembly Master Mix (New England BioLabs) in a ratio of 5:1 (insert:vector) following manufacturer's instructions.

3.2.5 Fluorescence confocal microscopy

For immunofluorescence assays, cells were plated onto slides coated with poly-L-Lysine (50 µg ml^{-1}, Sigma), incubated for 30 min, fixed with 2% Paraformaldehyde, blocked (BSA 5%) and stained with the indicated primary antibodies (at 5 µg ml^{-1} for the purified ones and directly adding the supernatants form those monoclonals available in the lab) followed by alexa488- or Rhodamine Red X-labeled secondary antibodies (5 µg ml^{-1}) (Life Thechnologies).

The antibodies used throughout this thesis for immunofluorescences were: Monoclonal anti-human antibodies produced in the laboratory: anti-CD63 mAb (Tea 3/18), anti-CD3

mAb (T3b), anti-CD45 (D3/9), and anti-MHC-II (DCIS1/21). Commercial antibodies: Rabbit polyclonal anti-Hrs (Abcam), rabbit polyclonal anti-Zcchc11 (TUT4), rabbit polyclonal anti-Zcchc11 (TUT4) (Proteintech), Anti tubulin-FITC (Sigma) and Phalloidin-alexa488 for F-actin labeling (Life Technologies).

For live-cell imaging, Raji (preloaded with CMAC and SEE) and J77-CD63-GFP cells were added to coverslips coated with fibronectin (20µg ml^{-1}, Sigma), mounted in Attofluor open chambers (Molecular Probes), and maintained at 37°C in a 5% CO2 atmosphere.

Samples were examined with a Leica SP5 confocal microscope fitted with a 63x objective, and images were processed and assembled using Leica software.

3.2.6 Immunoblotting

Cells were lysed in lysis buffer (50 mM Tris pH7.5, 150 mM NaCl, 2 mM MgCl2, 1%NP-40, 5mM EDTA) of RIPA (1% NP40, 0.5% deoxycholate, 0.1% SDS in TBS) depending on the experiment, both containing a protease inhibitor cocktail (Complete, Roche). Proteins were separated on 8 or 10% acrylamide/bisacrylamide gels and transferred to a nitrocellulose membrane. Membranes were blocked with 5% skim milk in TBS-T milk and incubated with specific primary antibodies (5 µg ml^{-1}) and peroxidase-conjugated secondary antibodies (5 µg ml^{-1}), and chemiluminescence was measured with LAS-6000 (Fujifilm). Band intensities were quantified with Image Gauge (Fujifilm) and results are expressed relative to the control condition. Proteo Extract subcellular proteome extraction kit (Calbiochem) was used for subcellular fractionation of proteins followed by western blot.

The following antibodies were used for western blot throughout this thesis: Anti-CD63 mAb produced in our laboratory (Tea 3/18), rabbit anti-Hrs (Abcam), anti-CD81 mAb (5A6, Santa Cruz), Anti-alpha Tubulin antibody (DM1A, Sigma) rabbit polyclonal anti-Zcchc11 (TUT4), rabbit polyclonal anti-Zcchc6 (TUT7) (Proteintech), goat polyclonal anit-Zcchc11 (ProSci), anti-$p150^{glued}$ (BD Transduction Laboratories), monoclonal anti-EZH2 (Cell Signaling), rabbit polyclonal anti-p85a (Millipore), polyclonal anti ezrin/moesin (ERMs) (90/3) (provided by Heinz Furthmayr, Stanford University, Stanford, CA). Secondary antibodies were goat anti-mouse Horseradish peroxidase (HRP) (31446,

Thermo Scientific) (1:5,000), goat anti-rabbit HRP (37460, Thermo Scientific) (1: 10,000) and donkey anti-goat HRP (Santa Cruz) (1:10,000).

3.2.7 Exosome purification

Exosome producing cells were cultured in RPMI-1640 supplemented with 10% FBS (depleted of bovine exosomes by overnight centrifugation at 100000g), and exosomes were prepared from cell supernatants by several centrifugation and filtration steps (Thery et al., 2006). Briefly, cells were centrifuged (320g for 5 min) and the supernatant filtered through 0.22 µm membranes. Exosomes were pelleted by ultracentrifugation at 100000g for 60 min at 4ºC (Beckman Coulter Optima L-100 XP).

3.2.8 Non-synaptic exosome uptake experiments

Exosomes were purified as described above and added to recipient cells in a ratio 1:25 (recipient:donor cells). After 16h, recipient cells were analyzed by flow cytometry.

3.2.9 Conjugate formation and Transwell assays

To distinguish B cells from T cells, B cells (Raji or Hom2) were loaded with the blue fluorescent tracker CMAC (chloromethyl derivative of aminocoumarin, Molecular Probes). B cells were incubated with SEE (Toxin Technology) or HA peptide (New England Peptide) as appropriate and mixed with J77 cells (native or expressing CD63-GFP ± miR-335 or miR-101) or CH7C17 cells at a ratio of 1:8. Conjugation at 37ºC was continued for times indicated in each case. Where indicated, J77 cells were preincubated with manumycin-A (10µM), brefeldin (10 mg ml^{-1}), nocodazol (5 µM), cytochalasin-D (20 µM) or latrunculin-A (1 µM) (all from Sigma). In experiments with Raji-CD63-GFP cells, J77 cells were labeled with CMAC. Where indicated, Raji and J77 cells were prevented from coming into direct contact by separating with a 0.4 µm pore-size transwell membrane (Costar). This allows the passage of exosomes but precludes direct cell-cell interaction. When indicated, T cells were activated with phorbol myristate acetate (PMA) (50ng ml^{-1}) plus Ionomycin (0.5 µg ml^{-1}), anti-CD3 plus anti-CD28 (both at 5µg ml^{-1}), or SEE (0.5 µg ml^{-1}).

3.2.10 Flow cytometry analysis and sorting

Cell samples were analyzed with a BD FACS Canto flow cytometer or BD LSR Fortessa and FACSDiva software (BD Biosciences) and FlowJo software. Viable cells were identified by propidium iodide or DAPI exclusion as convenient. Singlet cells were discerned with a stringent multiparametric gating strategy based on FSC and SSC (pulse width and height). For mouse CD4 T cells phenotyping to check purity of macs sorting and activation state (***Results 4.2*** and ***4.3***) the following antibodies were used: anti CD4, anti CD69, anti CD62L, anti CD25, and anti CD8 coupled with the appropriate fluorophore (All from BD Biosciences). For immune synapse experiments (***Results 4.1***) T cells and APCs were distinguished by CMAC staining and GFP fluorescence.

When stated, cells were sorted on a FACSAria flow cytometer (BD Biosciences). Raji cells were isolated after coculture with T cells by sorting for CMAC-positive singlet cells (***Results 4.1***). When indicated, Raji cells were also sorted based on CD63-GFP levels. Cocultures of cDCs or pDCs with CD4+ T cells (***Results 4.2***) were discriminated by staining of MHC-II and CD4 plus CD69.

3.2.11 UTR reporter assays

Psicheck2 dual luciferase reporter vector (Promega) have been used twice along this thesis. It comprise the gene of Firefly luciferase as a normalizing gene and the luciferease *Renilla reniformis* gene downstream of the cloning site. The vectors cloned with the full-length 3'UTRs of SOX4 and UBE2F and the SOX4 3'UTR segment (base pairs 449-509) containing the wild-type or mutated (base pair 483) miR-335 seed sequence were a gift from Dr. J. Massagué (Tavazoie et al., 2008) (Memorial Sloan-Kettering Cancer Center, NY). Raji cells were transfected by electroporation and, 16h later, cocultured with J-335 or J-101.

For validation of pik3r1 as a target of miR-132-3p, the dual reporter vector was cloned with the fragments for binding sites of miR-132-3p as mentioned above in section ***3.2.4 Cloning*** and cotransfected with control or miR-132-3p overexpressing vectors.

After 24h, cells were lysed and the ratio of Renilla and Firefly luciferase activities was measured by the dual luciferase assay (Promega). Renilla and Firefly Luciferase.

3.2.12 Mouse primary T cell polyclonal activation

Naive CD4+ T cells were obtained from cell suspensions of lymph nodes or spleen by negative selection as explained above in under ***Mouse primary cells***. After isolation naïve T cells were either directly lysed or cultured (10^6 cells ml^{-1}) with 2µg ml^{-1} of anti-CD28 on plates previously coated with 10 µg ml^{-1} of anti-CD3 (BD Biosciences). Alternatively, cells were maintained in the naive state in the presence of 4 ng ml^{-1} of interleukin 7 (Peprotech). The activation status of CD4 T cells was assessed at the indicated time points by flow cytometry after staining with antibodies against CD4, CD25, and CD69 (BD Biosciences). Data were acquired and analyzed with a FACSFortessa flow cytometer and FACSDiva (BD Biosciences) or FlowJo software.

3.2.13 Antigen specific primary T cell stimulation

When indicated, dendritic cells (DCs) were used to stimulate OT-II CD4 T cells. DCs were derived from bone marrow as described above under ***Mouse primary cells***. OT-II CD4 T cells were cocultured with the corresponding subset of DCs (8:1 T cell/DC ratio) in the presence or absence of ovalbumin (OVA) peptide for 18 h. When required, cells were stained for CD4 and MHCII for subsequent sorting of the CD4 T cell fraction on a FACSAria flow cytometer (BD Biosciences). The activation status of CD4 T cells was assessed by flow cytometry like in *3.2.12*.

3.2.14 Human T lymphoblast stimulation

Human T lymphoblasts were obtained as explained in page 37 in ***Human primary cells*** and later stimulated either with anti-CD3 and anti-CD28 coated beads (Gibco) or with phorbol myristate acetate (PMA) and ionomycin.

3.2.15 RNA isolation

Total RNA was extracted with QIAzol lysis reagent (Qiagen) and the miRNeasy mini kit (Qiagen). Purity and concentration were measured in a Nanodrop-1000 spectrophotometer (Thermo Scientific) and RNA integrity was assessed using the Agilent 2100 Bioanalyzer or by ethidium bromide labeling on a 1.5% agarose gel.

3.2.16 microRNA microarrays

The Agilent 2100 Bioanalyzer for total RNA (RNA nano chips) and for small RNA (small RNA chips) were used to assess the large and small RNA profiles. Microarray

experiments were performed using the human microRNA microarray from Agilent for data from *Results 4.1.* Arrays were performed on three different RNA preparations from Raji and J77 cells and their exosomes, and two preparations each from human dendritic cells, and their exosomes. Microarray for mouse microRNA from Agilent were used for *Results 4.2.*

3.2.17 Small RNA cloning and sequencing (miR-seq library preparation, sequencing and generation of FastQ files)

Total RNA (1 µg) was used to generate barcoded miR-seq libraries using the TruSeq smallRNA sample preparation kit (Illumina). Briefly, 3´ and 5´adapters were first ligated to the RNA sample. Next, reverse transcription followed by PCR amplification was used to enrich cDNA fragments with adapters at both ends. Adapter-ligated cDNA fragments from different samples were pooled and run on a 6% polyacrylamide gel. The band between 147 and 180 base pairs, corresponding to the pooled miRNA libraries including slightly longer fragments (potential IsomiRs with 3'NTAs), was purified from the gel. Finally, the quantity and quality of the pooled miR-seq libraries were determined using the Agilent 2100 Bioanalyzer High Sensitivity DNA chip. Libraries were sequenced on a Genome Analyzer IIx (Illumina). FastQ files for each sample were obtained using CASAVA v1.8 (Illumina). Library preparation and sequencing was performed by CNIC genomic unit.

3.2.18 Next generation sequencing analysis and statistics

Raw FASTQ files were trimmed for adapter contamination using REAPER from the Kraken package (Davis et al., 2013). All reads were mapped against miRNA precursors obtained from miRBase release 21 (Kozomara and Griffiths-Jones, 2014) using BLASTn. A custom pipeline interrogated each read to determine which miRNAs originated from which precursor and which arm (either 5' or 3'). Extra nucleotides that could not be explained by the associated miRNA precursor sequence were flagged as non-canonical 5' or 3' extensions. Count data for canonical matches and non-canonical extensions were stored for each sample in the tabular form. Count data were normalized and analyzed using R/BioConductor with the DeSeq2 package. Changes to either global miRNA levels or individual miRNA modifications were viewed as significant if they had an absolute

Log Fold-Change > 0.5 and an adjusted P-Value < 0.05. All data and scripts used are available.

3.2.19 mRNA reverse transcription and quantitative real time PCR

For data corresponding to *Results 4.1* mRNA quantification was performed by TaqMan real-time PCR (Applied Biosystems) according to the manufacturer's instructions. The following TaqMan Gene expression Assays (Applied Biosystems) were used: SMPD3 (nSMase2) (Hs00218713_m1) while GAPDH (Hs02758991_g1) and HPRT (Hs01003267_m1) were used as endogenous controls. For data corresponding to *Results 4.2.* and *4.3* cDNA was synthesized using the High Capacity cDNA Reverse Transcription Kit (Applied Biosystems). Expression analysis by quantitative PCR was performed with SYBRgreen PCR master mix (Applied Biosystems), and the corresponding primers (listed in *Table 3.1*). B-actin and Yhwaz (tyrosine 3-monooxygenase/tryptophan 5-monooxygenase activation protein, zeta) genes were used as endogenous controls.

Data were acquired and analyzed using the ABI Prism 7900HT Sequence Detection System (Applied Biosystems) and Biogazelle QBasePlus software (Biogazelle). Data are presented in relative mRNA levels to endogenous controls.

Oligo Name	Sequence (5' to 3')
Mouse YWHAZ (Forward)	CGTTGTAGGAGCCCGTAGGTCAT
Mouse YWHAZ (Reverse)	TCTGGTTGCGAAGCATTGGG
Mouse b Actin (Forward)	CAGAAGGAGATTACTGCTCTGGCT
Mouse b Actin (Reverse)	TACTCCTGCTTGCTGATCCACATC
Mouse B2M (Forward)	TTCTGGTGCTTGTCTCACTGA
Mouse B2M (Reverse)	CAGTATGTTCGGCTTCCCATTC
Mouse Pik3r1 v1 (Forward)	ACACCACGGTTTGGACTATGG
Mouse Pik3r1 v1 (Reverse)	GGCTACAGTAGTGGGCTTGG
Mouse Pik3r1 v2 (Forward)	ATTTCACCCCCTACTCCCAAG
Mouse Pik3r1 v2 (Reverse)	AGTCGAACATTCCAGTCCTTT
Mouse TUT4 (Forward)	AAGTCAGAAATTGGGACCAGC
Mouse TUT4 (Reverse)	TGGCAGCGTTTACTTTACATGAT
Mouse TUT2 (Forward)	AAACTCAATTTTGGGTCGTCCA
Mouse TUT2 (Reverse)	GTGCATCTATAAGTTGCTGGTGT
Human HPRT1 (Forward)	CCTGGCGTCGTGATTAGTGAT
Human HPRT1 (Reverse)	AGACGTTCAGTCCTGTCCATAA

Human B2M (Forward)	GAGGCTATCCAGCGTACTCCA
Human B2M (Reverse)	CGGCAGGCATACTCATCTTTT
Human PIK3R1 (Forward)	CGGCGAAGTAAAGCATTGTG
Human PIK3R1 (Reverse)	ACATTGAGGGAGTCGTTGTG
Human TUT4 (Forward)	TCAACAGGTGGCTGGTTCAGCTCAG
Human TUT4 (Reverse)	TAGCAGCTGACTGGGAAGAGTTCTG
Human TUT2 (Forward)	CTACTGTTTATTCACACCAGC
Human TUT2 (Reverse)	CTCTTCCTTCCTCGAAATAATG

Table 3.1 Primers for mRNA qPCR used in this thesis

3.2.20 Reverse transcription and RT-qPCR of mature canonical miRNA

For *Results 4.1* data mature miRNA quantification was performed by TaqMan real-time PCR (Applied Biosystems) according to the manufacturer's instructions using the following TaqMan miRNA Assays: hsa-miR-335 (000546), hsa-miR-92a (000431). HY3 (001214) and RNU19 (001003) were used as endogenous controls. For data corresponding to *Results 4.2.*and *4.3* cDNA was synthesized and mature miRNAs were quantified by miRCURY LNA Universal RT microRNA PCR (Exiqon), using miRNA LNA primers (Exiqon) and SYBRgreen PCR master mix (Applied Biosystems). RNU1A1 and RNU5G RNAs were used as endogenous controls

Quantitative miRNA expression data were acquired and analyzed using the ABI Prism 7900HT Sequence Detection System (Applied Biosystems). Data were further analyzed using BiogazelleQBasePlus software (Biogazelle). Results are expressed in arbitrary units relative to endogenous controls.

3.2.21 Reverse transcription and qPCR of synthetic miRs and isomiRs

Levels of the synthetic miRNAs previously nucleofected into T cells were analyzed by a variation of miQPCR method(Benes et al., 2015). In bief 60 ng of total RNA were ligated to an oligonucleotide adapter (miLINKER) followed by retrotranscripition to cDNA. Quantitative PCR was then performed with Taqman PCR master mix (Applied Biosystems) using both specific primers and LNA Taqman probes. Quantitative data of synthetic RNA levels were acquired and analyzed using the ABI Prism 7900HT Sequence Detection System (Applied Biosystems). Data were further analyzed using

BiogazelleQBasePlus software (Biogazelle). snoRNA 420 and snoRNA 412 were used as endogenous controls for normalization and results are expressed in arbitrary units.

RESULTS

4 RESULTS

4.1 Unidirectional transfer of microRNA-loaded exosomes from T-cells to Antigen Presenting Cells

4.1.1 miRNA profiles of immune cells and their exosomes

To determine the miRNA repertoire of exosomes secreted by immune cells, we isolated exosomes from cell supernatants of the Raji B cell line, the Jurkat-derived J77 T cell line, and primary dendritic cells (DCs) derived from human monocytes. Exosomes were isolated by a series of microfiltration and ultracentrifugation steps (Thery et al., 2006), and exosome identity was assessed by extensive protein analysis with LC-MS/MS technology. About 60% of proteins found in the analyzed exosome samples have been previously found in exosomes; these include the tetraspanins CD63, CD81 and CD9, proteins involved in membrane transport and fusion (Rab GTPases, annexins and fotillin), and other exosomal markers such as Tsg101 (*Annex Table 9.1*). Moreover, exosomes derived from T lymphocytes and from APCs both contained RNA. Profiling of RNA isolated from exosomes and their donor cells indicates that exosomes are highly enriched in small RNA species (*Figure 4.1*). Agilent miRNA microarray analysis showed that certain miRNAs are

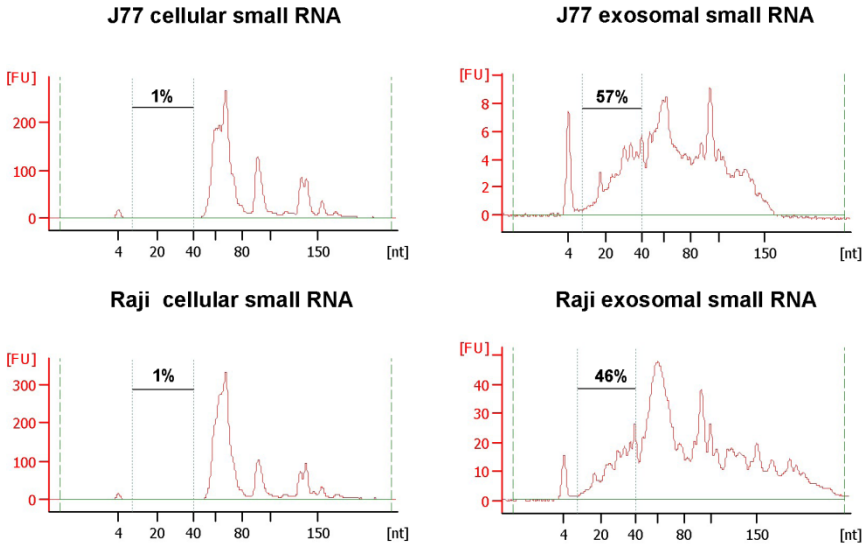

Figure 4.1 Exosomes are enriched in small RNA
RNA from immune cells and their exosomes was assessed with the Agilent 2100 Bioanalyzer. The percentage of small RNAs (<30 nucleotides) was higher in exosomes than in their donor cells. FU, fluorescence units; nt, nucleotides.

expressed at higher levels in exosomes than in their donor cells, and *vice versa* (*Figure 4.2* and *Annex Table 9.2*). The hierarchical clustering and the principal component analysis (PCA) of the array data grouped the samples according to their cellular or exosomal origin (*Figure 4.2A, B*). Several miRNAs (for example, miR-760, miR-632, miR-654-5p and miR-671-5p) were significantly more abundant in exosomal samples from all cell types; others, for example miR-335, were found only in exosomes derived from the primary DCs; in contrast, others (for example, miR-101, miR-32 and miR-21*) were more highly represented in cells than in exosomes (*Figure 4.2C*). These data indicate that specific miRNA populations are selectively sorted into exosomes.

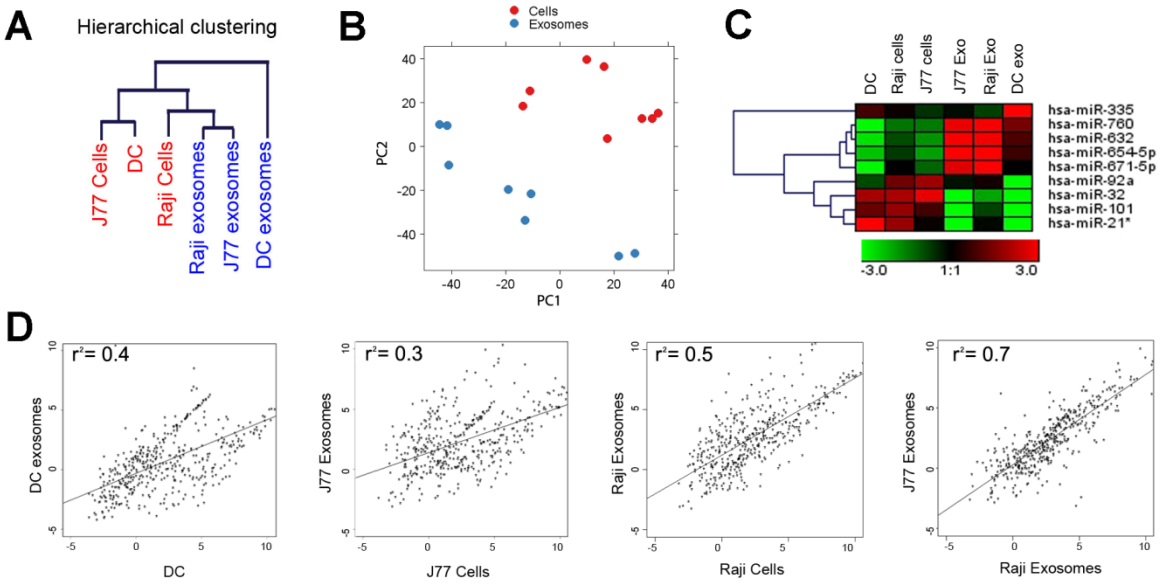

Figure 4.2 microRNA profiles of exosomes and their parental cells
(A) Microarray analysis of exosomal miRNAs vs the miRNAs of their respective donor cells. Exosomes were isolated by serial centrifugation and filtration steps from supernatants of donor cells cultured in RPMI-1640 supplemented with exosome-depleted FBS (10%). Total RNA, including microRNA, was isolated from exosomes and their donor cells and miRNA profiles were assessed by microarray technology. The panel shows the hierarchical clustering of the vsn-normalized array data in the log2 scale averaged per biological replicate for each origin (Exosomes/cells) and cell type (DC: dendritic cells; J77: Jurkat-derived J77 T cell line and Raji: Raji B cell line). **(B)** Principal component analysis (PCA) of all normalized array data. Each point represents a hybridized sample: i.e. different biological samples per origin and cell type. X-axis, first principal component (PC1); Y-axis, second principal component (PC2). Cell samples, red; exosomal samples, blue. **(C)** Heatmap of the vsn-normalized data for selected miRNAs. For visualization purposes the expression profiles were centered on the median of the profile. The scale bar across the bottom depicts standard deviation change from the mean. **(D)** Scatterplots of the exosome vs cell averaged array data in each cell type and of Raji exosomes vs J77 exosomes. The correlation is shown.

Consistently, there was lower overall similarity between the miRNA repertoire in exosomes and their corresponding cells than between the exosomes of different cellular origin (*Figure 4.2D*).

4.1.2 Multivesicular bodies from T lymphocytes polarize towards the IS

To analyze the capacity of cells to take up immune exosomes, we generated Raji B and J77 T cells stably expressing the exosomal marker CD63 fused to GFP. The tetraspanin CD63 is very abundant in exosomes, and inside cells localizes mainly to MVBs and lysosomes, with only a small pool present at the plasma membrane (Pols and Klumperman, 2009). Western blot and cytometry analyses confirmed the presence of CD63-GFP in exosomes released by these cells (*Figure 4.3*). The purified CD63-GFP exosomes were then incubated with non-transfected J77 cells or Raji cells (recipient cells) for 16h. Flow cytometry analysis revealed that both J77 T and Raji B cells have the capacity to take up immune exosomes (*Figure 4.4A*). It is important to highlight that Raji B cells take up T cell- derived exosomes to a greater extent than their own exosomes and *vice-versa*. Moreover, CD63-GFP was detected at the surface of recipient cells by confocal microscopy (*Figure 4.4*), suggesting that exosomes are not internalized but remain attached to the recipient plasma membrane.

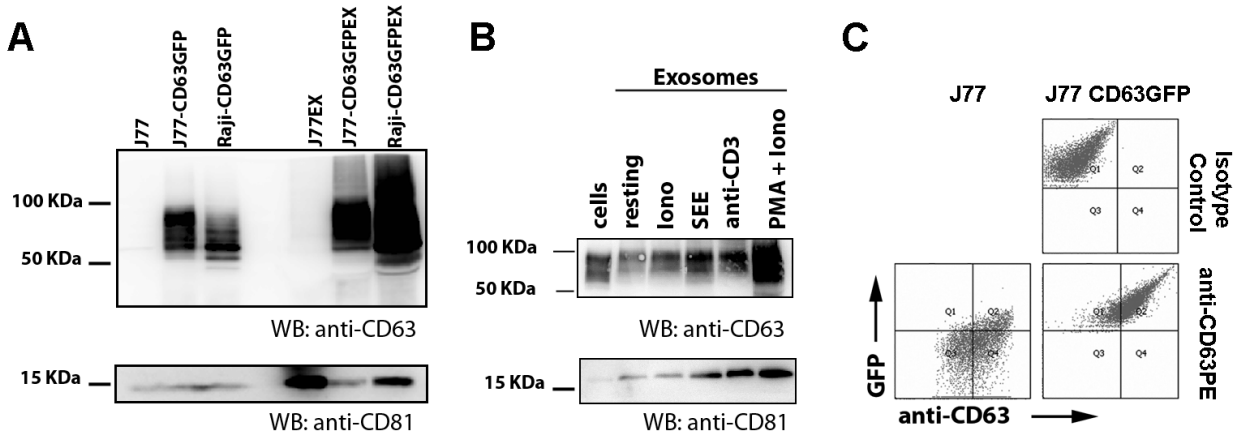

Figure 4.3 Exosomes contain CD63-GFP

(A) J77, J77-CD63GFP and Raji-CD63GFP cells were cultured in exosome-depleted medium for 24 h and released exosomes were purified from supernatant by ultracentrifugation. Both whole cell and exosomes (denoted as Ex) lysates from each cell type were analyzed by immunoblotting for the presence of CD81 and CD63 tetraspanins. **(B)** J77-CD63GFP cells were cultured in exosome-depleted medium for 24 h under resting conditions or with the indicated activation stimuli (Ionomycin (Iono), *Staphylococcus* enterotoxin superantigen-E (SEE), Phorbol myristate acetate (PMA) or anti-CD3). Released exosomes were purified from supernatant by ultracentrifugation and analyzed by immunoblot for the presence of CD81 and CD63 tetraspanins. **(C)** Untransfected J77

cells and J77 cells stably expressing CD63-GFP (J77-CD63-GFP cells) were cultured in exosome-depleted medium for 24 h and exosomes were purified from supernatants by ultracentrifugation. Exosomes were labeled with anti-CD63-phycoerythrin and analyzed by flow cytometry.

To address whether exosomes mediate the transfer of miRNA during cognate immune interactions, we first studied the intracellular distribution of MVBs—the compartments from which exosomes arise—during the formation of an IS. In these experiments, Raji B cells were pulsed with *Staphylococcus* enterotoxin superantigen-E (SEE) and then incubated with TCR-Vβ8$^+$ J77 cells. MVB localization was assessed by immunofluorescence analysis of CD63 and a component of the ESCRT-0 (endosomal sorting complex required for transport) Hrs. In the presence of SEE, which promotes formation of a fully functional IS, the MVBs of the J77 T lymphocyte lost their random cytoplasmic distribution and congregated near the IS (identified by CD3 and actin staining); in contrast, the localization of MVBs in the Raji B cell remained unchanged (*Figure 4.5A*). Similar results were obtained in experiments in which CH7C17 T cells, bearing an influenza hemagglutinin (HA) peptide-specific TCR, were conjugated to HA peptide-pulsed Hom2 B cells, thus confirming that antigen-induced formation of an IS polarizes T cell MVBs to the contact site (*Figure 4.5B, C*). Live cell imaging of CD63-GFP-

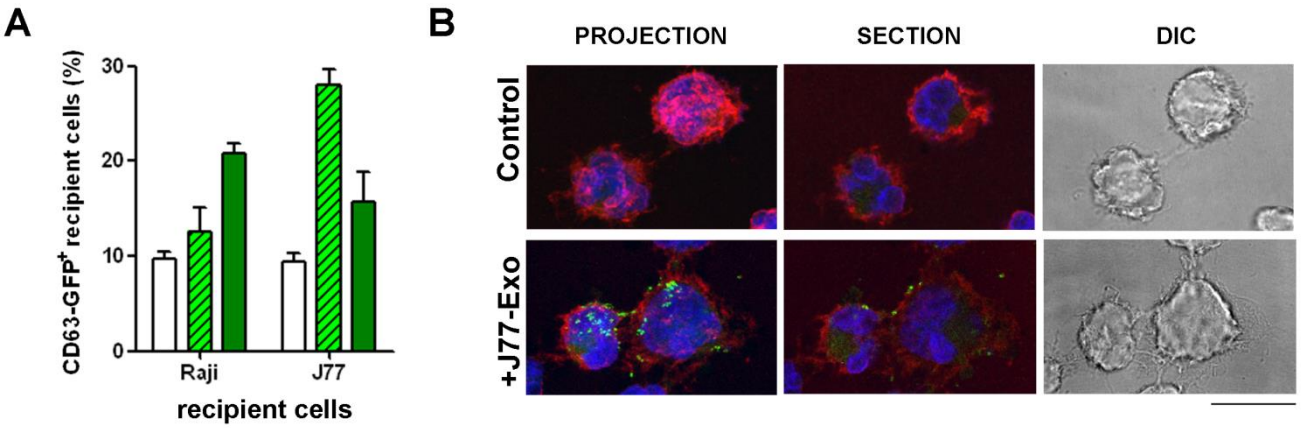

Figure 4.4 Uptake of CD63-GFP exosomes by immune cells
(A) Uptake of CD63-GFP exosomes by T cells and B cells (recipient cells). Untransfected cells were incubated with CD63-GFP exosomes for 16h and analyzed by flow cytometry. Data represent the percentage of GFP-positive cells (± s.e.m.) of three independent experiments. Open bars: no exosomes. Striped bars: Raji exosomes. Filled bars: J77 exosomes. **(B)** Confocal microscopy detection of CD63-GFP (green) on the surface of recipient cells (Raji) after incubation with J77-CD63-GFP exosomes. Cell membranes were stained for the cell surface molecule CD45 (red) and nuclei were stained with HOESCHT (blue). Images show maximal projections of confocal images (Projection), one representative confocal section (Section) and the DIC images. Scale bar: 10 µm.

expressing J77 T cells encountering SEE-pulsed Raji B cells revealed that the MVBs of the T cells move to the IS during the first 10 min (*Figure 4.5D, and Supplementary Movie1*)

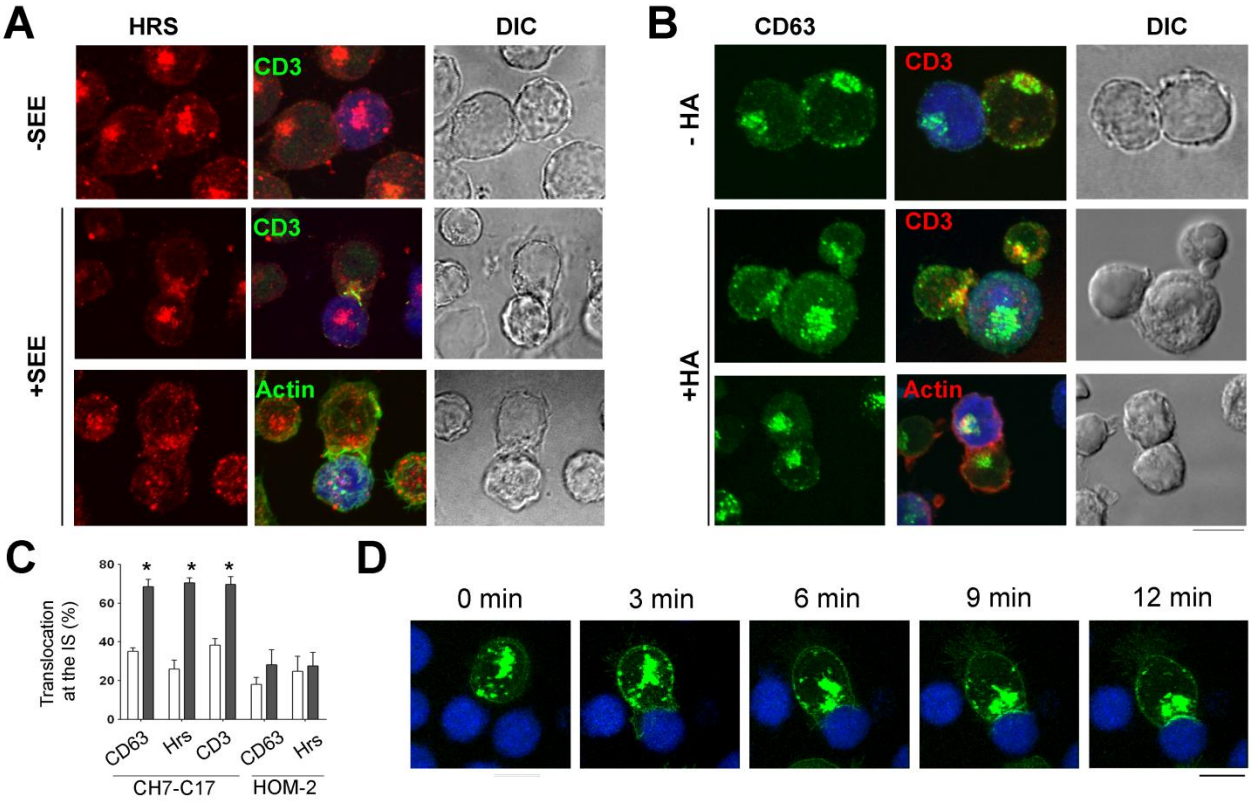

Figure 4.5 MVBs in T cells translocate to the IS
(A) J77 T cells were conjugated with SEE-pulsed or non-pulsed Raji B cells loaded with CMAC (blue). After 30 min, cells were fixed and stained for the MVB marker Hrs (red), CD3 and actin (both green). Plates show maximal projections of confocal images and the DIC images. **(B)** CH7C17 T cells were conjugated with HA-loaded or non-loaded HOM2 B cells (blue). After 30 min, cells were fixed and stained for CD63 (green), CD3 and actin (both red). Plates show maximal projections of confocal images and the DIC images. **(C)** Percentage of T and APC cells in which CD63, Hrs and CD3 relocalized to the T cell–APC contact area in the presence of HA peptide (filled bars) or its absence (open bars). Data are the arithmetic means ± s.e.m. of four experiments. * $p < 0.03$ compared with the absence of antigen (Mann Whitney test). **(D)** Live cell imaging of J77-CD63-GFP cells seeded on fibronectin-coated coverslips and conjugated with SEE-primed Raji cells (blue). Cells were monitored by time-lapse confocal microscopy at 30-s intervals. Plates show maximal projections of confocal images. Scale bars: 10 µm

4.1.3 The immune synapse promotes the transfer of exosomes from the T cell to the antigen presenting cell

To investigate whether the IS promotes the transfer of exosomes from T cells to APCs, CD63-GFP T cells were cultured with Raji cells (stained blue with CMAC) for 16 h, by which stage most conjugates will have separated. The coculture was analyzed by flow cytometry for the transfer of CD63-GFP. SEE-pulsed Raji cells acquired CD63-GFP from the T cells, whereas transfer in the absence of SEE was negligible (*Figure 4.6A*). No transfer of GFP signal was detected when the assay was performed in the opposite direction (from Raji-CD63-GFP to J77 cells) (*Figure 4.6A*) or when using J77 cells overexpressing non-exosomal membrane or cytoplasmic proteins (CD69-GFP and GFP) (*Figure 4.6B*). In addition, we also detected transfer of other molecules related to exosomes and vesicles, such as LAT (*Figure 4.6C)*.

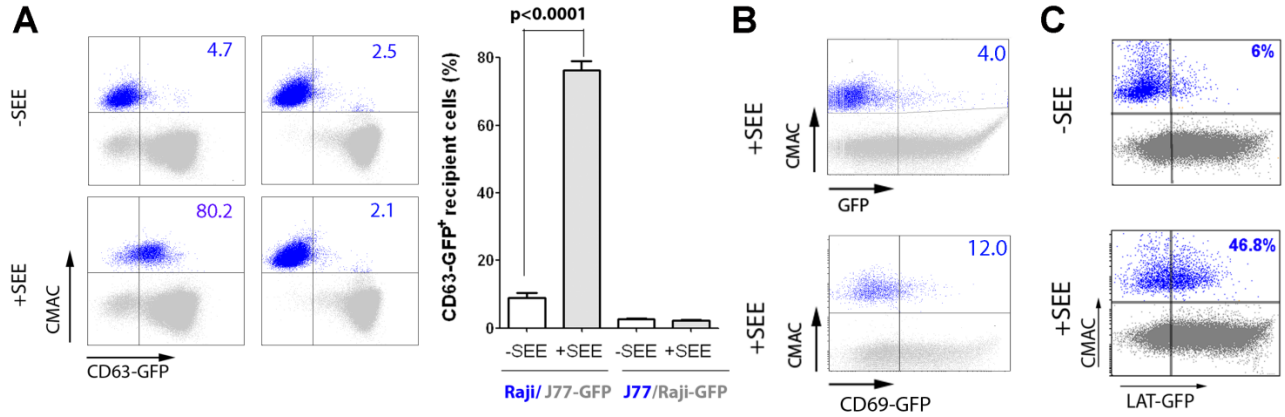

Figure 4.6 Ag recognition induces transfer of exosomes from T cell to APC
(A) *Left*: J77-CD63-GFP donor cells were conjugated with SEE-primed or unprimed Raji cells (recipient, in blue). *Right*: Raji-CD63-GFP donor cells (±SEE) were conjugated with blue-labeled J77 recipients. After 16 h cocultures were analyzed by flow cytometry. Bar chart shows the percentage ± s.e.m. of positive recipient cells (n=9, p<0.001, Student's t-test). **(B)** J77 cells transfected with CD69-GFP or GFP were conjugated with SEE-primed Raji cells (blue) and analyzed as in (A). **(C)** J77-LAT-GFP cells (donor) were conjugated with SEE-loaded or unloaded Raji cells (recipient; blue). Donor and recipient populations were analyzed by flow cytometry after 24 h coculture. Raji recipients acquired LAT-GFP in an antigen-dependent manner. Dot plot of one representative experiment is shown.

To define the requirement for cell-cell contact, we separated donor and recipient populations by a 0.4 μm pore-size Transwell membrane. J77-CD63-GFP T cells in transwell assays were treated with anti-CD3 plus anti-CD28 to activate them and therefore enhance exosome release ((Blanchard et al., 2002) and *Figure 4.3*). Although T cell CD69 levels indicated that cells had been activated to the same extent as after formation of an IS, no CD63-GFP was detected on APC recipient cells, whether or not

these were loaded with SEE (*Figure 4.7A and Figure 4.8A*). Also, in contact (non-Transwell) cocultures, stimulation with CD3 and CD28 Abs in the absence of SEE did not support CD63-GFP transfer (*Figure 4.7B,C*). Moreover, CD63-GFP transfer in standard (in the presence of SEE) contact cocultures was abolished by addition of the actin cytoskeleton inhibitors cytochalasin-D and latruculin-A, which disrupt the IS (Valitutti et al., 1995), whereas the microtubule inhibitor nocodazol had no effect (*Figure 4.8A*). These results indicate that cell-cell contact and T-cell activation by themselves do not support exosomal transfer.

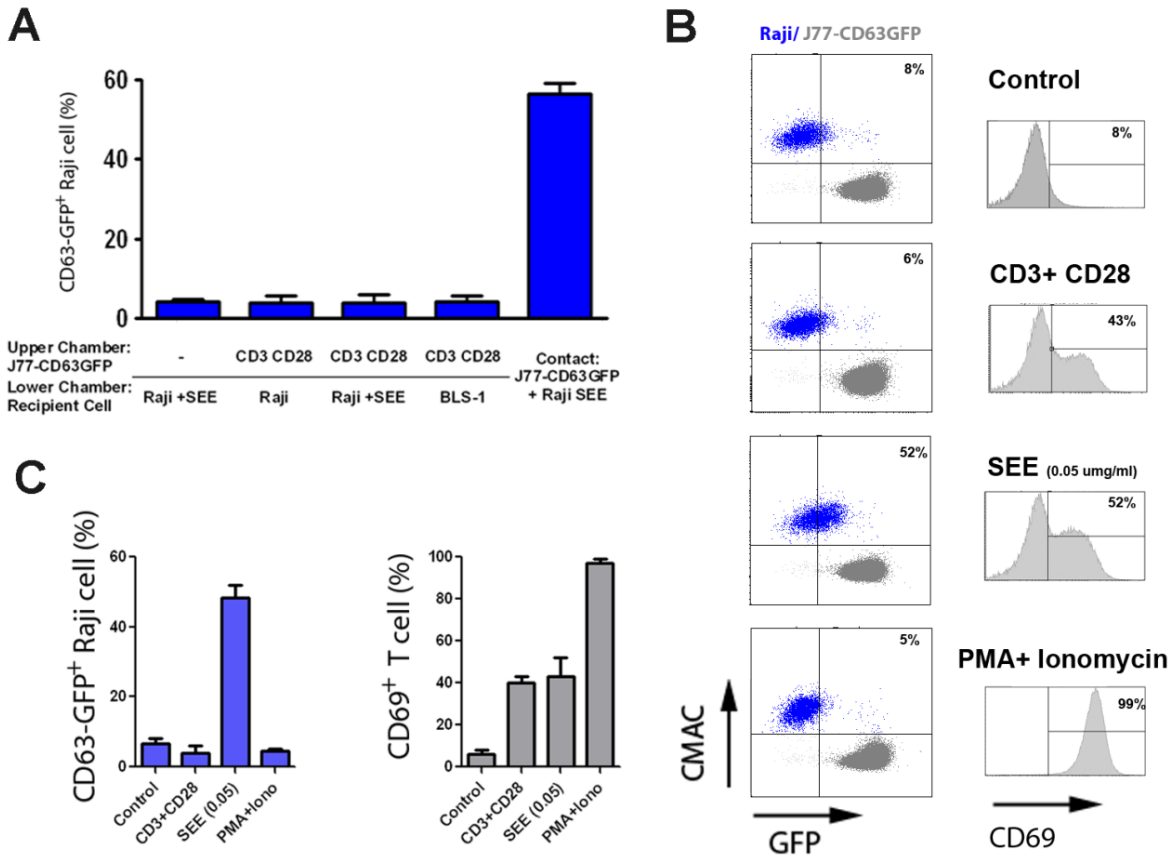

Figure 4.7 Cell-Cell contact and T cell activation are not sufficient for the exosomal transfer
(A) Transwell experiments were performed with donor and recipient cells placed in the upper and lower chambers as indicated. CD63-GFP signal was measured on the recipient cells after 16h by FACS, and compared with the signal from antigen-stimulated contact cultures at the same T-cell:APC ratio. **(B and C)** J77-CD63-GFP cells (donor) were conjugated with Raji cells (recipient; blue) in the presence of CD3 and CD28 Abs, SEE or PMA+Ionomycin. The cocultures were analyzed by flow cytometry 24 h later, donor cells for expression of the activation marker CD69 and recipients for the acquisition of CD63-GFP. A representative experiment is shown in **(B)** and the percentage ± s.e.m. of positive cells of 3 independent experiments in panel **(C)**.

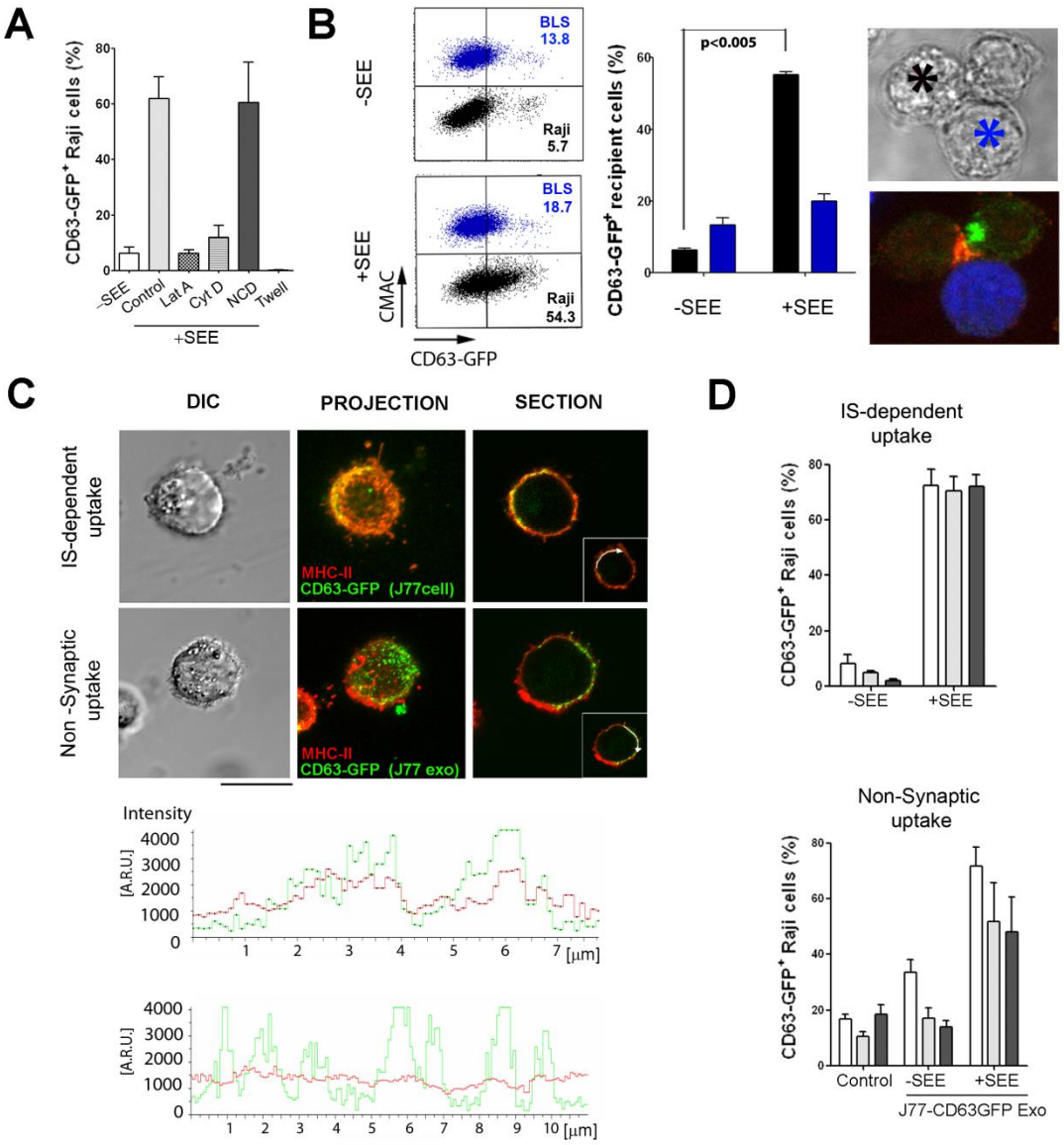

Figure 4.8 Cognate immune interactions induce exosomal uptake and fusion
(A) FACS analysis of the percentage of GFP-positive Raji cells after incubation with J77-CD63-GFP cells in contact coculture as in *Figure 4.6A* (control), in the presence of inhibitors of actin (latrunculin-A, LatA or cytochalasin-D, CytD) or tubulin (nocodazol, NCD), or after incubation with separation of donors and recipients by a 0.4 µm pore-size transwell membrane (Twell). T cells in transwells were activated with CD3+CD28 Abs and Raji cells were loaded with SEE. **(B)** J77-CD63-GFP donor cells were conjugated with a 1:1 mix of two B cell lines: Raji cells (black) and BLS-1 cells (blue) and analyzed as in (A). Bar chart shows percentages ± s.e.m. of positive recipient cells (n=6, p<0.005, Mann Whitney test). Maximal projections of confocal images and the DIC of a triple conjugated formed by J77-CD63-GFP (green), Raji cells (black asterisk) and BLS-1 (CMAC stained and blue asterisk), stained for CD3 (red) are shown. **(C)** Confocal analysis of Raji cells that acquired CD63-GFP directly from J77-CD63-GFP after IS formation (IS-dependent transfer) or after external administration of CD63-GFP exosomes isolated from J77-CD63GFP supernatants (non-synaptic uptake). Cell were stained for MHC-II (red). Images show maximal projections of confocal images, one representative confocal section, and the DIC images. Plots show cell perimeter fluorescence

intensity profiles of the green and the red signals. A.R.U.: arbitrary relative units. Scale bar: 10 µm **(D)** Raji cells (±SEE) were treated as in (C)**.** FACS analysis of the effect of trypsin on the CD63-GFP content of Raji cells that acquired exosomes by IS-dependent transfer or non-synaptic uptake. White bars, control; grey bars, 10' trypsin; black bars, 10'+10' trypsin. Bar chart shows percentages ± s.e.m. of positive cells (n=3).

To confirm that the exosomal transfer requires a functional IS, we cocultured J77-CD63-GFP T cells with a mix of Raji B cells and BLS-1 B cells, which lack HLA class II and cannot form an IS (Hume et al., 1989). After 16 h, GFP signal was detected on SEE-primed Raji B cells (*Figure 4.8B*). In contrast, BLS-1 B cells did not trigger CD63 translocation or CD3 clustering (*Figure 4.8B*, right panel). These findings indicate that while T and APCs can both take up immune exosomes, cognate immune interactions promote the transfer of exosomes from the T lymphocyte to the APC and their unidirectional acquisition by the conjugated APC.

We next analyzed the mechanism of exosome uptake by APCs. In post-conjugated Raji cells, which had acquired CD63-GFP upon IS formation, the CD63-GFP colocalized at the plasma membrane with endogenous MHC-II molecules, indicating that the exosomes either remained attached or had fused with the cell surface. Intensity profiles around the cell perimeter indicate similar distributions of both molecules in the plasma membrane (*Figure 4.8C*). In contrast, in Raji cells that had acquired CD63-GFP by direct addition of exosomes isolated from J77-CD63-GFP cells (non-synaptic uptake), the GFP signal appeared as aggregates attached to the plasma membrane and did not coincide with endogenous plasma membrane MHC-II (*Figure 4.8C*). To find out whether T cell exosomes are fused or only adhered to the APC plasma membrane, we treated the Raji cells with trypsin. Trypsin treatment did not decrease the GFP signal acquired by SEE-loaded Raji cells from conjugated J77-CD63-GFP, indicating that exosomes transferred upon immune synapsis can fuse with the APC plasma membrane or be internalized (*Figure 4.8D*). In contrast, trypsin decreased the fluorescence signal of Raji cells that acquired CD63-GFP by non-synaptic uptake (*Figure 4.8D*). These results suggest that the IS might not only promote the secretion of exosomes from T cell to APC, but might also induce the fusion of these exosomes with the plasma membrane of the recipient cell.

4.1.4 The immune synapse promotes the transfer of exosomal microRNA

To demonstrate delivery of exosomal miRNA from T cell to APC after IS formation, we stably over-expressed miR-335 in J77-CD63-GFP T cells (*Figure 4.9A*). This miRNA is not

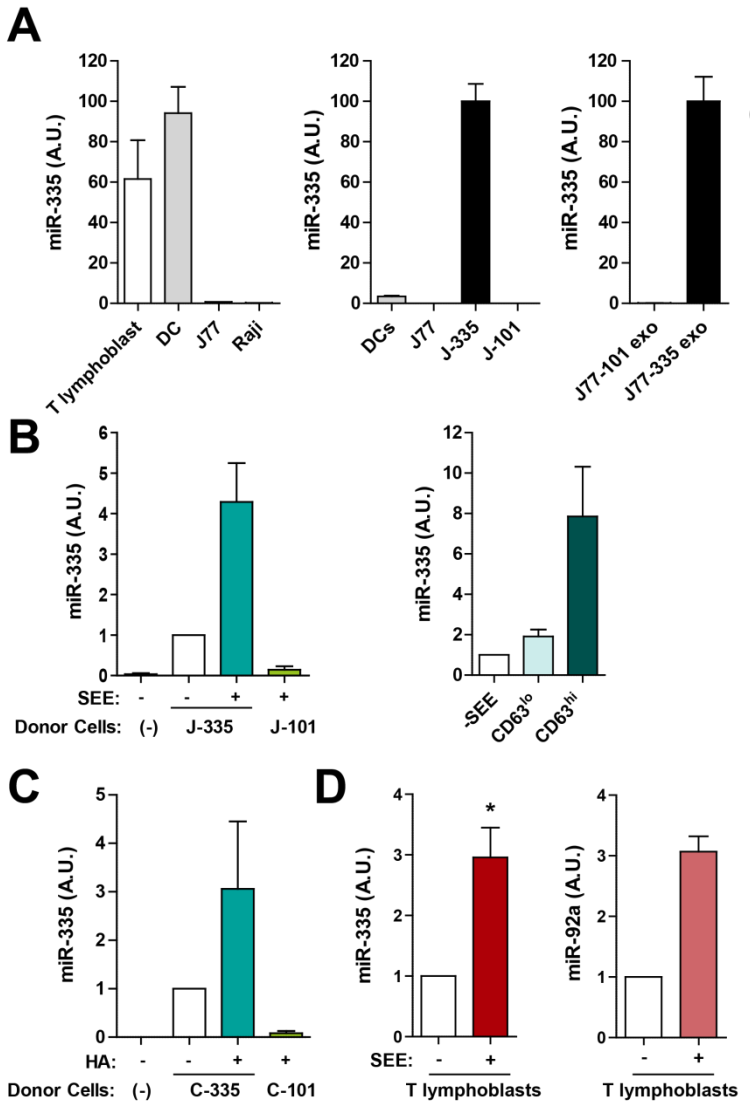

Figure 4.9 Exosomal miRNA-335 is transferred from T cell to APC in an Ag-specific manner **(A)** Levels of miR-335 were assessed by quantitative RT-PCR in primary dendritic cells and T lymphoblasts, and in Raji and J77 cells. J77-CD63-GFP cells were stably transduced with miR-335 (J-335 cells) or miR-101 (J-101 cells), and miR-335 levels were determined by qRT-PCR in cells and derived exosomes. **(B)** miR-335 levels in SEE-primed Raji cells sorted 24 h after conjugation with J-335 cells. J-101 were used as control donor cells. *Left panel,* Data are representative of seven independent experiments (mean and s.e.m), p=0.014 (one sample t test). *Right panel*, Raji cells that had acquired respectively low and high levels of C63GFP were sorted. n=5 independent experiments; p=0.04 (one sample t test); error bars represent s.e.m. **(C)** miR-335 levels in HA-primed HOM-2 cells sorted 24 h after conjugation with CH7C17 cells overexpressing miR-335 (C-335). CH7C17 cells overexpressing miR-101 (C-101) were used as control donor cells. Data are representative of five experiments (mean and s.e.m.). **(D)** miR-335 and miR-92a levels in SEE-primed Raji cells sorted 24h after conjugation with primary T lymphoblasts expressing miR-335 and miR-92a endogenously. Data are representative of three experiments (mean and s.e.m.), p=0.026 (one sample t test) A.U., Arbitrary Units.

normally expressed in the donor (J77) or recipient (Raji) cells, but is sorted to the exosomes of primary immune cells (DCs and T lymphoblasts) (*Figure 4.9A*, *Figure 4.2C*, *Annex Table 9.2*). J77-CD63-GFP cells expressing miR-335 (J-335) were co-cultured with unprimed or SEE-primed Raji B cells (stained blue with CMAC), and after 24h the Raji

cells were sorted by flow cytometry and their miR-335 content analyzed by RT-PCR. miR-335 was transferred to Raji cells only in the presence of SEE (*Figure 4.9B*). Raji cells that acquired high amounts of CD63-GFP contained correspondingly high amounts of miR-335, demonstrating correlation between the transfer of miR-335 and exosomal proteins (*Figure 4.9B*). To demonstrate that miR-335 is not expressed *de novo* in Raji cells after IS formation, we repeated the experiment with J77-CD63-GFP cells stably over-expressing miR-101 (J-101); conjugation with these cells did not induce expression of miR-335 in Raji cells (*Figure 4.9B*). The ability of a peptide antigen-specific IS to transfer miRNA was further demonstrated in CH7C17 cells overexpressing miR-335 (C-335) and conjugated to HA-loaded Hom-2 cells (*Figure 4.9C*), demonstrating antigen-specific directional transfer of exosomal miRNA from T cell to APC. We also investigated the transfer of endogenous miRNAs by primary SEE-specific T lymphocytes. These cells transferred endogenous miR-335 and miR-92 to Raji APCs in a SEE-specific manner (*Figure 4.9D*).

To confirm that microRNA transfer is mediated by exosomes, we blocked exosome production in J-335 cells. Ceramide, whose biosynthesis is regulated by neutral sphingomyelinase-2 (nSMase2), triggers the budding of exosomes into MVBs, and inhibition of nSMase2 therefore reduces the secretion of CD63-containing exosomes (Trajkovic et al., 2008) and miRNAs (Kosaka et al., 2010). Accordingly, the secretion of exosomes by J77 cells was impaired when nSMase2 activity was reduced either by addition of the inhibitor manumycin A (*Figure 4.10A*) or by shRNA silencing (*Figure 4.10B,C*). Targeting of nSMase2 activity inhibited the IS-dependent transfer of CD63-GFP (*Figure 4.10D,E*) and miRNA-335 (*Figure 4.10F,G*). Transfer of CD63-GFP and miR-335 was also blocked by brefeldin (*Figure 4.10D,F*), which inhibits the guanine nucleotide-exchange protein BIG2 and regulates the constitutive release of exosome-like vesicles (Islam et al., 2007). In contrast, transfer of CD63-GFP occurred normally from Hrs-interfered J77 cells (*Figure 4.10E,H*), in agreement with previous studies that demonstrated that the ESCRT system is unnecessary for the release of exosomes and microRNA (Kosaka et al., 2010; Trajkovic et al., 2008).

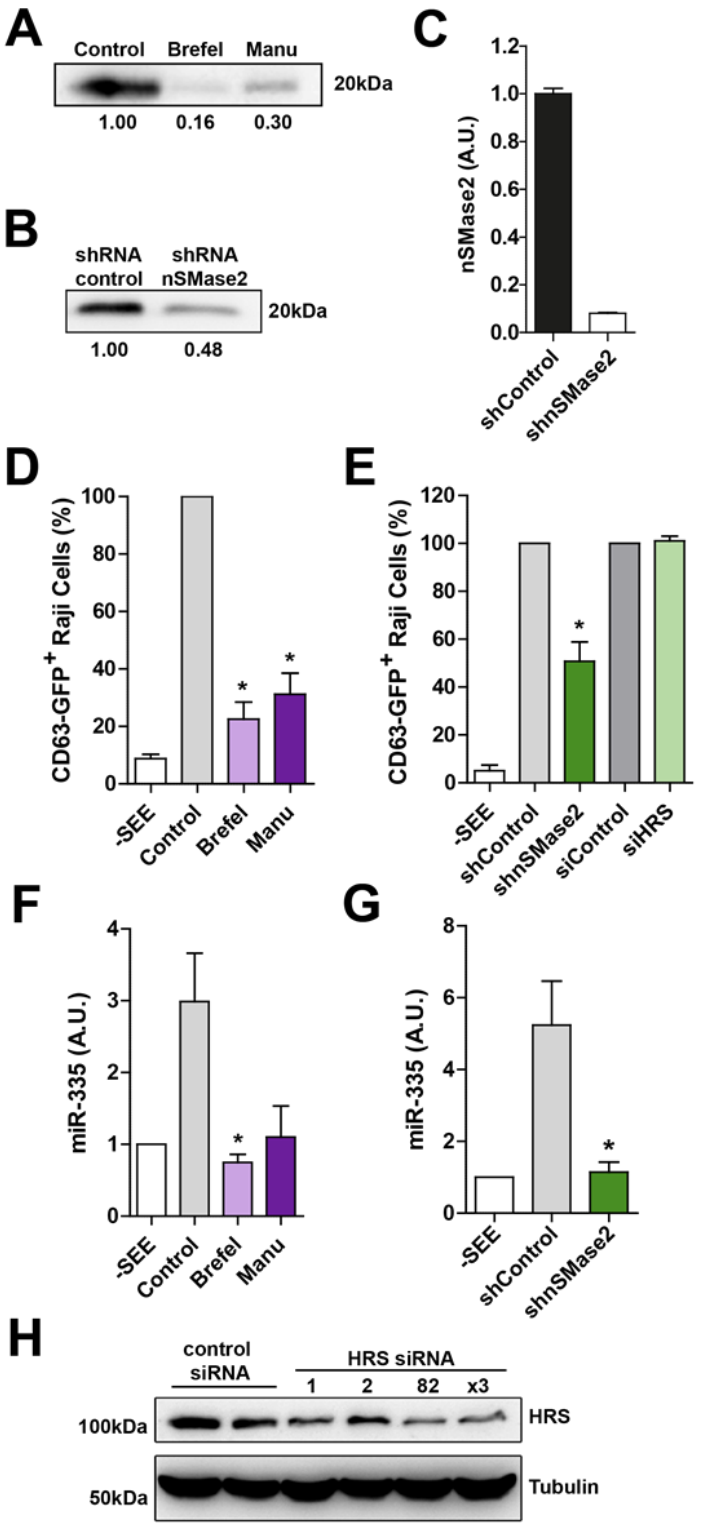

Figure 4.10 Inhibition of exosomes biogenesis impairs transfer of exosomal miRNAs and proteins through the IS

(A) J77 cells were cultured in exosome-depleted medium for 24 h, in the presence of inhibitors of nSMase2 (manumycin A, Manu) or BIG2 (brefeldin, Brefel). Purified exosomes secreted by equal numbers of control or treated cells were analyzed by immunoblotting for the presence of the exosome marker CD81. Densitometric analyses were performed, and the ratio between the treated and the control condition is shown. **(B)** CD81 immunoblot of exosomes purified from equal numbers of cells transduced with control or nSMase2 shRNA. Densitometric analyses were performed, and the ratio between the silenced and the control condition is shown. **(C)** TaqMan RT-PCR was performed to confirm the silencing of nSMAse2 mRNA on J-335 transduced with shnSMase2 or shControl. **(D)** FACS analysis of the CD63-GFP content of Raji recipients cells after conjugation with J-335 cells in the presence of manumycin or brefeldin. Data are the percentage ± s.e.m. of Raji-GFP positive recipient cells relative to the SEE-loaded control condition. n=5 independent experiments; $p \leq 0.001$ (one sample t test). **(E)** FACS analysis of the CD63-GFP content of Raji recipient cells after coculture with J77-CD63GFP cells expressing shnSMase2 or siHrs. Data are the percentage ± s.e.m. of Raji-GFP positive recipient cells relative to the SEE-loaded control condition. n=8 independent experiments, *, $p = 0.0005$ (one sample t-test). **(F)** RT-PCR analysis of miR-335 in Raji cells sorted after conjugation with J-335 cells in the presence of manumycin or brefeldin. n=3 independent experiments; *, $p = 0.03$ (unpaired t test) **(G)** qRT-PCR analysis of miR-335 in Raji cells sorted after conjugation with J-335 transduced with shnSMase 2 or shControl. n=4 independent experiments, * $p = 0.012$ (unpaired t test); error bars represent s.e.m.. **(H)** Control RNA duplex or different siRNA against Hrs were delivered by electroporation into J77-CD63GFP cells. The efficiency of the knock-down was demonstrated by Western blotting. Tubulin is shown as a loading control.

4.1.5 Transferred microRNAs regulate gene expression on the antigen presenting cell

To determine whether synaptically transferred miRNA-335 is functional in the recipient APC, we carried out luciferase reporter assays with full-length 3´UTR constructs of the miR-335 target SOX4 and the miR-335–insensitive UBE2F (Tavazoie et al., 2008). Raji cells transfected with luciferase constructs were cocultured with J-335 cells and luciferase activity was assessed. Expression from the SOX4 3´UTR was significantly reduced in SEE-primed Raji cells that had been in contact with J-335 cells, whereas expression from the

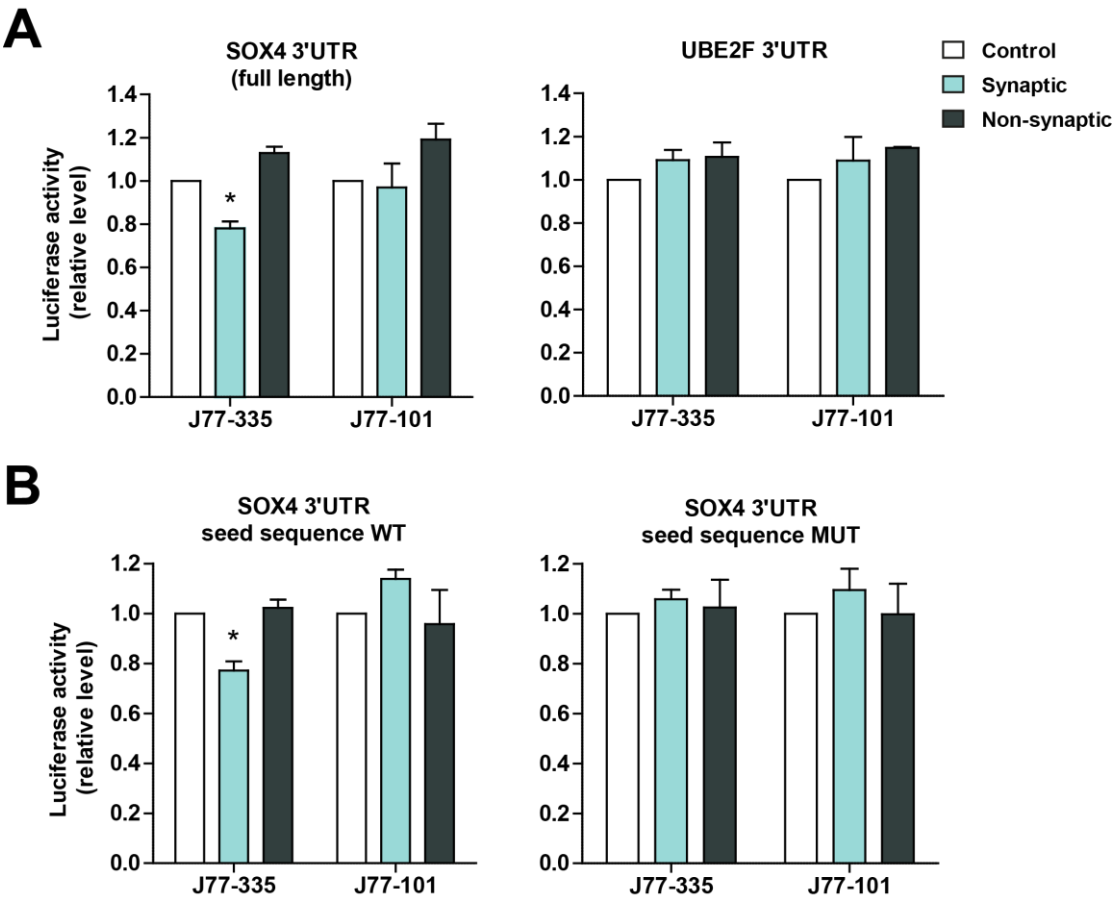

Figure 4.11 Synaptically transferred miR-335 down-regulates target gene expression in the APC
(A) Raji cells were transfected with reporter constructs consisting of the luciferase sequence placed upstream of the full length 3´UTR of either the miR-335 target gene SOX4 or the control gene UBE2F. Luciferase activity was assayed 24 h after coculture of SEE-loaded Raji with J77-miR-335 cells or control J-101 cells (synaptic transfer) or after addition of derived exosomes to SEE-loaded Raji cells (non-synaptic uptake). **(B)** Experiments as in (A) performed with Raji recipient cells expressing the wild-type of mutated seed sequence for miR-335 from the SOX4 3´UTR. Luciferase activities are shown relative to control incubations with untreated Raji cells. Data are means ± s.e.m.; n= 5 independent experiments, *p<0.05 (Newman-Keuls multiple comparison test).

UBE2F 3´UTR was unaffected (*Figure 4.11A*). Expression from these 3´UTR reporters was not affected by coculture of Raji cells with J-101 cells, indicating that the process is not a general effect of IS formation but rather involves the direct transfer of the specific miRNA. Reduction in luciferase activity after conjugate formation was also detected in Raji cells expressing base pairs 449-509 of the SOX4 3´UTR, which encompasses the miR-335 seed sequence; and inhibition of luciferase expression was abolished by mutation of this sequence (*Figure 4.11B*). The IS thus guides the transfer of functional miRNA from the T cell to the APC. Contrasting with IS-dependent miRNA transfer, addition of exosomes isolated from J-335 cells to transfected Raji cells had no effect on luciferase activity (*Figure 4.11A,B*), indicating that any miR-335 acquired in this way was non-functional.

4.2 Regulation of T cell miRNAs profile during activation

4.2.1 miRNA profile of CD4+ T cells after activation by different dendritic cells subsets.

To analyze the miRNA profile of CD4 T cells after cognate interactions with different types of APCs, we cocultured freshly isolated CD4 T cells from OT-II transgenic mice with *in vitro* derived conventional or plasmacytoid dendritic cells (cDCs or pDCs) in the presence or absence of ovalbumin (OVA) peptide. After 18 h of coculture we monitored the CD69 expression levels of the T cells (*Figure 4.12*) and subsequently we sorted them from the coculture by flow cytometry. As expected, activation was greater in the coculture with cDCs (*Figure 4.12A*) than with pDCs (*Figure 4.12B*) being the first one similar to the control of polyclonal activation with anti CD3 and anti CD28 (*Figure 4.12C*). Total RNA was then isolated and miRNA profile analyzed by Agilent microarray. We found 25 differentially expressed miRNAs (Log Fold Change < 0.5 or >-0.5 and adjusted p vale < 0.05) when we compared the presence or absence of antigen regardless the type of APC (*Figure 4.13A*). In T cells activated by cDCs-OVA we found 34 miRNAs differentially expressed being 21 of them coincident with the previous group (*Figure 4.13B*, in bold common ones). When we analyzed the changes in the case of pDCs-OVA we found only 10 miRNAs changing significantly (*Figure 4.13C*). However, when we compared the two types of activation, we detected only 1 miRNA specifically upregulated after the T cell

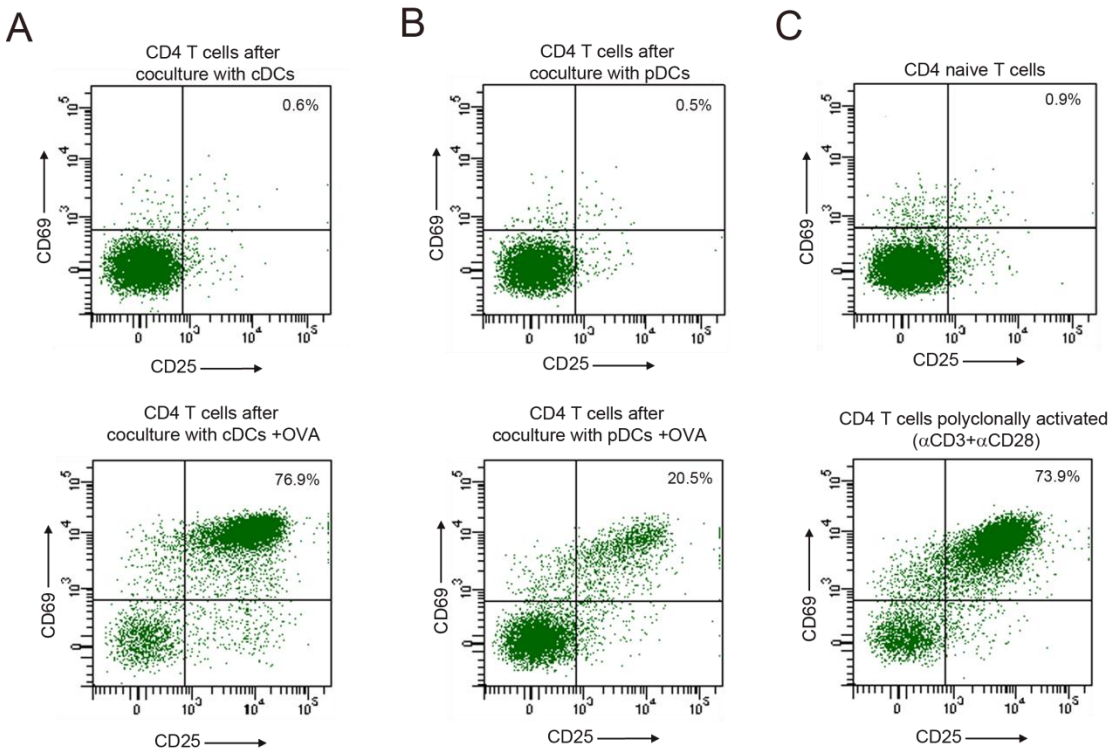

Figure 4.12 CD4 T cell activation after coculture with different DCs subsets
(A) CD4 T cells from OT-II mice were coculture with cDCs in the absence (upper panel) or presence (lower panel) of OVA peptide. CD4 T cells were gated and analyzed for the activation markers CD25 and CD69. **(B)** The same procedure was done with cocultures with pDCs in the absence (upper panel) or presence (lower panel) of OVA peptide. **(C)** CD4 T cells were analyzed in naïve conditions (upper panel) or after polyclonal stimulation with anti CD3 and anti CD28 antibodies (lower panel).

encounter with a cDCs as well as 5 miRNAs specific of the activation exerted by pDCs (*Figure 4.13D*). We next validated the microarray data by RT-qPCR for some of the miRNAs. miR-17, miR-18a and miR-132 were significantly upregulated in cDC mediated activation and also with pDC but in a lower extent (*Figure 4.14A*). miR-467b was significantly downregulated in cDC mediated activation. miR-26a and miR-150 show also a tendency of decrease both with cDCs and pDCs (*Figure 4.14B*).

Unfortunately, when we analyzed the miRNAs that appeared to be differentially expressed in microarray data between pDCs- or cDCs-driven activation, some of them were not even detectable by qPCR (miR-494, miR-188-5p, miR-1224, data not shown) or data were not reproduced (miR-680 *Figure 4.14D*). Only the specific upregulation miR-720 after cDC activation was detected although not in significant levels (*Figure 4.14C*).

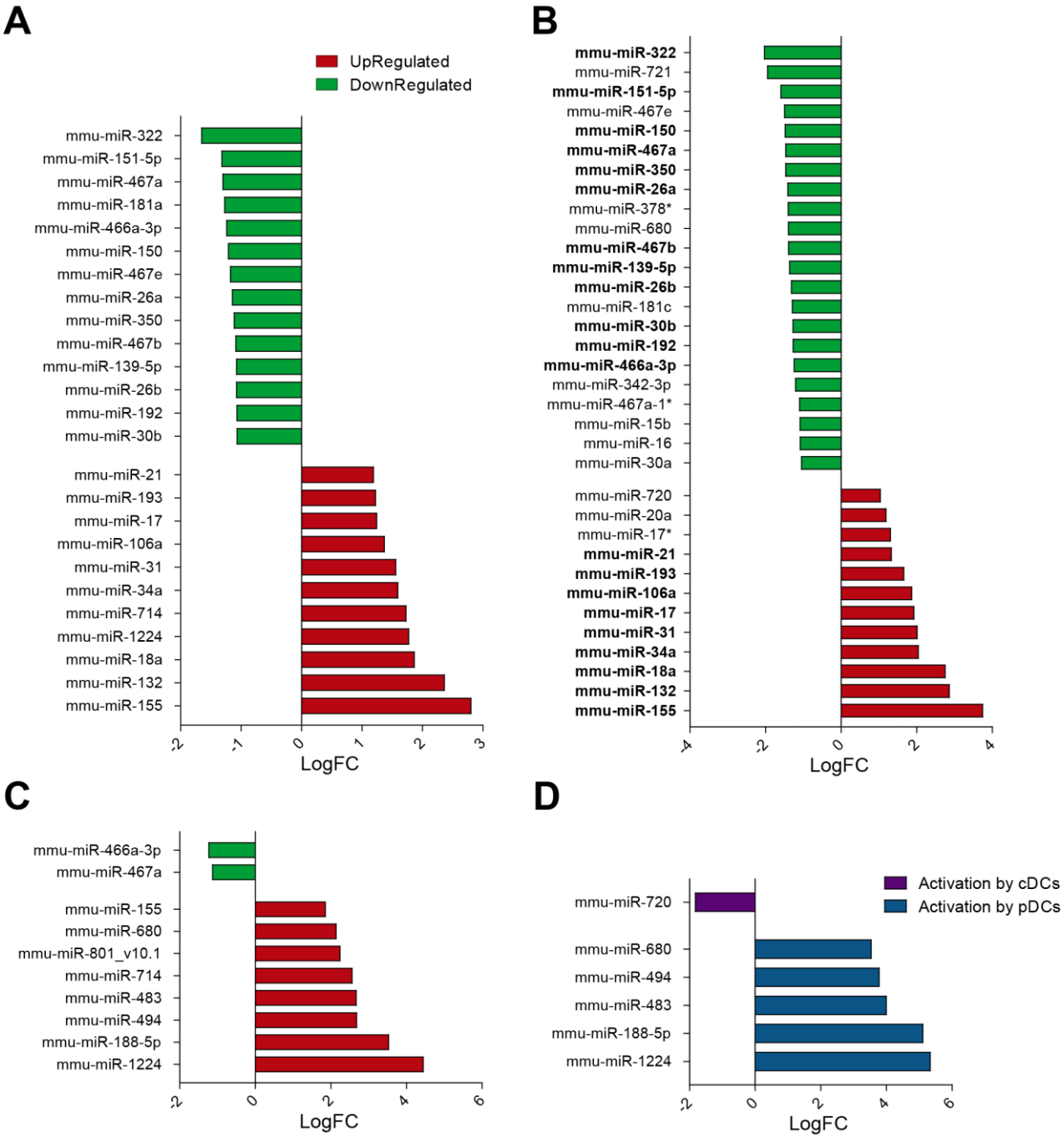

Figure 4.13 microRNA profile of CD4 T cells activated with different subsets of cDCs
CD4 T cells from OT-II mice were cocultured with either cDCs or pDCs in the presence or absence of OVA peptide and their microRNA analyzed by miRNA microarray. **(A)** Differential miRNA expression in the presence or absence of OVA peptide independently of the DC subset. **(B)** Comparison of miRNAs expression for specific stimulation by cDCs loaded or not with OVA peptide. **(C)** Same analysis for stimulation by pDCs without or with OVA. **(D)** Differentially expressed miRNAs for cDCs stimulation was compared to those for pDCs stimulation. miRNAs that were differentially upregulated in a significant level with each type of stimulation are represented.

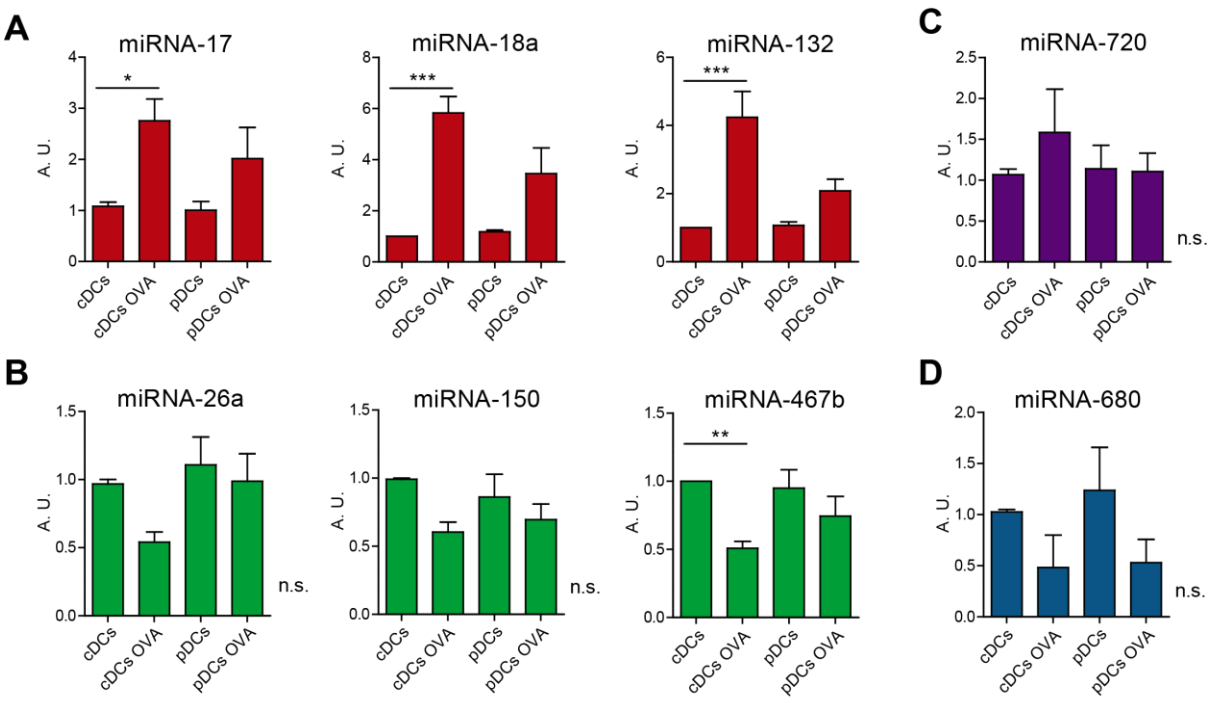

Figure 4.14 Several miRNAs are differentially expressed after CD4 T cells activation
Selected miRNAs detected by microarrays in *Figure 4.13* were validated by RT-qPCR. **(A)** miR-17, miR-18 and miR-132 were significantly upregulated after stimulation with cDCs-OVA. **(B)** miR-26a, miR-150 and miR-467b were downregulated after stimulation with cDCs-OVA although only miR-467b was significantly different by RT-qPCR analysis. **(C)** miR-720 was specifically upregulated with cDC stimulation but not in a significant level. pDCs stimulation did not change miR-720 level in concordance with microarray analysis **(D)** miR-680 levels by RT-qPCR were lower for both cDC-OVA and pDC-OVA although not in significant level, contrasting with microarray data. RNU1A1 and RNU5G were used as endogenous controls. A. U.: arbitrary units (n=8). ***P<0.001; **P<0.05; ns, non-significant.

The expression of the identified miRNAs was also assessed in CD4 T cell activation upon treatment with concanavalin-A (ConA) followed by expansion with recombinant interleukin 2 (IL-2). A clear upregulation of miR-17, miR-18 and miR-132 was detected. The three miRNAs showed the higher levels at 24h post stimulation but for miR-132 basal levels were recovered after around 4 d while miR-17 and miR-18 still maintain high levels after 8 d (*Figure 4.15A*). We observed similar behavior for the downregulated miRNAs. miR-26a and miR-150 decreased sharply their levels only 24h post stimulation being the lowest after 3 d and maintained until 8 d. However, miR-467b was only slightly decreased after 3 d and its levels were not consistent through time (*Figure 4.15B*). Finally, in the case of miR-720, there was only a very slight increase with this type of activation only after 3 d of stimulation (*Figure 4.15C*). Overall, these data indicate that there is a specific profile of

miRNAs regulated after T cell activation that changes depending on the APC that is stimulating the T cell. As expected, the profile of miRNAs that change after cDC exerted activation is more similar to that of the ConA activation that is a strong signal for T cell stimulation.

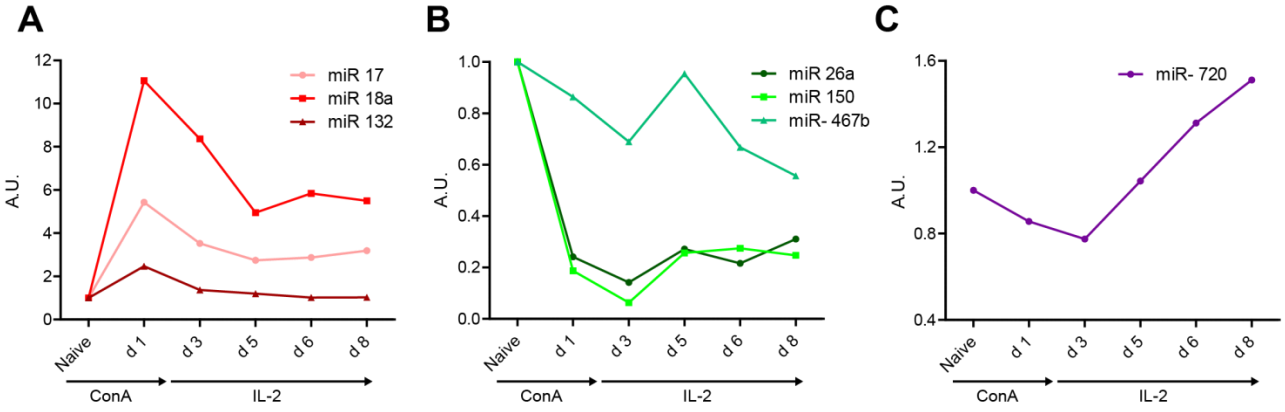

Figure 4.15 miRNAs regulation during time upon T cell activation
miRNA levels were assessed by RT-qPCR in freshly isolated mouse naive CD4 T cells in different time points of activation with ConA followed by IL-2. **(A)** Upregulated miRNAs kinetics: miR-17, miR-18 and miR-132. **(B)** Downregulated miRNAs kinetics: miR-26a, miR-150 and miR-467b. **(C)** miR-720 regulation during time. miRNA levels were normalized to RNU1A1 and RNU5G and are presented in arbitrary units (n=2).

4.2.2 Common predicted targets of miRNAs upregulated upon CD4 T cell activation

There are different tools available that predict *in silico* the mRNA targets of a given miRNA, but unfortunately due to the intrinsic difficulty of the prediction none of them is perfect. Thus, to improve the prediction we used a program that combines several prediction tools as well as databases for experimentally validated targets (Tabas-Madrid et al., 2014), to identify the possible common mRNA targets of the miRNAs that were down- or up-regulated after T cell activation. Signaling pathways where the target genes are implicated were studied with Ingenuity Pathway Analysis (IPA) tool. Interestingly, genes regulated by the miRNAs upregulated after T cell activation were related to immune response. The most represented ones are presented in *Figure 4.16*. We focus our attention on those mRNA targets that have the higher number of predicted miRNAs modulating them and specifically those interactions that have not been experimentally

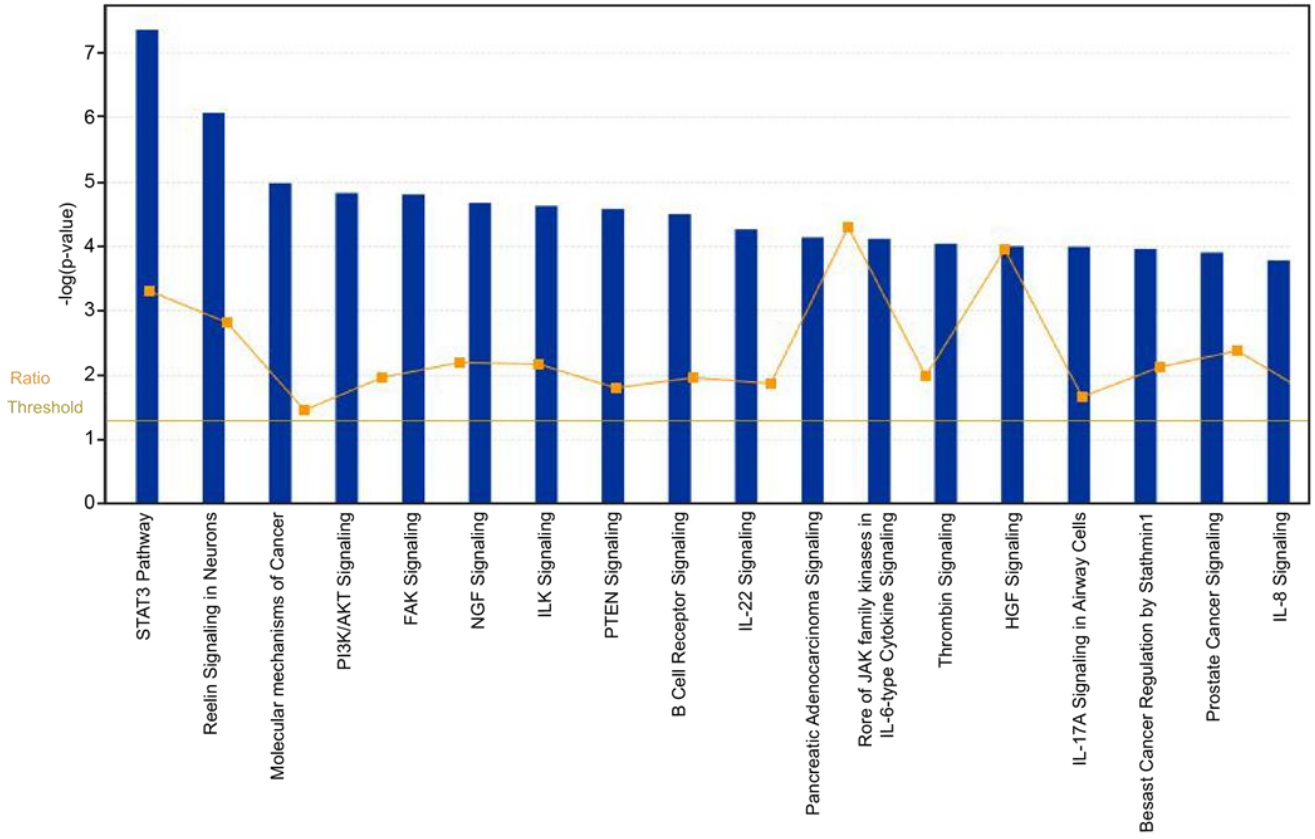

Figure 4.16 Signaling Pathways of upregulated miRNAs Targets
Genes regulated by 7 or more upregulated miRNAs during T cell activation were analyzed with Ingenuity Pathway Analysis to find common pathways of these targets. Those pathways with higher score are shown.

validated yet. Some of these genes are shown in *Table 4.1* with the combined prediction score of our prediction tool.

4.2.3 PIK3R1 is a target of the miRNAs upregulated during T cell activation

Pik3r1 (Phosphoinositide-3-Kinase, Regulatory Subunit 1 Alpha) gene encodes p50a, p55a and p85a, regulatory subunits of PI3Kinase that provide at least three functions to the catalytic subunits p110; stabilization, inactivation of kinase activity in the basal state and recruitment to pTyr residues in receptors and adaptor molecules. The engagement of the p85 SH2 domains by pTyr relieves the p85-mediated inhibition of the catalytic subunits and also brings them in contact with their lipid substrates in the membrane (Vanhaesebroeck et al., 2010). Thus, the proteins encoded by *pik3r1* are negative regulators of the PI3K signaling pathway which is one of the signaling pathways that arise from TCR and co-receptors engagement. Taking into account its described function, *pik3r1* gene

Gen	Number of miRNAs	Combined Prediction SCORE
Tnrc6b	12	0.8084745
Eif4g2	11	0.7353566
Tnrc6a	11	0.6859481
Sox5	11	0.6671118
Pik3r1	**11**	**0.6514733**
Tbc1d2b	11	0.5969837
Tbxas1	11	0.5769961
Syncrip	11	0.5662375
Gsk3b	11	0.5640294
Neo1	11	0.5611467
Zfp664	11	0.5451551
Rdx	11	0.5301558

Table 4.1 Targets of upregulated miRNAs in CD4 T cells
Prediction of the Targets of the miRNAs upregulated in CD4 T cells from OT-II Mice after stimulation with cDCs loaded with OVA peptide. Prediction was performed with a combinatorial method of different available prediction tools. Higher combined prediction score denotes more confidence in the prediction

specifically captured our interest among those predicted targets of the miRNAs upregulated after T cell activation. Indeed *pik3r1* was predicted to be inhibited by 11 of the 12 miRNAs upregulated in T cells after cognate interaction with cDCs (*Table 4.1*). The specific list of these miRNAs and their logFoldChange of naïve vs cDC-OVA stimulated CD4 T cells is presented in (*Table 4.2*).

We next studied the expression of the gene as well as some of the miRNAs predicted to target it during T cell activation. p85 and p50 proteins and mRNA levels of the two corresponding alternative transcripts of *pik3r1* were decreased during time in CD4 T cells stimulated with anti CD3 and anti CD28 for 7 d (*Figure 4.17A,B and C*). On the other hand miR-17-5p, miR-18a and miR-132 that are predicted to target pik3r1 were inversely regulated (*Figure 4.17D*). These data indicate that the negative regulator of PI3K, *pik3r1,* might be directly regulated by miRNAs during T cell activation.

miRNA	logFC	adjpv
mmu-miR-155-5p	3,746	0,003
mmu-miR-132-3p	2,865	0,031
mmu-miR-18a-5p	2,752	0,025
mmu-miR-34a-5p	2,041	0,012
mmu-miR-31-5p	2,012	0,042
mmu-miR-17-5p	1,928	0,008
mmu-miR-106a-5p	1,867	0,018
mmu-miR-193a-3p	1,661	0,018
mmu-miR-21a-5p	1,330	0,042
mmu-miR-17-3p	1,307	0,039
mmu-miR-20a-5p	1,190	0,031
mmu-miR-146a-5p	0,936	0,048

Table 4.2 miRNAs predicted to target pik3r1
A total of 11 out of the 12 miRNAs upregulated after CD4 T cell stimulation by cDC-OVA are predicted to be targeting pik3r1. The only miRNA not predicted to target is presented in gray.

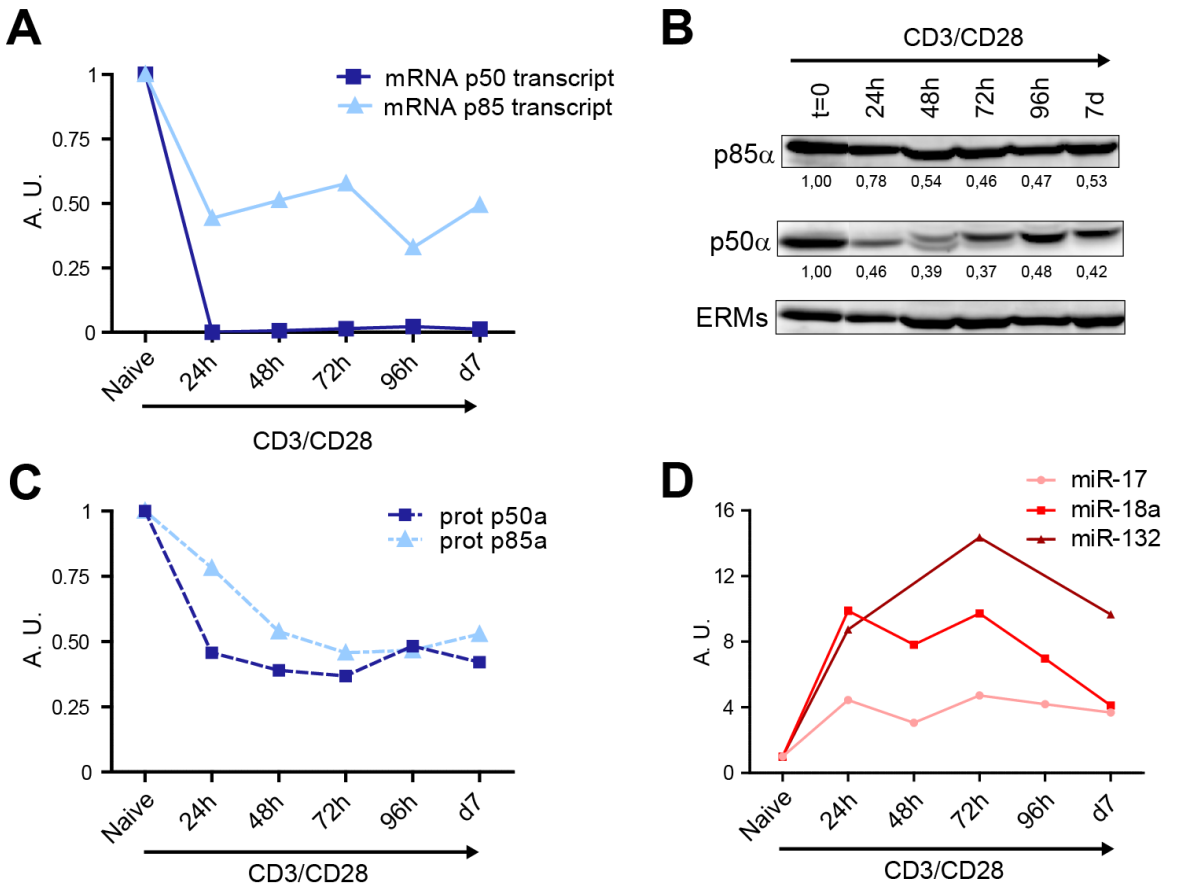

Figure 4.17 pik3r1 is downregulated during upon T cell activation
(A) mRNA relative levels of the two main transcripts of pik3r1 were measured by qPCR. Levels were normalized to Yhwaz and β-actin housekeeping genes (n=2). **(B)** Western blot analysis of p85α and p50α protein content in CD4 T cells after activation with anti-CD3 plus anti-CD28. Representative Immunoblots (n=3). ERMs were included as a loading control. **(C)** Protein levels of p85 and p50 in B normalized to ERMs. **(D)** miRNA levels in CD4 T cells after activation with anti-CD3 plus anti-CD28. Levels are normalized to RNU1A1 and RNU5G and presented in arbitrary units (n=2).

4.2.4 miR-132 targets pik3r1

Next, the predicted site sequences of miRNA binding were studied on the 3'UTR of *pik3r1* (*Table 4.3*) with a combination of prediction programs. Apart from canonical sites two unusual sites were also predicted in 3'UTR of *pik3r1*. We decided to study in depth the interaction between miR-132-3p with *pik3r1* because it has two different predicted binding sites and its role in the context of T cell activation has not been well analyzed. With this purpose, we cloned into luciferase reporter vectors two regions of the 3'UTR of *pik3r1* containing the two predicted target sites for miR-132-3p. For Site 1 we cloned the fragment from 71 to 362 bp and for Site 2 we cloned from 2957 to 3162 bp of 3'UTR.

(*Figure 4.18A*). We co-transfected into HEK cells the reporter plasmids either with a control plasmid or a plasmid for the overexpression of miR-132-3p. GFP positive cells were subsequently sorted by flow cytometry to analyze only cells transfected with the miRNA overexpression plasmid or the control. miRNA-132 levels were also assessed by RTqPCR (*Figure 4.18B*). Cells were then lysed and luciferase levels analyzed. Both sites resulted to be targeted by miR-132 since luciferase levels were significantly lower when cells were co-transfected with miR-132 plasmid compared to the control plasmid (*Figure 4.18C*). Thus our data experimentally demonstrate for the first time the inhibition of *pik3r1* by miR-132-3p.

Canonical sites

miRNA	Start	End	Seedmatch Sequence	Seedmatch type	3' pairing	# sites	Prediction Programs
mmu-miR-106a-5p	1377	1383	GCACTTT	7mer-m8	-	1	targetscan,miranda,findtar
mmu-miR-132-3p	**3082**	**3088**	**GACTGTT**	**7mer-m8**	**-**	**2**	targetscan,miranda,findtar
mmu-miR-132-3p	**175**	**181**	**GACTGTT**	**7mer-m8**	**-**		targetscan,miranda,findtar
mmu-miR-146a-5p	3359	3365	GTTCTCA	7mer-m8	13-17	1	targetscan,rnahybrid,findtar
mmu-miR-17-5p	1377	1383	GCACTTT	7mer-m8	-	1	targetscan,miranda,findtar
mmu-miR-20a-5p	1377	1383	GCACTTT	7mer-m8	-	1	targetscan,miranda,findtar
mmu-miR-21a-5p	2400	2406	TAAGCTA	7mer-m8	-	3	targetscan,findtar
mmu-miR-21a-5p	904	910	ATAAGCT	7mer-m8	-		targetscan,miranda,findtar
mmu-miR-21a-5p	2937	2943	TAAGCTA	7mer-m8	-		targetscan,findtar
mmu-miR-34a-5p	2299	2305	ACTGCCA	7mer-m8	-	1	targetscan,findtar

Unusual sites

miRNA	Start	End	Seedmatch Sequence				
mmu-miR-21a-5p	1154	1162	TGATAAGCT				
mmu-miR-155-5p	1442	1465	AGTTTGGTAGTCAT TAGCAATTAA				

Table 4.3 pik3r1 3'UTR miRNA binding sites sequences
The predicted binding sites for upregulated miRNAs at 3'UTR of pik3r1 mRNA were analyzed with a prediction tool that combines different prediction programs currently available. Seedmach type, sequence and location as well as the specific programs that predict this binding are shown for each interaction.

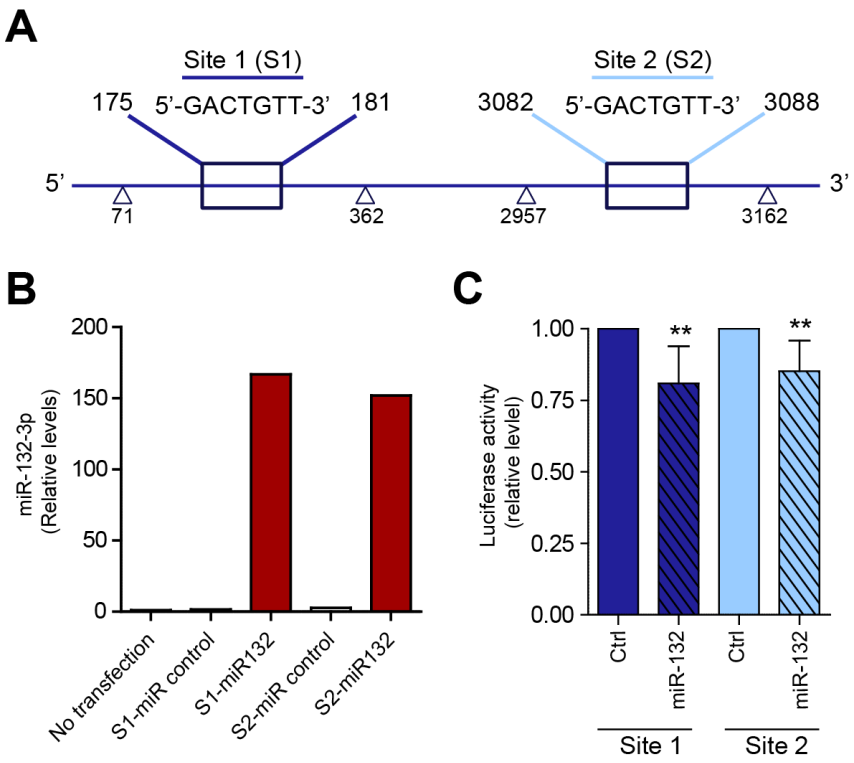

Figure 4.18 miR-132-3p targets pik3r1
(A) 3'UTR of pik3r1 cloning strategy. Fragments from 71 to 362 bp and from 2957 to 3162 bp containing the two binding sites predicted for miR-132-3p were cloned into the psiCheck2 vector. **(B)** miR-132-3p levels in HEK cells after transfection. Levels were normalized to RNU1A1 and RNU5G and presented in arbitrary units. **(C)** HEK cells were transfected with indicated plasmids, GFP+ cells sorted and Renilla and Firefly luciferase signal measured. Data are presented in Renilla Luciferase signal relative to Firefly (n=5). T test **P<0.05.

4.3 3' Nucleotide Additions to Mature miRNA control their turnover during T cell activation

4.3.1 TUT4 is downregulated during T cell activation

To investigate the molecular mechanism underlying the post-transcriptional modification of miRNAs during T cell activation, we studied the regulation of terminal uridyl transferases (TUTases) during this process. The mRNA transcript levels of TUTases 1,2,3,4,5 and 7 in CD4 T cells were determined before and after polyclonal stimulation with anti-CD3 and anti-CD28 antibodies for 48h. TUT4 and TUT7, the two enzymes predominately responsible for uridylation, were decreased upon T cell activation, whereas TUT1 and TUT5 were upregulated, and TUT2 and TUT3 were unaltered (*Figure 4.19A*). Reduction of TUT4 mRNA levels was confirmed in human T cell blasts stimulated polyclonally (*Figure 4.19B*) and in antigen-specific experiments in which CD4 T cells from transgenic OT-II mice were cocultured with bone marrow-derived dendritic cells loaded with OVA peptide (*Figure 4.19C*). We detected a very transient upregulation of TUT4

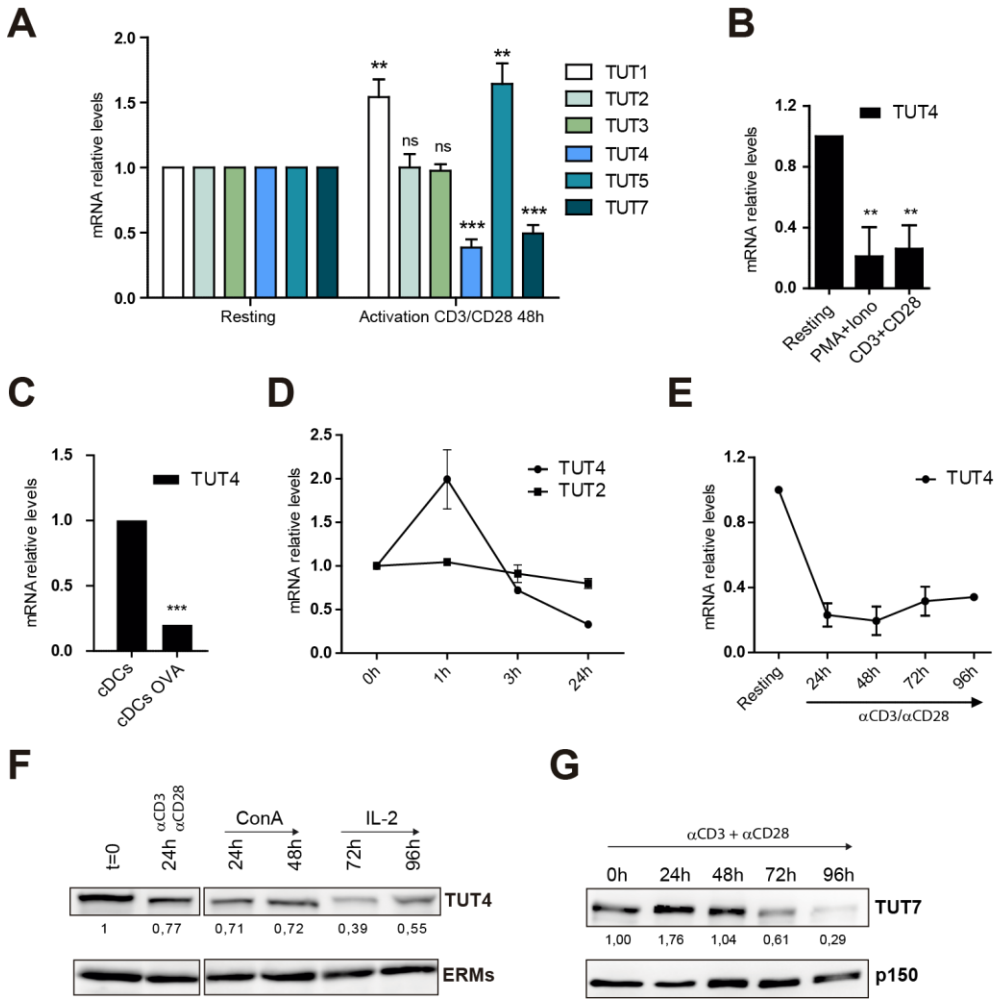

Figure 4.19 TUT4 expression is downregulated after T cell activation
(A) RNA levels of TUT1,2,3,4,5 and 7 assessed by RT-qPCR in freshly isolated mouse naive CD4 T cells or cells activated with anti-CD3 and anti-CD28 for 48 h. mRNA levels were normalized to β-actin and Yhwaz housekeeping genes and are presented in arbitrary units (n=7). **(B)** TUT4 mRNA levels in human T lymphoblasts measured by RT-qPCR after two different activation stimuli: PMA with Ionomycin and anti-CD3 plus anti-CD28 (n=3). **(C)** Mouse naive CD4 T cells from OT-II mice specific to OVA peptide were cocultured with cDCs in the absence or presence of the peptide. TUT4 mRNA levels were determined by RT-qPCR as in (A) (n=5). **(D)** Early time course of TUT4 mRNA levels quantified by RT-qPCR in activated mouse CD4 T cells (n=3). **(E)** Long-term time course of TUT4 mRNA levels in activated mouse CD4 T cells (n=3). **(F)** Western blot analysis of TUT4 protein content in CD4 T cells after activation with anti-CD3 plus anti-CD28 or with concanavalin A followed by expansion with interleukin 2. Representative Immunoblots (n=3). ERMs were included as a loading control. **(G)** Western blot analysis of TUT7 protein at different time points after antibody activation of CD4 T cells. Representative Immunoblots (n=3). p150 was included as a loading control. Numbers below blots show normalized densitometry values relative to naive T cells. Error bars in A-C represent standard deviation; ***P<0.001; **P<0.05; ns, non-significant.

mRNA at 1h after stimulation (*Figure 4.19D*), but TUT4 mRNA levels decreased over the subsequent 24h and remained low at 96h (*Figure 4.19E*). Western blot analysis of TUT4 protein showed a decrease at 24h after activation with anti-CD3 and anti-CD28 antibodies and upon treatment with concanavalin-A followed by expansion with recombinant interleukin 2 (*Figure 4.19F*). TUT7 protein content was also downmodulated after stimulation with CD3 and CD28 antibodies, albeit delayed compared with TUT4 (*Figure 4.19G*). Immunofluorescence and subcellular fractionation experiments showed a predominant cytoplasmic confinement of TUT4, and T cell activation did not provoke any significant subcellular redistribution (*Figure 4.20A and B*). These data indicate a clear downregulation of TUT4 and TUT7, the TUTases implicated in miRNA uridylation, upon T cell activation.

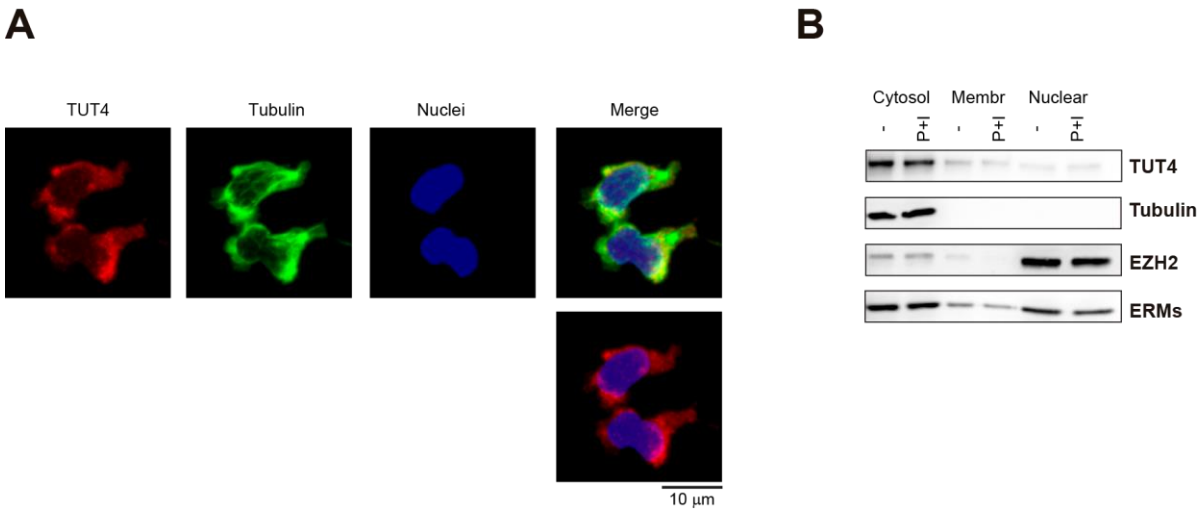

Figure 4.20 Subcellular localization of TUT4
(A) Subcellular localization of TUT4 was assessed by immunofluorescence in mouse blast T cells. Cells were fixed and stained for TUT4 (red) and tubulin (green), and nuclei were stained with DAPI (blue). Plates show maximal projections of confocal images. **(B)** Western blot analysis of subcellular fractions of resting and activated human T cells. Cells were activated with phorbol myristate acetate and ionomycin (P+I). TUT4 protein content is shown for each fraction, together with tubulin (cytosolic protein), EZH2(nuclear protein) and ERMs (submembranous proteins)

4.3.2 T cell activation alters the profile of miRNA 3′ non-templated nucleotide additions

To assess the dynamics of isomiR generation during T cell activation, we performed a deep sequencing analysis on small RNAs from mouse CD4+ T cells in naive conditions (CD25-, CD62L+) and upon stimulation with anti-CD3 and anti-CD28 antibodies. The

homogeneity of replicates for each condition was confirmed by their proximity on the principal components analysis (PCA) (*Figure 4.21A*). T cell activation was confirmed by staining of the activation markers CD25 and CD69 (*Figure 4.21B*) and by the analysis of canonical (unmodified) miRNAs that are modulated upon T cell activation, which showed clear upregulation of miR-155-5p and members of the miR-17~92 cluster (miR-17-5p, miR-18a-5p, miR-19a-3p and miR-20a-5p), whereas miR-150-5p and miR-26a-2-5p were

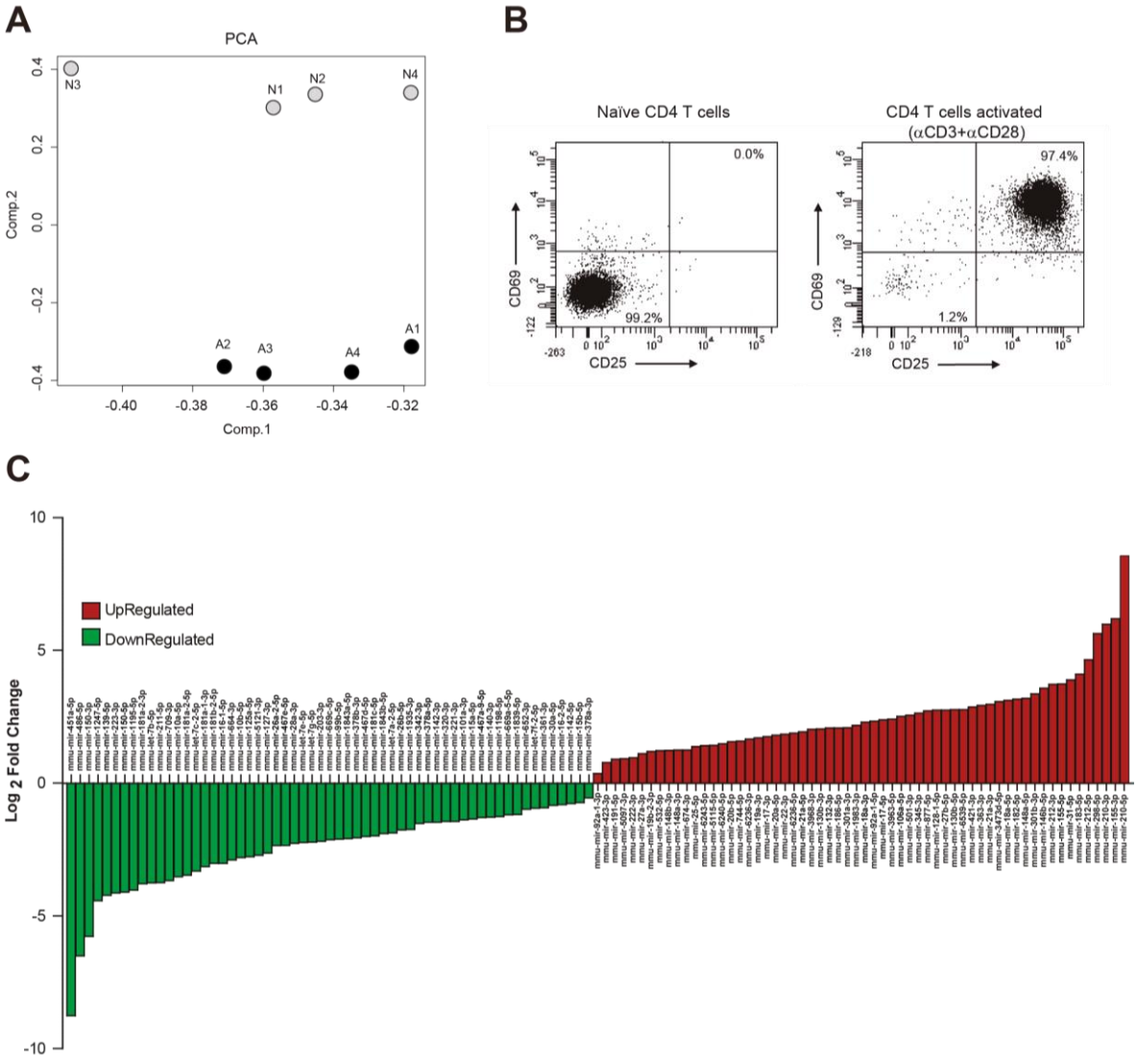

Figure 4.21 Small RNA deep sequencing analysis of naive and activated CD4 T cells
(A) Principal component analysis of the eight libraries in the experiment. Naïve (N); Activated (A). **(B)** Activation markers CD25 and CD69 were analyzed in naive and activated CD4 T cells by flow cytometry. **(C)** Canonical miRNA analysis. Statistically significant data are presented (fold change >0.5 or <-0.5; adjusted p value <0.05). Negative fold change corresponds to downregulated miRNAs (green) and positive fold change corresponds to upregulated miRNAs (red).

downregulated (*Figure 4.21C*). These data are also in accordance with previous microarray data mention above in in section *4.2.1* (*Figure 4.13D*). Moreover a global downregulation of miRNA was detected in our deep sequencing data when miRNA count distributions were analyzed with Kolmogorov Smirnoff test, P <= 1e-4).

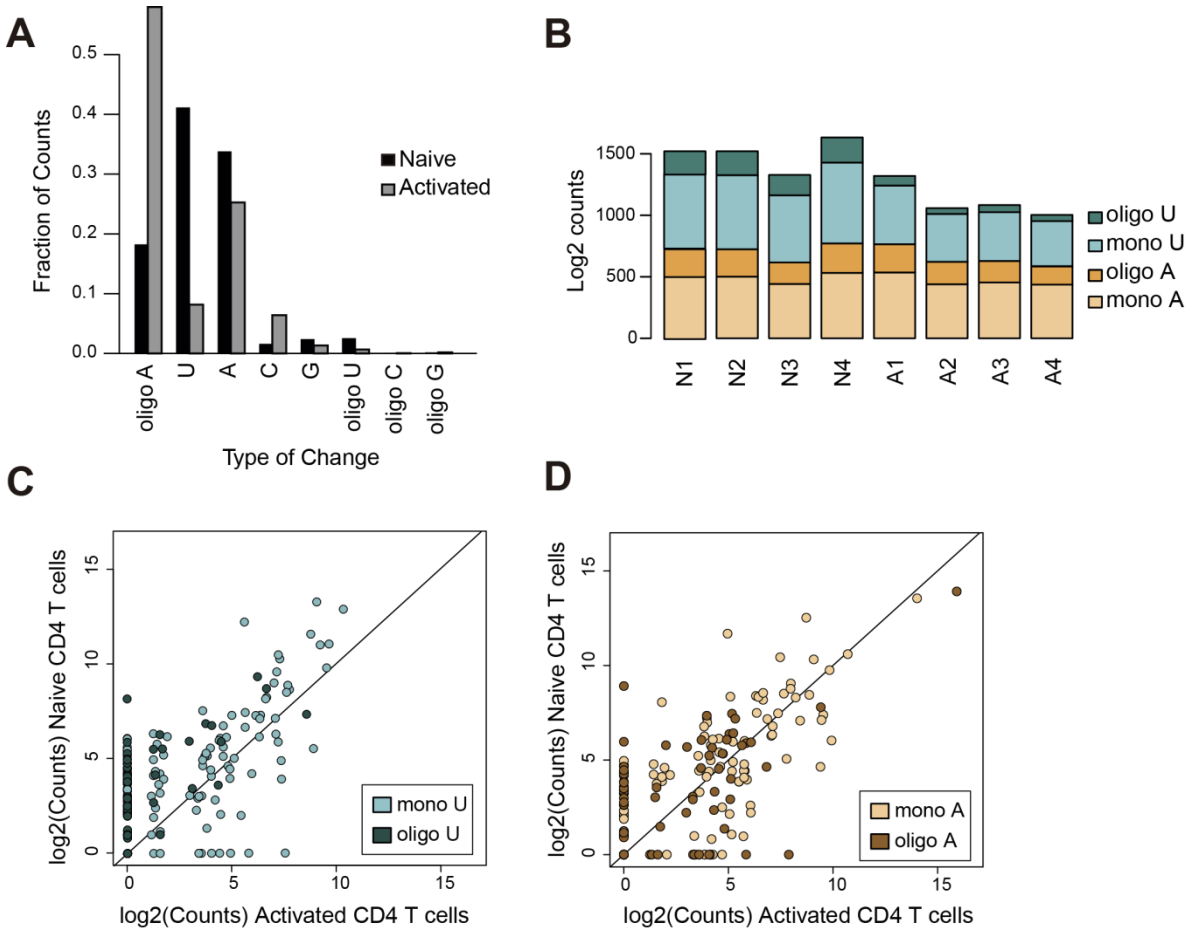

Figure 4.22 The miRNA 3′ non-templated nucleotide addition (3′NTA) profile changes during T cell activation

Deep sequencing libraries were generated from naive CD4 T cells or cells activated for 48h with anti-CD3 and anti-CD28 (n=4). **(A)** 3′ NTAs to all mature miRNAs are represented as the fraction of total counts (normalized) per mature miRNA in resting and activation conditions. **(B)** Total normalized counts of uridylated and adenylated miRNAs for the eight libraries examined (N: naive; A: activated CD3/CD28). **(C, D)** Comparison of the relative abundance of 3′ mono-uridine and oligo-uridines **(C)** and of 3′ mono-adenine or oligo-adenines **(D)** in individual miRNAs from naive and activated CD4 T cells.

MiRNA modifications were classified as mono addition (one nucleotide) or oligo addition (two or more nucleotides). Uridylation and adenylation were identified as the most common modifications of miRNAs in CD4 T cells (*Figure 4.22 A*). A clear reduction of

miRNA uridylation, both mono and oligo additions, was observed in activated T cells, both when the data were analyzed globally (*Figure 4.22B*) and when examining each miRNA individually (*Figure 4.22C*). In contrast, adenylation remained unaltered after activation, both in the global (*Figure 4.22B*) and individual analysis (*Figure 4.22D*).

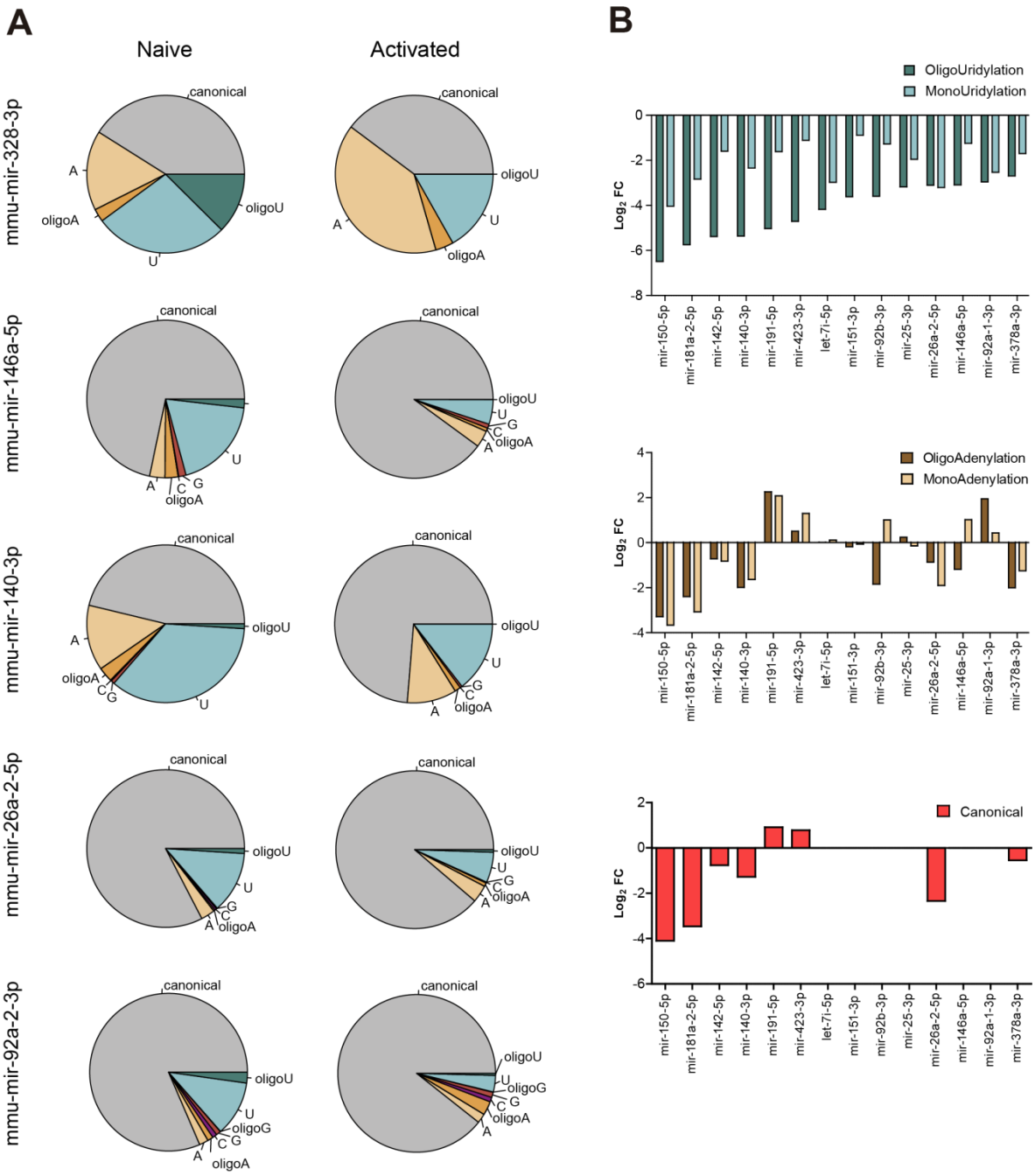

Figure 4.23 Uridylated miRNAs are decreased upon T cell activation
Individual miRNAs were analyzed for their 3′ end modifications by deep sequencing in naive and activated CD4 T cells. **(A)** Pie charts for selected miRNAs depict the fraction of counts for each type

of 3'NTA-modified and canonical miRNA dectected. A, adenine, C, cytosine, G, guanine and U, uracil. **(B)** A group of 14 miRNAs was selected from the set of uridylated miRNAs that decrease after T cell activation. Fold changes between the naive and activated state were calculated for the uridylated miRNAs (upper panel) and the corresponding adenylated miRNAs (middle panel) and canonical miRNA (lower panel). A negative log FC indicates downregulation after T cell activation.

Abundance profiles of isomiR forms of example miRNAs are shown in *Figure 4.23*. As mentioned above, all uridylated miRNAs decrease after T cell activation. For each of the selected miRNAs, *Figure 4.23A* depicts the fraction of counts corresponding to each 3'NTA and the canonical sequence, showing clear decreases in the percentages of the uridylated forms. The group of uridylated miRNAs that decreases after activation was selected and the log fold-changes in the abundance of each canonical and modified miRNA species between naive and activated conditions is shown in *Figure 4.23B*. This analysis shows that the reduction in uridylation (*Figure 4.23B* upper panel) does not correlate with alterations to the level of the corresponding canonical miRNA, which in many cases remained unchanged (*Figure 4.23B* lower panel). Moreover, the adenylated species corresponding to these miRNAs show a similar pattern of abundance changes to the canonical species, and thus do not appear to compensate the decrease in uridylation (*Figure 4.23B* middle panel). These data raise the conclusion that the regulation of uridylated miRNA levels is thus independent of the regulation of its canonical counterpart and of other 3'NTAs like adenylation.

4.3.3 Uridylation targets mature miRNA for activation-dependent degradation

Uridylation of mRNA is associated with its decay (Schmidt et al., 2011; Shen and Goodman, 2004) and a recent report shows that degradation of mRNA with shortened polyA-tails is promoted by 3' uridylation, mediated by TUT4 and TUT7 (Lim et al., 2014). To investigate whether uridylation targets mature miRNAs for degradation during T cell activation, we transfected naive CD4 T cells with synthetic RNAs corresponding to canonical or di-uridylated miRNA sequences. The cells were subsequently either activated with anti-CD3 and anti-CD28 or maintained in culture in the presence of IL-7 to prevent naive T cell apoptosis. Levels of the synthetic miRNAs were measured with a variation of miQPCR ((Benes et al., 2015) see materials and methods) that distinguishes single nucleotide changes in the miRNA sequence. Synthetic canonical miR-151 and miR-25 were stable upon T cell activation, whereas the levels of the di-uridylated forms

dropped sharply (*Figure 4.24*). These data indicate that miRNA uridine tailing is an important mechanism for targeting a specific set of miRNAs for degradation, and that this process is tightly regulated during T cell activation.

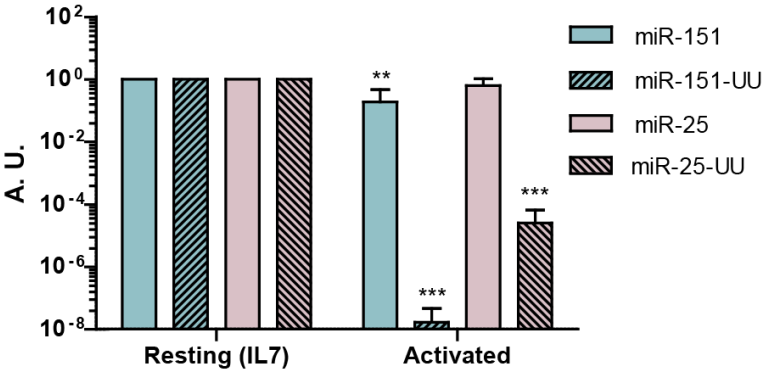

Figure 4.24 Uridylation promotes the decay of miRNAs during T cell activation
Synthetic miRNAs were nucleofected into naive CD4 T cells, which were then activated with anti CD3 and anti CD28 or left resting in the presence of IL7. Levels of the synthetic miRNAs were analyzed by a customized qPCR method (MiQPCR). Synthetic RNA levels were normalized to endogenous controls snoRNA 420 and snoRNA 412 and are presented in arbitrary units (n=3).

4.3.4 TUT4-dependent uridylation of mature microRNA

To assess the role of TUT4 in the uridylation of mature miRNAs in CD4 T lymphocytes we examined TUT4-deficient mice (Jones et al., 2012). TUT4-deficient mice showed no significant aberration in the percentage of CD4 and CD8 T lymphocytes in thymus, spleen or peripheral lymph nodes (*Figure 4.25A*), and TUT4-deficient CD4 T cells proliferated normally and could be activated to the same extent as wild type T cells (*Figure 4.25B and C*). Basal levels of miRNA mono- and oligo-uridylation were lower in naive TUT4-deficient CD4 T cells compared with wild type cells, as described for other tissues (Jones et al., 2012) (*Figure 4.26A and B*). Interestingly, miRNA mono- and oligo-adenylation were clearly higher in TUT4-deficient T cells. (*Figure 4.26C and D*). Previous reports indicate that TUT4 gene deficiency or knockdown does not modify the quantities of mature miRNAs in a variety of cellular contexts (Jones et al., 2012; Thornton et al., 2015). Accordingly, miR-seq data showed no significant differences in the levels of canonical miRNAs between TUT4-deficient and wild type CD4 T cells (data not shown), a finding validated for several mature miRNAs by qPCR (*Figure 4.27A*).

We next sought to identify the specific miRNA targets of TUT4 in T cells. We initially designated as "TUT4 targets" the miRNAs that were significantly less uridylated in TUT4-deficient CD4 T cells compared with wild type cells (*Figure 4.26A and B*). We considered

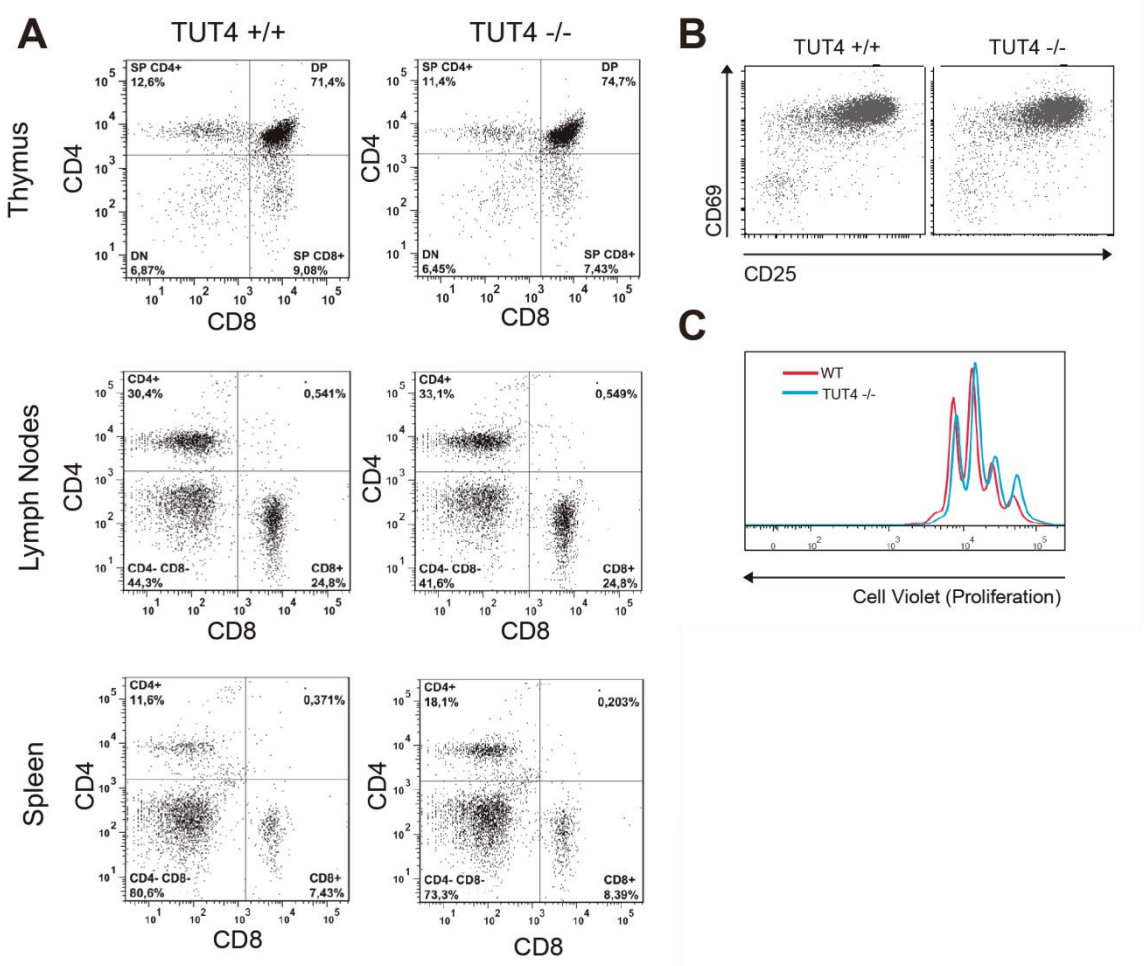

Figure 4.25 Analysis of TUT4-deficient lymphoid tissues and lymphocytes
(A) Flow cytometry analysis of CD4 and CD8 in lymphoid organs (thymus, spleen and lymph nodes) of wild type and TUT4-deficient mice. **(B)** Flow cytometry analysis of the activation markers CD69 and CD25 in CD4 T cells from wild type and TUT4-deficient mice 24h after stimulation with anti-CD3 and anti-CD28. **(C)** Proliferation of wild type and TUT4-deficient CD4 T cells. Cells were stained with cell violet and subsequently stimulated with anti-CD3 and anti-CD28. Cell violet staining was analyzed by flow cytometry after 72h.

both mono-uridylated and oligo-uridylated species as targets (*Annex Table 9.3A*), and miRNAs whose mono- and oligo-uridylated forms were both lower in TUT4-deficient CD4 T cells are listed in *Annex Table 9.3B*. Levels of the canonical miRNAs corresponding to these uridylated miRNAs were not modified in TUT4-deficient cells, as determined by miR-seq and RT qPCR analysis (*Figure 4.27A and B*). These data provide the first evidence that TUT4 controls the uridylation of mature miRNAs in T lymphocytes. Although uridylated miRNAs are clearly less abundant in TUT4-deficient CD4 T cells, we could still detect some miRNAs with 3' non-templated uridines. TUT4-deficient T cells showed no

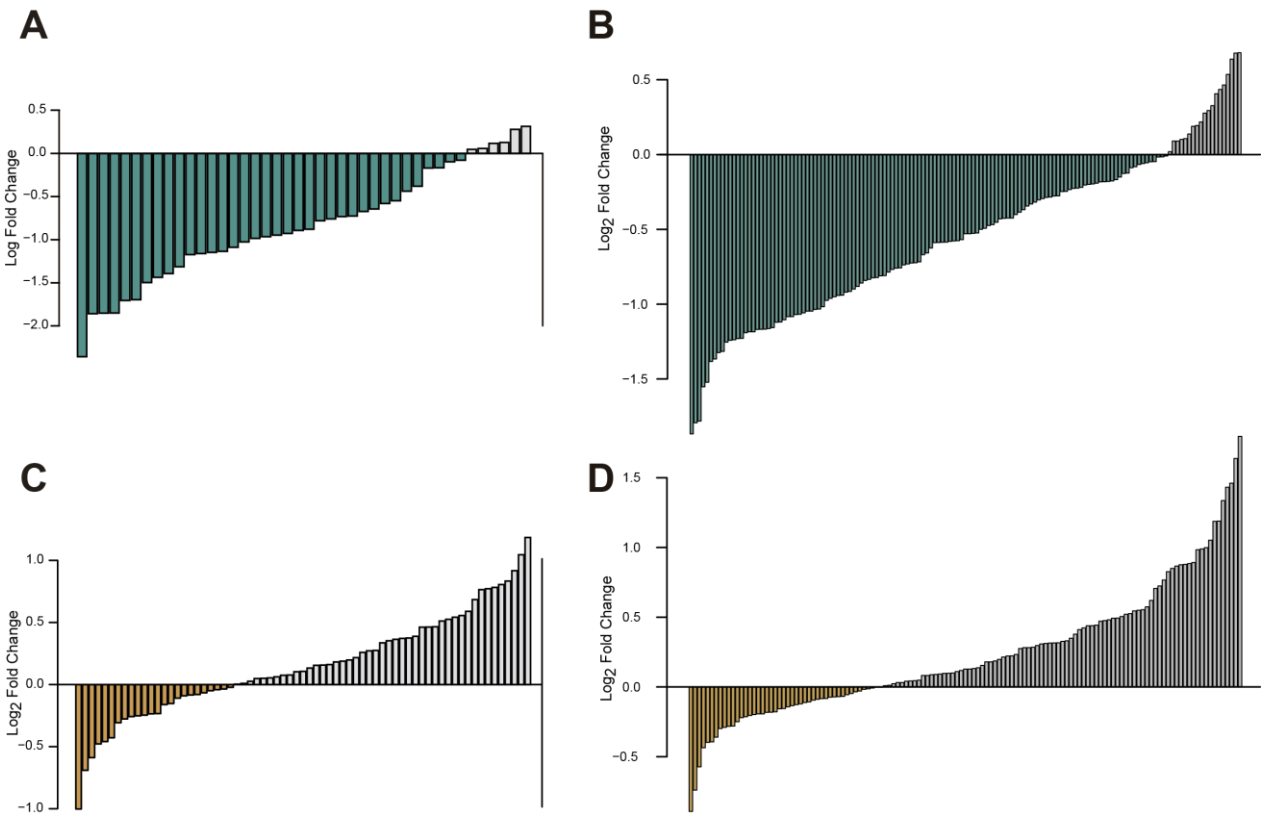

Figure 4.26 TUT4 dependent uridylation of mature microRNA
Small RNA from naive wild type or TUT4-deficient CD4 T cells was analyzed by deep sequencing. Fold changes between wild type and TUT4-/- CD4 T cells calculated for mono-uridylated **(A)**, oligo-uridylated **(B)**, mono-adenylated **(C)** and oligo-adenylated miRNAs **(D)**. A negative fold change indicates lower levels than in wild type.

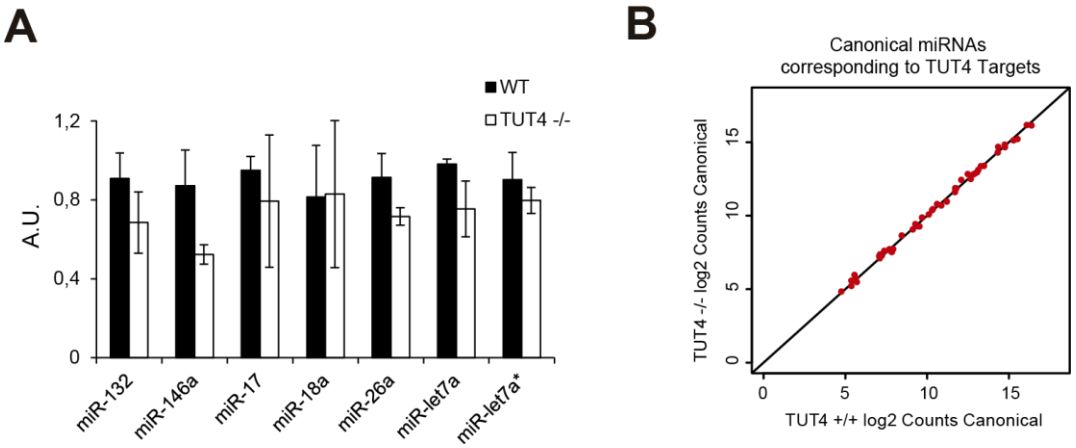

Figure 4.27 Canonical miRNAs are not modified in TUT4-deficient T cells
(A) RT-qPCR quantification of selected miRNAs in naive CD4 T cells from TUT4-deficient mice. miRNA levels are normalized to the mean levels of RNU1A1 and RNU5G RNAs and are presented in arbitrary units (n=3). **(B)** Comparison of the levels of the individual canonical miRNAs corresponding to the identified TUT4 uridylation targets between wild type nd TUT4-deficient CD4 T cells.

compensatory increase in the levels of TUT7 or any other TUTase (*Figure 4.28A and B*), but given the presence of TUT7 protein, it is likely that the remaining miRNA uridylation in TUT4-deficient mice is attributable to this enzyme.

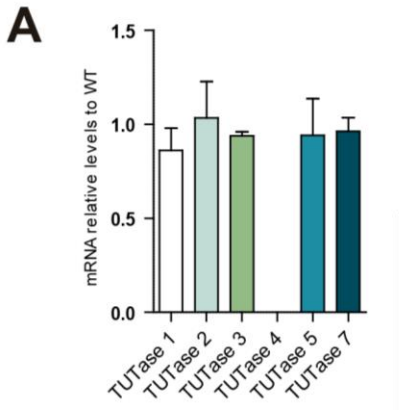

Figure 4.28 Expression of other TUTases are not modified in TUT4 deficient T cells.
(A) RT-qPCR quantification of TUT1,2,3,4,5 and 7 mRNA in naive CD4 T cells from TUT4-deficient mice. Data are expressed relative to the mRNA levels in wild type cells (n=2). **(B)** TUT7 protein content in wild type and TUT4-deficient CD4 T cells. ERMs were included as a loading control.

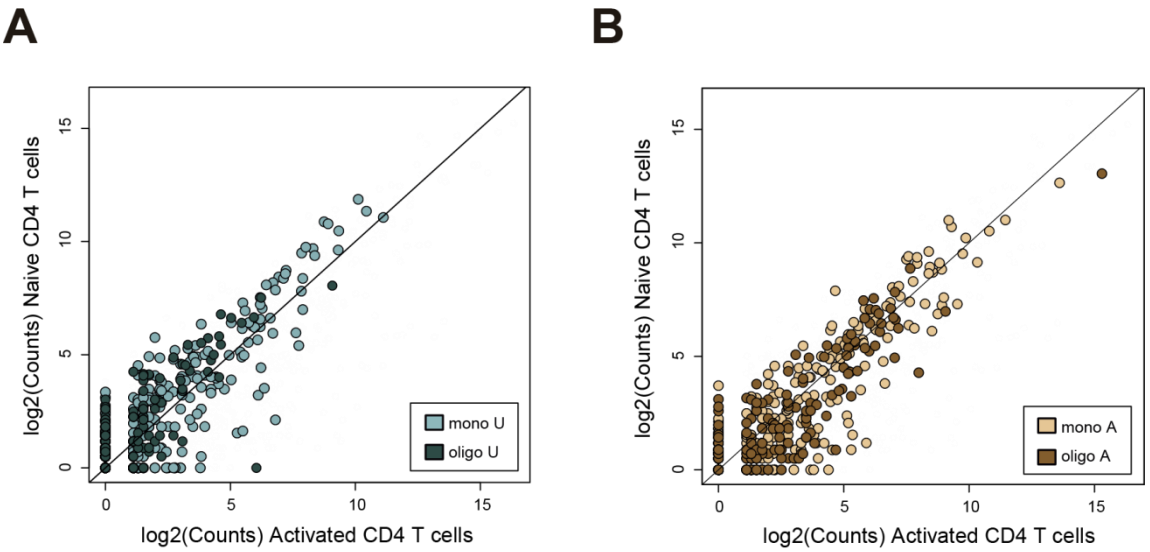

Figure 4.29 The remaining uridylated miRNAs in TUT4 deficient T cells are downregulated after T cell activation
Comparison of the relative abundance of 3′ mono-uridine and oligo-uridines **(A)** and of 3′ mono-adenine and oligo-adenines **(B)** in individual miRNAs from naive and activated TUT4-deficient CD4 T cells.

We further determined the impact of the lack of TUT4 on uridylated miRNAs during T cell activation. Despite the already low basal levels of uridylation in TUT4-deficient CD4 T cells (*Figure 4.26A and B*), cell activation still led to a reduction of the remaining uridylated miRNAs, while adenylation was again stable (*Figure 4.29A and B*). Analysis of the identified TUT4 miRNA targets (*Annex Table 9.3.* Targets of TUT4. during activation

of wild type T cells revealed that these species were downregulated while the corresponding canonical miRNAs remained stable (*Figure 4.30 and Annex Table 9.4*). TUT4 targets thus account for a substantial proportion of the uridylated miRNAs degraded upon T cell activation.

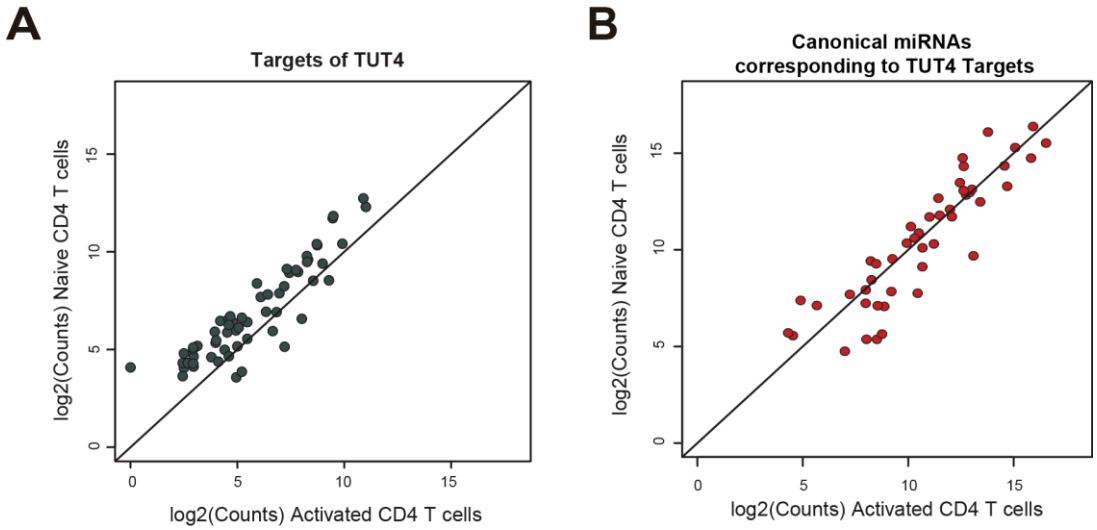

Figure 4.30 TUT4 Targets and their corresponding canonicals during T cell activation
(A) Comparison of the levels of individual uridylated miRNAs identified as TUT4 targets between naive and activated wild type CD4 T cells. **(B)** Comparison of the levels of the individual canonical miRNAs corresponding to the identified TUT4 uridylation targets between naive and activated wild type CD4 T cells.

DISCUSSION

5 DISCUSSION

5.1 microRNAs are transferred during IS from T lymphocytes to Antigen Presenting Cells shuttled by exosomes

5.1.1 EVs in cell-cell communication

Cells release different types of vesicles into the extracellular space being exosomes those of endosomal origin. Extracellular Vesicles are increasingly recognized as important mediators of cell-to-cell communication (Simons and Raposo, 2009). They can transfer receptors, proteins, mRNA and microRNA to target cells via interaction with specific receptors. Extracellular vesicles derived from embryonic stem cells have been reported to reprogram hematopoietic progenitors through the delivery of mRNA (Ratajczak et al., 2006a). The transfer of RNA species via microvesicles to endothelial cells induces angiogenesis (Deregibus et al., 2007; Skog et al., 2008) and progenitor mobilization (Zernecke et al., 2009). In the immune system, exosomal transfer of mRNA occurs between mast cells (Valadi et al., 2007), and viral miRNAs secreted by EBV-infected cells can be taken up by uninfected recipient cells (Pegtel et al., 2010). Synthetic miRNA mimetics and viral miRNAs have been reported to be transferred between leukocytes, although the direct involvement of exosomes/microvesicles in this case was not demonstrated (Rechavi et al., 2009). Exchange of proteins between immune cells has been extensively reported, but the mechanism of this transfer remains unclear (Davis, 2007). This phenomenon, which has been called trogocytosis, is considered to be an antigen-specific event that requires the formation of an IS. Data presented in the first section of this thesis suggest that the mechanism for the transfer of certain proteins during IS is the directional release of exosomes. It is worth to mention that other mechanisms of intercellular transfer of molecules have been described in the IS like trans-endocytosis, nanotubes and gap junctions.

5.1.2 IS as enhancer of directed intercellular communication

In accordance with other reports, our data show that exosomes can be transferred between cells at a distance. T lymphocytes and DCs can acquire exosomes from the extracellular milieu (Izquierdo-Useros et al., 2009; Montecalvo et al., 2008; Segura et al.,

2005a; Segura et al., 2005b). Uptake of isolated exosomes seems to be influenced by activation of donor T cells (Nolte-'t Hoen et al., 2009), the maturation state of recipient DCs (Izquierdo-Useros et al., 2009), and the presence of specific proteins like LFA-1 or ICAM-1 on exosomal or cellular membranes (Nolte-'t Hoen et al., 2009; Segura et al., 2005b; Xie et al., 2010). TCR specificity was suggested not to be required for exosomal uptake (Nolte-'t Hoen et al., 2009); however, we found that TCR specificity and the presence of antigen enhance their acquisition. Interestingly, we observed that CD63 was not transferred in T-B contact cocultures in the presence of stimuli that activate T cells without forming an IS. These results indicate that cell-cell contact and T cell activation are not sufficient for the observed exosomal transfer, and that the presence of specific antigen that induces the formation of an IS is critical.

Moreover, we have described that the exchange of exosomes is dependent on the formation of a fully functional IS. IS is such an intimate intercellular contact that provides ample opportunity for cell-cell communication often involving membrane fusion and the formation of several membrane structures. These processes facilitate the exchange of molecules not only from cell surfaces but also from the cytoplasm of the cells involved. However, the exact mechanism of IS-driven exosome transfer is still unsolved. At least two possibilities can be considered: i) transfer may occur through the IS itself; ii) exosomes could be released to the surrounding medium and acquired by the recipient cell, the IS thus making uptake more efficient than in the absence of cell-cell contact. Both possible routes have been described for IS-dependent transfer of cytokines and lytic factors (Huse et al., 2008). While cytokines such as TNFα and the chemokine CCL3 are released multidirectionally, IL2 and IFNγ are secreted within the IS between CD4+ T cell and APC (Huse et al., 2006). Directional secretion also occurs with lytic granules and factors released by CD8+ T cells during cytotoxic synapse with a target cell. In this case, directional and confined communication is especially important to safeguard surrounding cells from the cytotoxic action (Stinchcombe et al., 2001). In the IS between a CD4+ T cell and an APC, which occurs in the context of a cell-dense scenario such as a lymph node, directionality may ensure exclusive delivery of the exosomal signal to the specific target cell, without affecting surrounding bystander cells. Similarities between lytic-granule

release, exosome release at the IS, and neurotransmitter secretion at neuronal synapses are becoming increasingly evident (Huse et al., 2008).

5.1.3 Polarization of the T-cell MVBs

Polarized secretion is guided by the reorientation of the microtubule-organizing center (MTOC) toward the IS, which is accompanied either by the Golgi apparatus in cytokine-releasing helper T cells or by lytic granules in cytotoxic T cells (Griffiths et al., 2010) (Calabia-Linares et al., 2011). Our data and others demonstrate that the formation of an IS also induces the polarization of T cell MVBs toward the IS and enhances the release of exosomes (Blanchard et al., 2002). Preliminary evidence suggests that the mechanism of MTOC reorientation and MVB traffic for polarized secretion at the IS involves local production of second messenger lipids such as diacylglcyerol and its negative regulator, diacylgycerol kinase α (Quann et al., 2009). Further work is needed to better define the mechanism of directed exosomal release and uptake. Nevertheless, plasma-membrane fusion of MVBs at the IS zone is supported by or findings of the specific translocation of T-cell MVBs toward a functional IS and the selective uptake of exosomes only by APCs expressing MHCII and therefore able to form this functional IS. On the other hand, the MVBs of APCs, whether DCs or B cells, do not translocate to the IS, indicating that although APCs might release exosomes during cognate interaction, polarized release as occurs in T cells is very unlikely.

5.1.4 Exosomes uptake by the recipient cell

In order for the exosomal cargo (both protein and genetic material) to be functional after delivery, it must avoid degradation in the recipient cell. Using fluorescently labeled exosomes, several studies have demonstrated internalization of exosomes by DCs and other phagocytes (Feng et al., 2010; Izquierdo-Useros et al., 2009; Montecalvo et al., 2012; Montecalvo et al., 2008). Although internalized exosomes colocalize with late endosomes/lysosomes (Feng et al., 2010; Morelli et al., 2004), alopeptides of exosomal origin are processed and later presented on the DC surface, demonstrating that exosomal cargo is not completely degraded (Morelli et al., 2004). Moreover, tumor-derived exosomes have been shown to fuse directly with melanoma cells membrane at low pH (Parolini et al., 2009), although in other cell lines internalization occurs via the endocytic

pathway, with proteins directed to lysosomes while lipids appear to be recycled (Tian et al., 2010). Previous works detected the transfer of functional mRNA and viral miRNA by isolated exosomes (Pegtel et al., 2010; Valadi et al., 2007). More recently luciferin-loaded exosomes have been reported to induce luciferase activity in luciferase-transfected DCs (Montecalvo et al., 2012) and functional Cre mRNA has been described to be transferred by exosomes between hematopoietic cells to neurons leading to loxP excision in target cells (Ridder et al., 2014). Altogether, these works demonstrate the functional release of exosomal content into the cytosol.

Exosomes have a similar protein and lipid content to retroviruses, and both use the same biogenesis pathway and cell-to-cell transmission mechanisms (Gould et al., 2003; Izquierdo-Useros et al., 2009). The finding that HIV can be delivered through the virological synapse between infected and uninfected T cells and successfully infects the recipient cell (Hubner et al., 2009) thus strengthens the case for exosomal delivery of functional cargo via the IS. In this regard, our work using 3'UTR-luciferase vectors to sense miRNA activity demonstrates that exosomally-transferred miRNA is functional only in IS-mediated cell-cell contacts: isolated exosomes added directly to recipient cells do not transfer functional miRNA. We propose that the IS acts as a highly-efficient platform that enhances functional, antigen-specific delivery of exosomal cargo to the cytosol of the recipient APC. It is however conceivable that in other systems (for example with a more phagocytic target) free exosomes might be able to deliver functional cargo. The elucidation of the mechanism by which exosomes are taken up by the recipient cell awaits conclusive direct live-cell imaging of exosome fusion and will help to explain these differences.

5.1.5 Specific sorting of miRNAs into exosomes

Complex mechanisms underlie the sorting of cargo into different populations of ILVs that in turn will determine their fate. Ubiquitinated proteins require the action of the ESCRT machinery to mediate degradative protein sorting (Raiborg and Stenmark, 2009) while other cargos such as CD63 and miRNAs are sorted in a ceramide-dependent pathway that generates another population of ILVs destined for secretion as exosomes (Kosaka et al., 2010; Trajkovic et al., 2008). Indeed, our mechanistic studies with chemical inhibitors and

nSMase2 siRNA support this fact. Tetraspanins are also implicated in the recruitment of transmembrane proteins to exosomes and determine their composition (Chairoungdua et al., 2010; Perez-Hernandez et al., 2013). Our data and previous reports (Pegtel et al., 2010; Zhang et al., 2010) indicate that not all microRNAs can be incorporated into exosomes, and therefore that the packaging of specific miRNA populations into exosomes is selective. The mechanisms controlling this sorting are now beginning to be elucidated. Since proteins of the RNA-induced silencing complex (RISC) have been detected in exosomes (Gibbings et al., 2009), it is feasible that association with RISC components controls the packaging of miRNAs in exosomes. Blocking MVB formation by ESCRT depletion results in impaired miRNA silencing (Gibbings et al., 2009; Lee et al., 2009), thus suggesting that MVBs could be a miRNA crossroad to secretory pathway and gene silencing. Following the findings presented in this thesis, our lab also described a novel mechanism for the specific sorting of miRNAs inside exosomes. Exosomal miRNAs were found to contain specific sequence motifs that control their localization into exosomes. The protein heterogeneous nuclear ribonucleoprotein A2B1 (hnRNPA2B1) binds exosomal miRNAs and this binding is controlled by hnRNPA2B1 sumoylation (Villarroya-Beltri et al., 2013). Other potential mechanisms for the packaging of specific miRNAs in exosomes have been proposed like the 3′ NTA. Uridylated miRNAs were found to be more represented in extracellular vesicles produced by B cell lymphoma cells claiming that this type of post-transcriptional modification was sort of a label for miRNAs export (Koppers-Lalic et al., 2014). However this mechanism of sorting was not occurring in T cells as we will comment on the third section of the thesis (see section *5.3.3* on page 101).

5.1.6 Functional delivery of microRNAs to the recipient cell

Today there is no doubt that microRNAs are important modulators of the immune system (O'Connell et al., 2010; Sonkoly et al., 2008; Xiao and Rajewsky, 2009). Modification of gene expression in recipient cells by transferred genetic material could account for several exosome functions. This exosomal transfer of regulatory RNAs is potentially a powerful means of orchestrating gene expression during the generation of the immune response, and increases the complexity of communication between cells.

Our results show that the transfer of CD63 correlates with the transfer of one microRNA, miR-335, from the T cell to the APC being functional in the later. miRNA-335 is especially suitable for our technical approach since it is expressed in primary leukocytes, is highly enriched in exosomes, and its expression is negligible in Raji B cells. We demonstrate that miRNA-335 down-regulates translation of SOX-4 mRNA. This miRNA-335 target gene has been reported in breast cancer cells (Tavazoie et al., 2008). In contrast, Raji cells that were exposed to isolated exosomes without cellular contact showed no microRNA activity, and the exosomal protein signal could be removed by trypsin treatment. It is feasible that other exosomal microRNAs can also be transferred during immune synapsis. Our data show that levels of miR-92a, another miRNA abundant in exosomes, increase in Raji cells after conjugation with T lymphoblasts. However, since this miRNA is endogenously expressed by B cells we cannot distinguish between endogenous upregulation and horizontal transfer.

In conclusion, the data obtained in the first section of this thesis establish a highly efficient intercellular mechanism for the transfer of regulatory genetic information exclusively in the microenvironment of the IS. Unlike other examples of RNA transfer via microvesicles, where non-synaptic release potentially allows the exchange of genetic material at a distance, our data indicate that during cognate immune interactions there is a unidirectional transfer of microRNA from the T to the APC. This genetic communication is antigen-driven and appears to be linked to the formation of the IS. The importance of exosome release in this process is demonstrated by the correlation of miRNA transfer with that of CD63 and by its blockade with inhibitors of exosome production. Our proposed model is presented in ***Figure 5.1***

There are however several issues that will require further investigation. Different activation states alter the repertoire of RNAs packaged into the EVs, so it is possible that different types of immune cells, for example differentiated T-helper lymphocyte subsets (Th1, Th2, Th17 and Treg), might secrete different EV-shuttled RNAs. The physiological relevance of protein exchange during IS formation is still unclear depending on the biological context, although its occurrence has been widely demonstrated. Some authors claim that trogocytosis-mediated uptake of MHC-peptide complexes by T cells might aid the selection of high-affinity T cells, or in contrast induce 'fratricidal' killing by CTLs. A

broader function of this kind of exchange, involving transfer of other molecules, might enable cells to acquire molecules (proteins, lipids and RNAs) that they do not synthesize themselves. It is very likely that these processes will affect signal transduction, allowing intercellular communication to modify the physiology of the recipient cell. The impact of the transfer of miRNAs on the function of the recipient cell still needs to be addressed. This knowledge will give us a better understanding of how the IS works and of what are the consequences of this mode of communication. Detailed understanding of how EVs are exchanged between immune cells would permit therapeutic exploitation of these vesicles, which are promising vehicles for gene therapy in diseases of the immune system and in other scenarios.

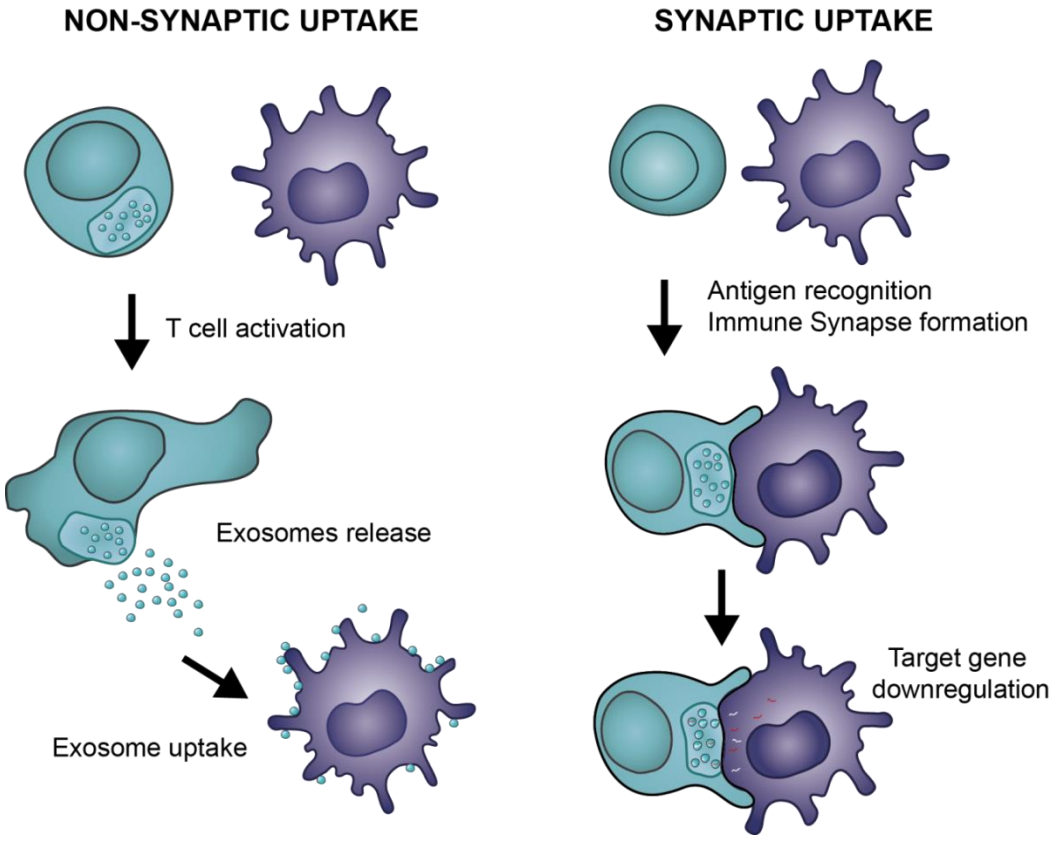

Figure 5.1 Proposed model for intercellular communication between T cell and APC
According to our results, exosomes released by T cells after activation can be uptaken by the APC. However, only exosomes transferred during the immune synapsis are able to transfer functional miRNAs that will in turn modulate the gene expression of the recipient cells. Thus, there is a cualitative difference between non-synaptic uptake and immune synapse mediated uptake of exosomes bearing miRNAs.

5.2 microRNA profile of T cells is regulated during activation

Different cell types of the immune system show specific expression of defined subsets of miRNAs. It has been described that microRNAs changes to very specific profiles after T cell activation and Th cell differentiation (Kuchen et al., 2010; Landgraf et al., 2007; Monticelli et al., 2005). Our data are in accordance with previous studies on miRNA profile changes on T cells after activation and add the finding of the specific changes that occur after cognate interaction not only with conventional DCs but with plasmacytoid DCs. Moreover, we were able to identify common targets for the miRNAs regulated after T cell activation and validate experimentally the relationship between one of the most upregulated miRNAs, miR-132-3p, and the common target *pik3r1* that resulted to be regulated inversely to this miRNA.

5.2.1 miRNAs changes in T cells are specific of the type of activation

pDCs are a particular subset of DCs that produces large amounts of type I interferons in response to viruses. It is largely accepted that in immature cDCs antigen presentation promotes T cell tolerance while after maturation they acquire capacity to induce effector T cell responses. However for pDCs it is not simply their activation status what determines their ability to promote tolerance or immunity. Activated pDCs function depends more on the anatomical localization and cytokine milieu although the precise mechanisms are still not well stablished (Guery and Hugues, 2013). Moreover, pDCs have been related to Tregs development as well as the generation of hyporesponsiveness of CD4 T cells (Kang et al., 2007; Loschko et al., 2011). It has been described that spleen pDCs induce minimal proliferation and no cytokine polarization in antigen specific transgenic T cells that do not further proliferate and acquire regulatory activity (Martin et al., 2002). Moreover, bone marrow derived pDCs showed a very limited immunogenic capacity although they could still induce T cell activation (Mittelbrunn et al., 2009). Accordingly, our data of *in vitro* co-culture of mature pDCs with OT-II CD4 T cells, suggest that although the T cells are still activated at some extent, pDCs are not as efficient as cDCs or anti CD3 plus anti CD28 antibodies in activating T cells, at least in terms of CD69 and CD25 expression. Indeed, the microRNA profile of the T cells after encounter with pDCs differed substantially from the one of T cells activated with cDCs. Unfortunately, validation by qPCR of those miRNAs

was not successful. This may be due to a combination of false positives on the arrays like the viral miRNA miR-801-v10.1 detected; the lack of good characterization of some rare new miRNAs that in turn implies bad qPCRs probes designs (miR-1224); and the low expression of these miRNAs in general. Due to these unexpected difficulties we decided to focus on the group of miRNAs regulated after the interaction with cDCs that is a well characterized immunogenic activation.

5.2.2 miRNAs regulated after T cell activation have common targets

Different studies have reported the miRNA profile of CD4 T cells after T cell activation with CD3 and CD28 antibodies assessed by different techniques from northenblot to microarrays (Bronevetsky et al., 2013; Grigoryev et al., 2011; Jindra et al., 2010; Monticelli et al., 2005) However, all these works have in common that T cell activation was polyclonal with antibodies that do not resemble a physiological immune interaction and thus, *bona fide* T cell activation. In our study, CD4 T cells from transgenic OT-II mice expressing TCR specific for the OVA peptide are cocultured with DCs in presence or absence of the peptide in order to analyze their microRNA profile in a more physiological scenario that better resemble what is happening *in vivo*. Differences between the results of previous studies and ours might come precisely because of the different approach. For example miR-214 was highly upregulated in mouse T cells after 24h of stimulation but we do not detect a differential expression of this miRNA (Jindra et al., 2010). Another source of difference may reside on different animal models although the degree of conservation of miRNAs through different organisms is high, it is not complete. That was nicely confirmed by Rossi and coworkers who analyzed previous published data showing that only 12 of the miRNAs found in human lymphocytes were expressed in mouse lymphocytes but only 6 share expression profiles in human and mouse lymphocytes (Rossi et al., 2011). Moreover, especially with microarray data, normalization is particularly important. Bronevetsky *et al* used tRNAs to normalize miRNA microarrays (Bronevetsky et al., 2013) but tRNAs are actually unrelated to miRNAs regarding to their biogenesis or their turnover. Therefore it is not the most suitable housekeeping gene in this case. We used VSN-invariant method (Huber et al., 2002), as this method normalizes data with the group of miRNAs that are the most stable among the whole group of samples. In our case around 100 miRNAs were considered as "invariants". Finally, when

we compared our miRNA microarrays data with data we obtained later by next generation sequencing from T cells polyclonally activated with anti CD3 and anti CD28, we found that in the later the list was indeed increased in number. This is likely due to a higher depth of this technique, the different type of activation or the different length of incubation time. At any rate, the 75% of miRNAs detected with microarrays to be upregulated in T cells after 20 h of the encounter with cDCs-OVA was represented in the group of miRNAs detected by deep sequencing to be upregulated after activation with anti CD3 and anti CD28 for 48h. No miRNAs were detected to be regulated in the opposite direction indicating that data are robust. Finally, the specific kinetics of the individual miRNAs must be different as we determined for seven miRNAs by qPCR.

To establish a relationship between miRNAs and their possible mRNA targets, some authors directly compare mRNA expression levels to miRNA expression levels assuming that mRNA targets of miRNA will be decreased when the miRNA is upregulated and viceversa (Fu et al., 2012; Li et al., 2013). It is noteworthy to highlight that mRNAs are not always degraded when targeted by a miRNA so this comparative approach will not be detecting every potential interaction. Our choice was instead to analyze the miRNAs regulated in the same direction (i.e. upregulated or downregulated) as a whole and look for common targets by *in silico* prediction. By this approach we were not missing any potential interaction and the fact that we were able to validate the interaction between miR-132 and *pik3r1* gene points out that the prediction method was appropriate. Further validation of other relationships between the targets on the list and the miRNAs might strengthen our analysis.

5.2.3 miR-132-3p in immunity

miR-132 shares both its primary transcript and seed sequence with miR-212 in mouse and human. However, although they are transcribed together, in some studies one of the two miRNAs was found to be more induced than the other. Actually, this was our case since we observed a clear upregulation of miR-132 after T cell activation while miR-212 remained unchanged. Whether this is due to either different stability or a preferential processing of one of the miRNAs still needs to be elucidated.

miR-132 has been mainly described in the nervous system with only a few recent emerging examples in the immune system including the regulation of hematopoietic stem cell function (Mehta et al., 2015b). It has been described that miR-132-3p facilitates viral infection both in innate immune cells (Lagos et al., 2010) and CD4 T cells (Chiang et al., 2013) and it has been recently related to resistance to experimental autoimmune encephalomyelitis (EAE) since it induces cholinergic anti-inflammatory system by targeting Acetylcholinesterase after ayrl hydrocarbon receptor activation (Hanieh and Alzahrani, 2013; Shaked et al., 2009). Mice deficient in the miR132/212 cluster exhibited significantly higher resistance to develop EAE and lower Th1 and Th17 cells in draining lymph nodes (Nakahama et al., 2013). Overexpression of miR-132 in encephalitogenic CD4 T cells decreased cell proliferation (Hanieh and Alzahrani, 2013). Very recently, miR-132/212 cluster has been implicated in B cell development (Mehta et al., 2015a). However none of these works studied the role of miR-132 in naïve CD4 T cell activation. Our data indicate that it is upregulated being functional on targeting genes. Loss of function experiments will provide insights with the specific function of miR-132 in the context of CD4 T cell activation. Altogether, taking into account the available information, we hypothesize that miR-132-3p role in T cell activation might be more a cooperative role together with the other miRNAs regulated in the process that in turn will finely tune the correct T cell activation and T helper cell differentiation.

5.2.4 Involvement of Pik3r1 in T cell activation

miR-132-3p was experimentally validated to target *pik3r1* gene and in fact, we predicted that this mRNAs is targeted by 11 of the 12 miRNAs upregulated after T cell activation. Moreover, we detected a downregulation of the gene both at protein and mRNA level after different time points of T cell activation. P*ik3r1* gene encodes p50a, p55a and p85a, regulatory subunits of Class IA phosphatidylinositol 3-kinases (PI3K) that catalyze the conversion of phosphatidylinositol-4,5-bisphosphate (PIP_2) to phosphatidylinositol-3,4,5-trisphosphate (PIP_3) and act downstream of receptors such as TCR and CD28 in T cells. The major roles of the regulatory subunits of I_A PI3K are to bind and stabilize p110, the catalytic subunit (Conley et al., 2012), inhibit p110 kinase activity (Burke et al., 2011), and recruit the PI3K complex to phosphotyrosine that in turn will relieve the inhibitory contact with the catalytic subunit. The existence of p85a subunit unbound to p110 is still

an open question. Hence, the specific loss of p85a (with the other regulatory subunits intact like p50a) inhibited the activation of Akt under conditions promoting the differentiation of Th1, Th2 and Th17 cells but only Th17 differentiation was affected (Kurebayashi et al., 2012). Recently, it has been described that patients with mutations on PIK3R1 undergo lymphoproliferation and exhibit hyperactive PI3K signaling since the resulting mutant p85a is expressed in abnormal low levels in the patients (Lucas et al., 2014). Taking these data into account we hypothesize that pik3r1 is downregulated by miRNAs after T cell activation enabling the increase on PI3K signaling. miRNAs gain and loss of function experiments where we could study PI3K signaling as well as pik3r1 levels would help us to prove our hypothesis.

5.3 Post-transcriptional modification of miRNAs during T cell activation

In the third section of this thesis we aimed to study of the regulation of miRNA by post-transcriptional modifications, i.e. addition of extra nucleotides to the transcribed sequence. Our results demonstrate that additions of nucleotides to the 3′ end of the miRNAs are functional modifications that impact the stability and turnover of this small RNA species. Our data indicate that miRNA uridylation is tightly regulated during T cell activation. We further identify TUT4 as the main enzyme responsible for uridylation of mature miRNA, and show that the turnover of uridylated microRNAs in T cells differs between resting and activated conditions, indicating that this is likely an important mechanism controlling the fate and function of miRNAs during T cell activation.

5.3.1 Uridylated mature miRNA in T cell activation

The study of miRNA variants or isomiRs is relatively recent and has expanded thank to the development of new analyzing techniques like next generation sequencing. Originally, there were some concerns about that isomiRs might be simply sequencing artefacts. However, "spike in" synthetic RNA oligonucleotide experiments indicated that isomiR identification far exceeds error rates (Wyman et al., 2011).

As mentioned before, uridylation of pre-miRNAs can impact their fate depending on the context since it can promote pre-miRNAs degradation (poly-uridylation in stem cells (Heo et al., 2009)) or facilitate their processing (mono-uridylation in somatic cells (Heo et al.,

2012)). For mature miRNAs the scenario varies also depending on the organism and the miRNA studied (Ibrahim et al., 2010; Zhao et al., 2012). The examples studied in mammals until now only describe that uridylation specifically reduces the function of miR-26a, miR-126-5p and miR-379 (Jones et al., 2012; Jones et al., 2009) but this work does not address any changes in miRNAs turnover. Our data describe a set of miRNAs that appears uridylated in naïve CD4 T cells that specifically decrease after T cells activation. Moreover, we demonstrate that uridylation impacts the stability of mature miRNAs in the context of T cell activation.

The 3'UTR of mRNAs are shortened upon T cell activation, which in turn implies an inhibition of the regulation of gene expression dependent on miRNA (Sandberg et al., 2008). Additionally, upon T cell activation, a global downregulation of mature miRNAs has been reported using microarray techniques (Bronevetsky et al., 2013). Similar results were detected by deep sequencing in our data after normalization. Although miRNA uridylation does not alter the levels of canonical mature miRNAs, it is conceivable that these changes in post-transcriptional modifications target specificity as well as functionality as has been described previously for specific miRNAs (Jones et al., 2009). More importantly, according to our results, miRNA stability can be altered also by these modifications. This process points to the same direction of the described miRNAs global downregulation during T cell activation.

Our data indicate that not all the miRNAs are uridylated and that the modification is restricted to a specific group. Moreover, this group is widely coinciding with the group identified as TUT4 targets. We have attempted to find common sequence motives for the group of uridylated miRNAs as we did in the past for miRNAs sorted into extracellular vesicles (Villarroya-Beltri et al., 2013). Unfortunately, in this case we did not find any specific motif represented in the sequence of this group of uridylated miRNAs. However, the restriction of the process to a specific group of miRNAs indicates that there must be a biological reason for their specific degradation in activated T cells. The contrasting degradation of uridylated miRNAs and maintenance of adenylated miRNAs may represent an additional mechanism for the cell to eliminate less stable miRNAs that are not important or even detrimental for the cell at this specific stage.

It is finally worth to mention that due to the strong biological changes that lymphocytes undergo during the process of activation, that makes this biological context a specially suitable scenario for the study of miRNA tailing and turnover regulation were these molecular processes acquire their biological relevance.

5.3.2 Terminal Uridyl transferases in T cells

We found that there is a paired downregulation of the two TUTases responsible of miRNA uridylation, TUT4 and TUT7, concomitant with the decrease in miRNA uridylation itself after T cell activation. This fact indicates that degradation of uridylated miRNA plays an important role during T cell activation. When TUT4 deficient lymphocytes were analysed, we found a clear decrease of uridylated miRNAs compared to wild type, Interestingly, adenylated miRNAs are increased in TUT4 deficient cells strongly suggesting that miRNA uridylation and adenylation are coordinated processes that can compensate each other in steady state. Taking advantage of TUT4 knock out mice, we have also been able to identify the miRNA species that are target of TUT4 uridylation. As mentioned above, TUT4 targets represent a large proportion of the uridylated miRNAs that is downregulated upon T cell activation in wild type cells. These results suggest that TUT4 controls a specific set of modified miRNAs that will be specifically decreased upon T cell activation. Moreover, we found that there is still a proportion of uridylated miRNAs in TUT4 deficient cells. This may reflect the activity of TUT7, which can uridylate miRNAs (Thornton et al., 2015) and is still present in the TUT4 deficient cells. Gain-of-function experiments were technically unfeasible in our system due to the difficulty of transfecting naive T cells and transducing such a large plasmid with lentivirus, but might have provided interesting additional data.

TUT4 has been described to be acting together with Lin28 in the processing pathway of pre-miRNAs in stem cells (Heo et al., 2009). In somatic cells TUT4, TUT7 or TUT2 were described to add only one nucleotide to a pre-miRNAs (Heo et al., 2012). In this case they are believe to act alone, however it has not been well explored yet whether in somatic cells (that include lymphocytes) TUT4 and TUT7 could be acting in concert with an unknown cofactor. Lin28 recognize a specific motif on let-7 precursors terminal loop guiding TUT4 to oligouridylate this specific family of pre-miRNAs (Heo et al., 2009). Similarly, the

potential unidentified TUT4 cofactor in somatic cells could be conferring the specificity for its miRNA targets.

Recently, additional piece of knowledge was obtained by N. Kim's group where they described that mRNA can be uridylated by TUT4 and TUT7 after the shortening of the polyA tail of this mRNAs. This way, mRNAs are targeted for degradation. This work supports both the function of TUT4 and TUT7 independently of Lin28 or other cofactor and the role of uridylation as a molecular mark for RNA decay (Lim et al., 2014).

Moreover, it might be worth to mention that TUT4 has been described to regulate cell cycle progression and proliferation independently of its uridyltransferase activity (Blahna et al., 2011). However, the authors of this work do not describe which is the biological activity that mediates this function and only characterize the involvement of the N-terminal region of the protein.

5.3.3 Alternative mechanisms for the reduction of uridylated miRNAs after T cell activation

Aside degradation into the cell we explored alternative fate for uridylated miRNAs: their export to the extracellular medium shuttled by exosomes. As explained in the first section of this thesis, we have described that the repertoire of miRNAs from exosomes secreted by T cell lymphocytes differs from their cellular counterpart (Mittelbrunn et al., 2011) and that a specific sequence motives determine the sorting of miRNAs inside exosomes (Villarroya-Beltri et al., 2013). Moreover, it has been recently stated that uridylated miRNAs are more represented in extracellular vesicles produced by B cell lymphoma cells (Koppers-Lalic et al., 2014). However, when we assessed the representation of the different isomiRs within mouse lymphoblasts and their extracellular vesicles we did not detect any 3' NTA more represented inside extracellular vesicles compared to the producing cells (data not shown). This made us to rule out this hypothesis for our system.

5.3.4 The missing 3' exonuclease

A key outstanding question about miRNA decay is the identity of the enzymes that catalyze the degradation of these small RNAs during T cell activation. The pathway of miRNA catabolism is not very well established yet. Several mammalian exoribonucleases

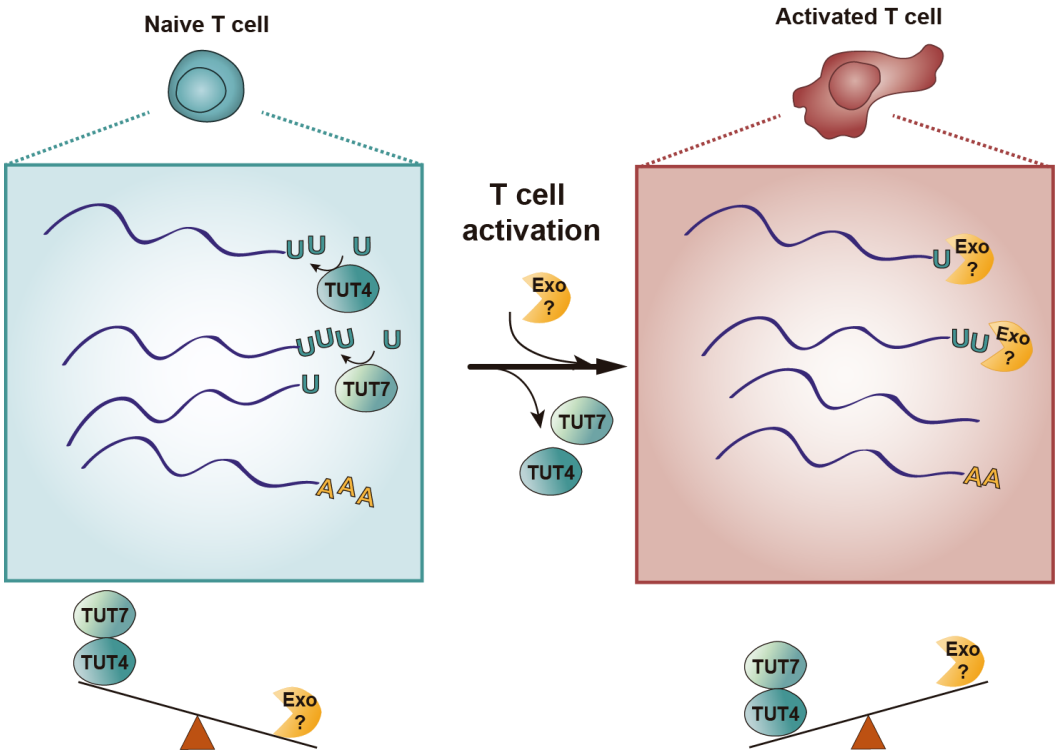

Figure 5.2 Diagram of the proposed mechanism of miRNA post-transcriptional regulation during T cell activation
Naïve cells under steady state contain basal levels of uridylated miRNAs that are downregulated after T cell activation. This decrease is accompanied by the downregulation of uridyltransferases TUT4 and TUT7. Additionally we hypothesize that an still unidentified exonuclease might be expressed in activated T cells responsible for uridylated miRNAs degradation.

have been described that show certain substrate specificity (Ruegger and Grosshans, 2012). XRN1 affects the decay of miR-378 and miR-382 (Bail et al., 2010), whereas several exome subunits degrade specific miRNAs. For example, PNPT1 (PNPaseold-35) degrades miR-221 and RRP41 degrades miR-382 (Bail et al., 2010; Das et al., 2010). Moreover, Dsi3L2 has been shown to degrade uridylated pre-miRNAs (Chang et al., 2013), while poly(A)-specific ribonuclease (PARN) catalyzes the trimming needed for the final maturation step of non-canonical pre-miRNAs (Yoda et al., 2013). Finally, exoribonuclease 1 (Eri1), an enzyme essential for T lymphocyte development and immunity, has been reported to globally target small RNAs in mouse lymphocytes (Thomas et al., 2012). Further research will be needed to identify the specific exoribonucleases that mediate the specific degradation of uridylated miRNAs observed after T cell activation. Once

identified, we could knock down this exonouclease and study the functional impact of the aberrant maintenance of uridylated miRNAs during T cell activation.

Altogether, data presented in this section indicate that NTA modifications and TUTases enzymes are tightly regulated during T cell activation. *Figure 5.2* represents our hypothesized scenario for 3'NTA of miRNAs during T cell activation. Future studies defining the mechanisms and functional significance of miRNA 3' NTAs will be important for understanding the post-transcriptional regulation of miRNA function and turnover, and could also inform strategies for therapeutic modulation of miRNA activity.

CONCLUSIONS/CONCLUSIONES

6 CONCLUSIONS

1. Immune cells secrete exosomes that contain a specific and enriched miRNA repertoire that differs from the cell of origin.

2. MVBs of the T cell translocate towards functional Immune Synapse

3. T cell exosomes bearing microRNA are transferred during Immune Synapsis to the APC. This transfer is unidirectional and functional since acquired microRNAs regulate gene expression at the APC.

4. miRNA repertoire of T cells is modified after cognate interactions with different subsets of DCs. miRNAs upregulated after T cell activation have several common target genes.

5. *pik3r1* gene is directly regulated by miR-132-3p.

6. Terminal Uridyltransferases responsible for miRNAs 3' uridylation, TUT4 and TUT7, are downregulated after T cell activation as well as uridylated miRNAs being other types of modifications as adenlylation unchanged.

7. Uridylated microRNAs are degraded more rapidly as compared to its canonical counterpart after T cell activation

8. TUT4 is essential to maintain miRNA uridylation in steady state. Uridylated miRNAs are reduced in TUT4 deficient CD4 T cells while adenylated miRNAs are increased.

7 CONCLUSIONES

1. Las células inmunes secretan exosomas que contienen un repertorio enriquecido y específico de miARNs distinto del de la célula que los ha producido.

2. Los cuerpos multivesiculares del linfocito T se translocan hacia la sinapsis inmunológica functional

3. Los exosomas de las células T que contienen miRNAs se transfieren a la CPA durante la sinapsis inmunológica. Esta transferencia es unidireccional y funcional ya que los miARNs adquiridos por la CPA son capaces de regular la expresión génica en dicha célula receptora.

4. El repertorio de miARNs de los linfocitos T se ve modificado después de la interacción con distintos tipos de células dentríticas. Los miARNs que aumentan su expresión después de la activación de la célula T tienen dianas comunes.

5. El gen *pik3r1* se regula directamente por el miARN miR-132-3p.

6. Las uridiltransferasas terminales TUT4 and TUT7 responsables de la uridilación en 3' de los miARNs, disminuyen después de la activación del linfocito T. Lo mismo ocurre con los miARNs uridilados mientras que los miARNs con otros tipos de modificaciones como la adenilación no se modifican.

7. Los miARNs uridilados se degradan más rápido comparado con su correspondiente miARN canónico específicamente después de la activación T.

8. TUT4 es esencial para mantener el estado de uridilación de los miARNs en estados basales. Los miARNs uriiylados están disminuidos en el los linfocitos CD4 deficientes en TUT4 mientras que los miARNs adenilados están aumentados.

BIBLIOGRAPHY

8 BIBLIOGRAPHY

Alcover, A., and Thoulouze, M.I. (2009). Vesicle traffic to the immunological synapse: a multifunctional process targeted by lymphotropic viruses. Curr Top Microbiol Immunol *340*, 191-207.

Alonso, R., Mazzeo, C., Rodriguez, M.C., Marsh, M., Fraile-Ramos, A., Calvo, V., Avila-Flores, A., Merida, I., and Izquierdo, M. (2011). Diacylglycerol kinase alpha regulates the formation and polarisation of mature multivesicular bodies involved in the secretion of Fas ligand-containing exosomes in T lymphocytes. Cell death and differentiation *18*, 1161-1173.

Alonso, R., Rodriguez, M.C., Pindado, J., Merino, E., Merida, I., and Izquierdo, M. (2005). Diacylglycerol kinase alpha regulates the secretion of lethal exosomes bearing Fas ligand during activation-induced cell death of T lymphocytes. The Journal of biological chemistry *280*, 28439-28450.

Ameres, S.L., and Zamore, P.D. (2013). Diversifying microRNA sequence and function. Nature reviews Molecular cell biology *14*, 475-488.

Baietti, M.F., Zhang, Z., Mortier, E., Melchior, A., Degeest, G., Geeraerts, A., Ivarsson, Y., Depoortere, F., Coomans, C., Vermeiren, E., *et al.* (2012). Syndecan-syntenin-ALIX regulates the biogenesis of exosomes. Nature cell biology *14*, 677-685.

Bail, S., Swerdel, M., Liu, H., Jiao, X., Goff, L.A., Hart, R.P., and Kiledjian, M. (2010). Differential regulation of microRNA stability. RNA *16*, 1032-1039.

Baj-Krzyworzeka, M., Szatanek, R., Weglarczyk, K., Baran, J., Urbanowicz, B., Branski, P., Ratajczak, M.Z., and Zembala, M. (2006). Tumour-derived microvesicles carry several surface determinants and mRNA of tumour cells and transfer some of these determinants to monocytes. Cancer Immunol Immunother *55*, 808-818.

Barreiro, O., de la Fuente, H., Mittelbrunn, M., and Sanchez-Madrid, F. (2007). Functional insights on the polarized redistribution of leukocyte integrins and their ligands during leukocyte migration and immune interactions. Immunol Rev *218*, 147-164.

Benes, V., Collier, P., Kordes, C., Stolte, J., Rausch, T., Muckentaler, M.U., Haussinger, D., and Castoldi, M. (2015). Identification of cytokine-induced modulation of microRNA expression and secretion as measured by a novel microRNA specific qPCR assay. Sci Rep *5*, 11590.

Blahna, M.T., Jones, M.R., Quinton, L.J., Matsuura, K.Y., and Mizgerd, J.P. (2011). Terminal uridyltransferase enzyme Zcchc11 promotes cell proliferation independent of its uridyltransferase activity. J Biol Chem *286*, 42381-42389.

Blanchard, N., Lankar, D., Faure, F., Regnault, A., Dumont, C., Raposo, G., and Hivroz, C. (2002). TCR activation of human T cells induces the production of exosomes bearing the TCR/CD3/zeta complex. J Immunol *168*, 3235-3241.

Bronevetsky, Y., Villarino, A.V., Eisley, C.J., Barbeau, R., Barczak, A.J., Heinz, G.A., Kremmer, E., Heissmeyer, V., McManus, M.T., Erle, D.J., *et al.* (2013). T cell activation induces proteasomal degradation of Argonaute and rapid remodeling of the microRNA repertoire. The Journal of experimental medicine *210*, 417-432.

Bunnell, S.C. (2010). Multiple microclusters: diverse compartments within the immune synapse. Current topics in microbiology and immunology *340*, 123-154.

Burke, J.E., Vadas, O., Berndt, A., Finegan, T., Perisic, O., and Williams, R.L. (2011). Dynamics of the phosphoinositide 3-kinase p110delta interaction with p85alpha and membranes reveals aspects of regulation distinct from p110alpha. Structure *19*, 1127-1137.

Burroughs, A.M., Ando, Y., de Hoon, M.J., Tomaru, Y., Nishibu, T., Ukekawa, R., Funakoshi, T., Kurokawa, T., Suzuki, H., Hayashizaki, Y., *et al.* (2010). A comprehensive survey of 3' animal miRNA modification events and a possible role for 3' adenylation in modulating miRNA targeting effectiveness. Genome Res *20*, 1398-1410.

Calabia-Linares, C., Robles-Valero, J., de la Fuente, H., Perez-Martinez, M., Martin-Cofreces, N., Alfonso-Perez, M., Gutierrez-Vazquez, C., Mittelbrunn, M., Ibiza, S., Urbano-Olmos, F.R., *et al.* (2011). Endosomal clathrin drives actin accumulation at the immunological synapse. J Cell Sci *124*, 820-830.

Carthew, R.W., and Sontheimer, E.J. (2009). Origins and Mechanisms of miRNAs and siRNAs. Cell *136*, 642-655.

Cifuentes, D., Xue, H., Taylor, D.W., Patnode, H., Mishima, Y., Cheloufi, S., Ma, E., Mane, S., Hannon, G.J., Lawson, N.D., *et al.* (2010). A novel miRNA processing pathway independent of Dicer requires Argonaute2 catalytic activity. Science *328*, 1694-1698.

Cobb, B.S., Hertweck, A., Smith, J., O'Connor, E., Graf, D., Cook, T., Smale, S.T., Sakaguchi, S., Livesey, F.J., Fisher, A.G., *et al.* (2006). A role for Dicer in immune regulation. The Journal of experimental medicine *203*, 2519-2527.

Cocucci, E., Racchetti, G., and Meldolesi, J. (2009). Shedding microvesicles: artefacts no more. Trends Cell Biol *19*, 43-51.

Conley, M.E., Dobbs, A.K., Quintana, A.M., Bosompem, A., Wang, Y.D., Coustan-Smith, E., Smith, A.M., Perez, E.E., and Murray, P.J. (2012). Agammaglobulinemia and absent B lineage cells in a patient lacking the p85alpha subunit of PI3K. The Journal of experimental medicine *209*, 463-470.

Chairoungdua, A., Smith, D.L., Pochard, P., Hull, M., and Caplan, M.J. (2010). Exosome release of beta-catenin: a novel mechanism that antagonizes Wnt signaling. The Journal of cell biology *190*, 1079-1091.

Chang, H.M., Triboulet, R., Thornton, J.E., and Gregory, R.I. (2013). A role for the Perlman syndrome exonuclease Dis3l2 in the Lin28-let-7 pathway. Nature *497*, 244-248.

Cheloufi, S., Dos Santos, C.O., Chong, M.M., and Hannon, G.J. (2010). A dicer-independent miRNA biogenesis pathway that requires Ago catalysis. Nature *465*, 584-589.

Chiang, K., Liu, H., and Rice, A.P. (2013). miR-132 enhances HIV-1 replication. Virology *438*, 1-4.

Chong, M.M., Rasmussen, J.P., Rudensky, A.Y., and Littman, D.R. (2008). The RNAseIII enzyme Drosha is critical in T cells for preventing lethal inflammatory disease. The Journal of experimental medicine *205*, 2005-2017.

Das, S.K., Sokhi, U.K., Bhutia, S.K., Azab, B., Su, Z.Z., Sarkar, D., and Fisher, P.B. (2010). Human polynucleotide phosphorylase selectively and preferentially degrades microRNA-221 in human melanoma cells. Proceedings of the National Academy of Sciences of the United States of America *107*, 11948-11953.

Das, V., Nal, B., Dujeancourt, A., Thoulouze, M.I., Galli, T., Roux, P., Dautry-Varsat, A., and Alcover, A. (2004). Activation-induced polarized recycling targets T cell antigen receptors to the immunological synapse; involvement of SNARE complexes. Immunity *20*, 577-588.

Davis, D.M. (2007). Intercellular transfer of cell-surface proteins is common and can affect many stages of an immune response. Nat Rev Immunol *7*, 238-243.

Davis, M.P., van Dongen, S., Abreu-Goodger, C., Bartonicek, N., and Enright, A.J. (2013). Kraken: a set of tools for quality control and analysis of high-throughput sequence data. Methods *63*, 41-49.

Deregibus, M.C., Cantaluppi, V., Calogero, R., Lo Iacono, M., Tetta, C., Biancone, L., Bruno, S., Bussolati, B., and Camussi, G. (2007). Endothelial progenitor cell derived microvesicles activate an angiogenic program in endothelial cells by a horizontal transfer of mRNA. Blood *110*, 2440-2448.

Diederichs, S., and Haber, D.A. (2007). Dual role for argonautes in microRNA processing and posttranscriptional regulation of microRNA expression. Cell *131*, 1097-1108.

Dustin, M.L. (1998). A novel adaptor protein orchestrates receptor patterning and cytoskeletal polarity in T-cell contacts. Cell *94*, 667-677.

Ecker, J.R., and Davis, R.W. (1986). Inhibition of gene expression in plant cells by expression of antisense RNA. Proceedings of the National Academy of Sciences of the United States of America *83*, 5372-5376.

Feng, D., Zhao, W.L., Ye, Y.Y., Bai, X.C., Liu, R.Q., Chang, L.F., Zhou, Q., and Sui, S.F. (2010). Cellular internalization of exosomes occurs through phagocytosis. Traffic *11*, 675-687.

Fire, A., Xu, S., Montgomery, M.K., Kostas, S.A., Driver, S.E., and Mello, C.C. (1998). Potent and specific genetic interference by double-stranded RNA in Caenorhabditis elegans. Nature *391*, 806-811.

Fu, J., Tang, W., Du, P., Wang, G., Chen, W., Li, J., Zhu, Y., Gao, J., and Cui, L. (2012). Identifying microRNA-mRNA regulatory network in colorectal cancer by a combination of expression profile and bioinformatics analysis. BMC Syst Biol *6*, 68.

Ghildiyal, M., and Zamore, P.D. (2009). Small silencing RNAs: an expanding universe. Nat Rev Genet *10*, 94-108.

Gibbings, D.J., Ciaudo, C., Erhardt, M., and Voinnet, O. (2009). Multivesicular bodies associate with components of miRNA effector complexes and modulate miRNA activity. Nat Cell Biol *11*, 1143-1149.

Gibson, D.G., Young, L., Chuang, R.Y., Venter, J.C., Hutchison, C.A., 3rd, and Smith, H.O. (2009). Enzymatic assembly of DNA molecules up to several hundred kilobases. Nat Methods *6*, 343-345.

Gorska, M.M., Liang, Q., Karim, Z., and Alam, R. (2009). Uncoordinated 119 protein controls trafficking of Lck via the Rab11 endosome and is critical for immunological synapse formation. J Immunol *183*, 1675-1684.

Gould, S.J., Booth, A.M., and Hildreth, J.E. (2003). The Trojan exosome hypothesis. Proceedings of the National Academy of Sciences of the United States of America *100*, 10592-10597.

Griffiths-Jones, S. (2004). The microRNA Registry. Nucleic Acids Res *32*, D109-111.

Griffiths, G.M., Tsun, A., and Stinchcombe, J.C. (2010). The immunological synapse: a focal point for endocytosis and exocytosis. J Cell Biol *189*, 399-406.

Grigoryev, Y.A., Kurian, S.M., Hart, T., Nakorchevsky, A.A., Chen, C., Campbell, D., Head, S.R., Yates, J.R., 3rd, and Salomon, D.R. (2011). MicroRNA regulation of molecular networks mapped by global microRNA, mRNA, and protein expression in activated T lymphocytes. Journal of immunology *187*, 2233-2243.

Guery, L., and Hugues, S. (2013). Tolerogenic and activatory plasmacytoid dendritic cells in autoimmunity. Front Immunol *4*, 59.

Gutierrez-Vazquez, C., Villarroya-Beltri, C., Mittelbrunn, M., and Sanchez-Madrid, F. (2013). Transfer of extracellular vesicles during immune cell-cell interactions. Immunological reviews *251*, 125-142.

Ha, M., and Kim, V.N. (2014). Regulation of microRNA biogenesis. Nature reviews Molecular cell biology *15*, 509-524.

Hamilton, A.J., and Baulcombe, D.C. (1999). A species of small antisense RNA in posttranscriptional gene silencing in plants. Science *286*, 950-952.

Hammond, S.M., Bernstein, E., Beach, D., and Hannon, G.J. (2000). An RNA-directed nuclease mediates post-transcriptional gene silencing in Drosophila cells. Nature *404*, 293-296.

Hanieh, H., and Alzahrani, A. (2013). MicroRNA-132 suppresses autoimmune encephalomyelitis by inducing cholinergic anti-inflammation: a new Ahr-based exploration. European journal of immunology *43*, 2771-2782.

Heo, I., Ha, M., Lim, J., Yoon, M.J., Park, J.E., Kwon, S.C., Chang, H., and Kim, V.N. (2012). Mono-uridylation of pre-microRNA as a key step in the biogenesis of group II let-7 microRNAs. Cell *151*, 521-532.

Heo, I., Joo, C., Kim, Y.K., Ha, M., Yoon, M.J., Cho, J., Yeom, K.H., Han, J., and Kim, V.N. (2009). TUT4 in concert with Lin28 suppresses microRNA biogenesis through pre-microRNA uridylation. Cell *138*, 696-708.

Hewitt, C.R., Lamb, J.R., Hayball, J., Hill, M., Owen, M.J., and O'Hehir, R.E. (1992). Major histocompatibility complex independent clonal T cell anergy by direct interaction of Staphylococcus aureus enterotoxin B with the T cell antigen receptor. J Exp Med *175*, 1493-1499.

Hsu, C., Morohashi, Y., Yoshimura, S., Manrique-Hoyos, N., Jung, S., Lauterbach, M.A., Bakhti, M., Gronborg, M., Mobius, W., Rhee, J., *et al.* (2010). Regulation of exosome secretion by Rab35 and its GTPase-activating proteins TBC1D10A-C. The Journal of cell biology *189*, 223-232.

Huber, W., von Heydebreck, A., Sultmann, H., Poustka, A., and Vingron, M. (2002). Variance stabilization applied to microarray data calibration and to the quantification of differential expression. Bioinformatics *18 Suppl 1*, S96-104.

Hubner, W., McNerney, G.P., Chen, P., Dale, B.M., Gordon, R.E., Chuang, F.Y., Li, X.D., Asmuth, D.M., Huser, T., and Chen, B.K. (2009). Quantitative 3D video microscopy of HIV transfer across T cell virological synapses. Science *323*, 1743-1747.

Hume, C.R., Shookster, L.A., Collins, N., O'Reilly, R., and Lee, J.S. (1989). Bare lymphocyte syndrome: altered HLA class II expression in B cell lines derived from two patients. Hum Immunol *25*, 1-11.

Huse, M., Lillemeier, B.F., Kuhns, M.S., Chen, D.S., and Davis, M.M. (2006). T cells use two directionally distinct pathways for cytokine secretion. Nat Immunol *7*, 247-255.

Huse, M., Quann, E.J., and Davis, M.M. (2008). Shouts, whispers and the kiss of death: directional secretion in T cells. Nat Immunol *9*, 1105-1111.

Ibrahim, F., Rymarquis, L.A., Kim, E.J., Becker, J., Balassa, E., Green, P.J., and Cerutti, H. (2010). Uridylation of mature miRNAs and siRNAs by the MUT68 nucleotidyltransferase promotes their degradation in Chlamydomonas. Proceedings of the National Academy of Sciences of the United States of America *107*, 3906-3911.

Islam, A., Shen, X., Hiroi, T., Moss, J., Vaughan, M., and Levine, S.J. (2007). The brefeldin A-inhibited guanine nucleotide-exchange protein, BIG2, regulates the constitutive release of TNFR1 exosome-like vesicles. J Biol Chem *282*, 9591-9599.

Izquierdo-Useros, N., Naranjo-Gomez, M., Archer, J., Hatch, S.C., Erkizia, I., Blanco, J., Borras, F.E., Puertas, M.C., Connor, J.H., Fernandez-Figueras, M.T., *et al.* (2009). Capture and transfer of HIV-1 particles by mature dendritic cells converges with the exosome-dissemination pathway. Blood *113*, 2732-2741.

Jiang, S., Li, C., Olive, V., Lykken, E., Feng, F., Sevilla, J., Wan, Y., He, L., and Li, Q.J. (2011). Molecular dissection of the miR-17-92 cluster's critical dual roles in promoting Th1 responses and preventing inducible Treg differentiation. Blood *118*, 5487-5497.

Jindra, P.T., Bagley, J., Godwin, J.G., and Iacomini, J. (2010). Costimulation-dependent expression of microRNA-214 increases the ability of T cells to proliferate by targeting Pten. Journal of immunology *185*, 990-997.

Jonas, S., and Izaurralde, E. (2015). Towards a molecular understanding of microRNA-mediated gene silencing. Nat Rev Genet *16*, 421-433.

Jones, M.R., Blahna, M.T., Kozlowski, E., Matsuura, K.Y., Ferrari, J.D., Morris, S.A., Powers, J.T., Daley, G.Q., Quinton, L.J., and Mizgerd, J.P. (2012). Zcchc11 uridylates mature miRNAs to enhance neonatal IGF-1 expression, growth, and survival. PLoS Genet *8*, e1003105.

Jones, M.R., Quinton, L.J., Blahna, M.T., Neilson, J.R., Fu, S., Ivanov, A.R., Wolf, D.A., and Mizgerd, J.P. (2009). Zcchc11-dependent uridylation of microRNA directs cytokine expression. Nat Cell Biol *11*, 1157-1163.

Kang, H.K., Liu, M., and Datta, S.K. (2007). Low-dose peptide tolerance therapy of lupus generates plasmacytoid dendritic cells that cause expansion of autoantigen-specific regulatory T cells and contraction of inflammatory Th17 cells. Journal of immunology *178*, 7849-7858.

Katoh, T., Sakaguchi, Y., Miyauchi, K., Suzuki, T., Kashiwabara, S., and Baba, T. (2009). Selective stabilization of mammalian microRNAs by 3' adenylation mediated by the cytoplasmic poly(A) polymerase GLD-2. Genes & development *23*, 433-438.

Kawahara, Y., Zinshteyn, B., Chendrimada, T.P., Shiekhattar, R., and Nishikura, K. (2007). RNA editing of the microRNA-151 precursor blocks cleavage by the Dicer-TRBP complex. EMBO reports *8*, 763-769.

Kim, V.N., Han, J., and Siomi, M.C. (2009). Biogenesis of small RNAs in animals. Nature reviews Molecular cell biology *10*, 126-139.

Koppers-Lalic, D., Hackenberg, M., Bijnsdorp, I.V., van Eijndhoven, M.A., Sadek, P., Sie, D., Zini, N., Middeldorp, J.M., Ylstra, B., de Menezes, R.X., *et al.* (2014). Nontemplated

nucleotide additions distinguish the small RNA composition in cells from exosomes. Cell Rep *8*, 1649-1658.

Kosaka, N., Iguchi, H., Yoshioka, Y., Takeshita, F., Matsuki, Y., and Ochiya, T. (2010). Secretory Mechanisms and Intercellular Transfer of MicroRNAs in Living Cells. J Biol Chem *285*, 17442-17452.

Kozomara, A., and Griffiths-Jones, S. (2014). miRBase: annotating high confidence microRNAs using deep sequencing data. Nucleic Acids Res *42*, D68-73.

Krol, J., Loedige, I., and Filipowicz, W. (2010). The widespread regulation of microRNA biogenesis, function and decay. Nat Rev Genet *11*, 597-610.

Kuchen, S., Resch, W., Yamane, A., Kuo, N., Li, Z., Chakraborty, T., Wei, L., Laurence, A., Yasuda, T., Peng, S., *et al.* (2010). Regulation of microRNA expression and abundance during lymphopoiesis. Immunity *32*, 828-839.

Kupfer, A., and Dennert, G. (1984). Reorientation of the microtubule-organizing center and the Golgi apparatus in cloned cytotoxic lymphocytes triggered by binding to lysable target cells. J Immunol *133*, 2762-2766.

Kurebayashi, Y., Nagai, S., Ikejiri, A., Ohtani, M., Ichiyama, K., Baba, Y., Yamada, T., Egami, S., Hoshii, T., Hirao, A., *et al.* (2012). PI3K-Akt-mTORC1-S6K1/2 axis controls Th17 differentiation by regulating Gfi1 expression and nuclear translocation of RORgamma. Cell Rep *1*, 360-373.

Lagos-Quintana, M., Rauhut, R., Lendeckel, W., and Tuschl, T. (2001). Identification of novel genes coding for small expressed RNAs. Science *294*, 853-858.

Lagos, D., Pollara, G., Henderson, S., Gratrix, F., Fabani, M., Milne, R.S., Gotch, F., and Boshoff, C. (2010). miR-132 regulates antiviral innate immunity through suppression of the p300 transcriptional co-activator. Nature cell biology *12*, 513-519.

Landgraf, P., Rusu, M., Sheridan, R., Sewer, A., Iovino, N., Aravin, A., Pfeffer, S., Rice, A., Kamphorst, A.O., Landthaler, M., *et al.* (2007). A mammalian microRNA expression atlas based on small RNA library sequencing. Cell *129*, 1401-1414.

Lau, N.C., Lim, L.P., Weinstein, E.G., and Bartel, D.P. (2001). An abundant class of tiny RNAs with probable regulatory roles in Caenorhabditis elegans. Science *294*, 858-862.

Laulagnier, K., Grand, D., Dujardin, A., Hamdi, S., Vincent-Schneider, H., Lankar, D., Salles, J.P., Bonnerot, C., Perret, B., and Record, M. (2004a). PLD2 is enriched on exosomes and its activity is correlated to the release of exosomes. FEBS letters *572*, 11-14.

Laulagnier, K., Motta, C., Hamdi, S., Roy, S., Fauvelle, F., Pageaux, J.F., Kobayashi, T., Salles, J.P., Perret, B., Bonnerot, C., *et al.* (2004b). Mast cell- and dendritic cell-derived exosomes display a specific lipid composition and an unusual membrane organization. The Biochemical journal *380*, 161-171.

Lee, R.C., and Ambros, V. (2001). An extensive class of small RNAs in Caenorhabditis elegans. Science *294*, 862-864.

Lee, R.C., Feinbaum, R.L., and Ambros, V. (1993). The C. elegans heterochronic gene lin-4 encodes small RNAs with antisense complementarity to lin-14. Cell *75*, 843-854.

Lee, Y.S., Pressman, S., Andress, A.P., Kim, K., White, J.L., Cassidy, J.J., Li, X., Lubell, K., Lim do, H., Cho, I.S., *et al.* (2009). Silencing by small RNAs is linked to endosomal trafficking. Nat Cell Biol *11*, 1150-1156.

Li, Q.J., Chau, J., Ebert, P.J., Sylvester, G., Min, H., Liu, G., Braich, R., Manoharan, M., Soutschek, J., Skare, P., *et al.* (2007). miR-181a is an intrinsic modulator of T cell sensitivity and selection. Cell *129*, 147-161.

Li, Y., Xu, J., Chen, H., Bai, J., Li, S., Zhao, Z., Shao, T., Jiang, T., Ren, H., Kang, C., *et al.* (2013). Comprehensive analysis of the functional microRNA-mRNA regulatory network identifies miRNA signatures associated with glioma malignant progression. Nucleic Acids Res *41*, e203.

Lim, J., Ha, M., Chang, H., Kwon, S.C., Simanshu, D.K., Patel, D.J., and Kim, V.N. (2014). Uridylation by TUT4 and TUT7 Marks mRNA for Degradation. Cell *159*, 1365-1376.

Lodish, H.F., Zhou, B., Liu, G., and Chen, C.Z. (2008). Micromanagement of the immune system by microRNAs. Nat Rev Immunol *8*, 120-130.

Loeb, G.B., Khan, A.A., Canner, D., Hiatt, J.B., Shendure, J., Darnell, R.B., Leslie, C.S., and Rudensky, A.Y. (2012). Transcriptome-wide miR-155 binding map reveals widespread noncanonical microRNA targeting. Molecular cell *48*, 760-770.

Loschko, J., Heink, S., Hackl, D., Dudziak, D., Reindl, W., Korn, T., and Krug, A.B. (2011). Antigen targeting to plasmacytoid dendritic cells via Siglec-H inhibits Th cell-dependent autoimmunity. Journal of immunology *187*, 6346-6356.

Lu, L.F., Boldin, M.P., Chaudhry, A., Lin, L.L., Taganov, K.D., Hanada, T., Yoshimura, A., Baltimore, D., and Rudensky, A.Y. (2010). Function of miR-146a in controlling Treg cell-mediated regulation of Th1 responses. Cell *142*, 914-929.

Lu, S., Sun, Y.H., and Chiang, V.L. (2009). Adenylation of plant miRNAs. Nucleic Acids Res *37*, 1878-1885.

Lucas, C.L., Zhang, Y., Venida, A., Wang, Y., Hughes, J., McElwee, J., Butrick, M., Matthews, H., Price, S., Biancalana, M., *et al.* (2014). Heterozygous splice mutation in PIK3R1 causes human immunodeficiency with lymphoproliferation due to dominant activation of PI3K. The Journal of experimental medicine *211*, 2537-2547.

Martin-Cofreces, N.B., Baixauli, F., and Sanchez-Madrid, F. (2014). Immune synapse: conductor of orchestrated organelle movement. Trends in cell biology *24*, 61-72.

Martin, P., Del Hoyo, G.M., Anjuere, F., Arias, C.F., Vargas, H.H., Fernandez, L.A., Parrillas, V., and Ardavin, C. (2002). Characterization of a new subpopulation of mouse CD8alpha+ B220+ dendritic cells endowed with type 1 interferon production capacity and tolerogenic potential. Blood *100*, 383-390.

Mehta, A., Mann, M., Zhao, J.L., Marinov, G.K., Majumdar, D., Garcia-Flores, Y., Du, X., Erikci, E., Chowdhury, K., and Baltimore, D. (2015a). The microRNA-212/132 cluster regulates B cell development by targeting Sox4. The Journal of experimental medicine.

Mehta, A., Zhao, J.L., Sinha, N., Marinov, G.K., Mann, M., Kowalczyk, M.S., Galimidi, R.P., Du, X., Erikci, E., Regev, A., *et al.* (2015b). The MicroRNA-132 and MicroRNA-212 Cluster Regulates Hematopoietic Stem Cell Maintenance and Survival with Age by Buffering FOXO3 Expression. Immunity *42*, 1021-1032.

Minoda, Y., Saeki, K., Aki, D., Takaki, H., Sanada, T., Koga, K., Kobayashi, T., Takaesu, G., and Yoshimura, A. (2006). A novel Zinc finger protein, ZCCHC11, interacts with TIFA and modulates TLR signaling. Biochem Biophys Res Commun *344*, 1023-1030.

Mittelbrunn, M., Gutierrez-Vazquez, C., Villarroya-Beltri, C., Gonzalez, S., Sanchez-Cabo, F., Gonzalez, M.A., Bernad, A., and Sanchez-Madrid, F. (2011). Unidirectional transfer of microRNA-loaded exosomes from T cells to antigen-presenting cells. Nat Commun *2*, 282.

Mittelbrunn, M., Martinez del Hoyo, G., Lopez-Bravo, M., Martin-Cofreces, N.B., Scholer, A., Hugues, S., Fetler, L., Amigorena, S., Ardavin, C., and Sanchez-Madrid, F. (2009). Imaging of plasmacytoid dendritic cell interactions with T cells. Blood *113*, 75-84.

Mittelbrunn, M., and Sanchez-Madrid, F. (2012). Intercellular communication: diverse structures for exchange of genetic information. Nature reviews Molecular cell biology *13*, 328-335.

Monks, C.R.F., Freiberg, B.A., Kupfer, H., Sclaky, N., and Kupfer, A. (1998). Three-dimensional segregation of supramolecular activation clusters in T cells. Nature *395*, 82-86.

Montecalvo, A., Larregina, A.T., Shufesky, W.J., Stolz, D.B., Sullivan, M.L., Karlsson, J.M., Baty, C.J., Gibson, G.A., Erdos, G., Wang, Z., *et al.* (2012). Mechanism of transfer of functional microRNAs between mouse dendritic cells via exosomes. Blood *119*, 756-766.

Montecalvo, A., Shufesky, W.J., Stolz, D.B., Sullivan, M.G., Wang, Z., Divito, S.J., Papworth, G.D., Watkins, S.C., Robbins, P.D., Larregina, A.T., *et al.* (2008). Exosomes as a short-range mechanism to spread alloantigen between dendritic cells during T cell allorecognition. Journal of immunology *180*, 3081-3090.

Monticelli, S., Ansel, K.M., Xiao, C., Socci, N.D., Krichevsky, A.M., Thai, T.H., Rajewsky, N., Marks, D.S., Sander, C., Rajewsky, K., *et al.* (2005). MicroRNA profiling of the murine hematopoietic system. Genome Biol *6*, R71.

Morelli, A.E., Larregina, A.T., Shufesky, W.J., Sullivan, M.L., Stolz, D.B., Papworth, G.D., Zahorchak, A.F., Logar, A.J., Wang, Z., Watkins, S.C., *et al.* (2004). Endocytosis, intracellular sorting, and processing of exosomes by dendritic cells. Blood *104*, 3257-3266.

Mosmann, T.R., Cherwinski, H., Bond, M.W., Giedlin, M.A., and Coffman, R.L. (1986). Two types of murine helper T cell clone. I. Definition according to profiles of lymphokine activities and secreted proteins. Journal of immunology *136*, 2348-2357.

Muljo, S.A., Ansel, K.M., Kanellopoulou, C., Livingston, D.M., Rao, A., and Rajewsky, K. (2005). Aberrant T cell differentiation in the absence of Dicer. The Journal of experimental medicine *202*, 261-269.

Nakahama, T., Hanieh, H., Nguyen, N.T., Chinen, I., Ripley, B., Millrine, D., Lee, S., Nyati, K.K., Dubey, P.K., Chowdhury, K., *et al.* (2013). Aryl hydrocarbon receptor-mediated induction of the microRNA-132/212 cluster promotes interleukin-17-producing T-helper cell differentiation. Proceedings of the National Academy of Sciences of the United States of America *110*, 11964-11969.

Niedergang, F., Hemar, A., Hewitt, C.R., Owen, M.J., Dautry-Varsat, A., and Alcover, A. (1995). The Staphylococcus aureus enterotoxin B superantigen induces specific T cell receptor down-regulation by increasing its internalization. J Biol Chem *270*, 12839-12845.

Nolte-'t Hoen, E.N., Buschow, S.I., Anderton, S.M., Stoorvogel, W., and Wauben, M.H. (2009). Activated T cells recruit exosomes secreted by dendritic cells via LFA-1. Blood *113*, 1977-1981.

O'Connell, R.M., Rao, D.S., Chaudhuri, A.A., and Baltimore, D. (2010). Physiological and pathological roles for microRNAs in the immune system. Nat Rev Immunol *10*, 111-122.

Ostrowski, M., Carmo, N.B., Krumeich, S., Fanget, I., Raposo, G., Savina, A., Moita, C.F., Schauer, K., Hume, A.N., Freitas, R.P., *et al.* (2010). Rab27a and Rab27b control different steps of the exosome secretion pathway. Nat Cell Biol *12*, 19-30; sup pp 11-13.

Parolini, I., Federici, C., Raggi, C., Lugini, L., Palleschi, S., De Milito, A., Coscia, C., Iessi, E., Logozzi, M., Molinari, A., *et al.* (2009). Microenvironmental pH is a key factor for exosome traffic in tumor cells. J Biol Chem *284*, 34211-34222.

Pegtel, D.M., Cosmopoulos, K., Thorley-Lawson, D.A., van Eijndhoven, M.A., Hopmans, E.S., Lindenberg, J.L., de Gruijl, T.D., Wurdinger, T., and Middeldorp, J.M. (2010). Functional delivery of viral miRNAs via exosomes. Proc Natl Acad Sci U S A *107*, 6328-6333.

Perez-Hernandez, D., Gutierrez-Vazquez, C., Jorge, I., Lopez-Martin, S., Ursa, A., Sanchez-Madrid, F., Vazquez, J., and Yanez-Mo, M. (2013). The intracellular interactome of tetraspanin-enriched microdomains reveals their function as sorting machineries toward exosomes. The Journal of biological chemistry *288*, 11649-11661.

Pols, M.S., and Klumperman, J. (2009). Trafficking and function of the tetraspanin CD63. Exp Cell Res *315*, 1584-1592.

Quann, E.J., Merino, E., Furuta, T., and Huse, M. (2009). Localized diacylglycerol drives the polarization of the microtubule-organizing center in T cells. Nature immunology *10*, 627-635.

Raiborg, C., and Stenmark, H. (2009). The ESCRT machinery in endosomal sorting of ubiquitylated membrane proteins. Nature *458*, 445-452.

Raphael, I., Nalawade, S., Eagar, T.N., and Forsthuber, T.G. (2015). T cell subsets and their signature cytokines in autoimmune and inflammatory diseases. Cytokine *74*, 5-17.

Ratajczak, J., Miekus, K., Kucia, M., Zhang, J., Reca, R., Dvorak, P., and Ratajczak, M.Z. (2006a). Embryonic stem cell-derived microvesicles reprogram hematopoietic progenitors: evidence for horizontal transfer of mRNA and protein delivery. Leukemia *20*, 847-856.

Ratajczak, J., Wysoczynski, M., Hayek, F., Janowska-Wieczorek, A., and Ratajczak, M.Z. (2006b). Membrane-derived microvesicles: important and underappreciated mediators of cell-to-cell communication. Leukemia *20*, 1487-1495.

Rechavi, O., Erlich, Y., Amram, H., Flomenblit, L., Karginov, F.V., Goldstein, I., Hannon, G.J., and Kloog, Y. (2009). Cell contact-dependent acquisition of cellular and viral nonautonomously encoded small RNAs. Genes Dev *23*, 1971-1979.

Ridder, K., Keller, S., Dams, M., Rupp, A.K., Schlaudraff, J., Del Turco, D., Starmann, J., Macas, J., Karpova, D., Devraj, K., *et al.* (2014). Extracellular vesicle-mediated transfer of genetic information between the hematopoietic system and the brain in response to inflammation. PLoS Biol *12*, e1001874.

Robles-Valero, J., Martin-Cofreces, N.B., Lamana, A., Macdonald, S., Volkov, Y., and Sanchez-Madrid, F. (2010). Integrin and CD3/TCR activation are regulated by the scaffold protein AKAP450. Blood *115*, 4174-4184.

Rodriguez, A., Vigorito, E., Clare, S., Warren, M.V., Couttet, P., Soond, D.R., van Dongen, S., Grocock, R.J., Das, P.P., Miska, E.A., *et al.* (2007). Requirement of bic/microRNA-155 for normal immune function. Science *316*, 608-611.

Rossi, R.L., Rossetti, G., Wenandy, L., Curti, S., Ripamonti, A., Bonnal, R.J., Birolo, R.S., Moro, M., Crosti, M.C., Gruarin, P., *et al.* (2011). Distinct microRNA signatures in human lymphocyte subsets and enforcement of the naive state in CD4+ T cells by the microRNA miR-125b. Nature immunology *12*, 796-803.

Ruby, J.G., Jan, C.H., and Bartel, D.P. (2007). Intronic microRNA precursors that bypass Drosha processing. Nature *448*, 83-86.

Ruegger, S., and Grosshans, H. (2012). MicroRNA turnover: when, how, and why. Trends Biochem Sci *37*, 436-446.

Sancho, D., Vicente-Manzanares, M., Mittelbrunn, M., Montoya, M.C., Gordon-Alonso, M., Serrador, J.M., and Sanchez-Madrid, F. (2002). Regulation of microtubule-organizing center orientation and actomyosin cytoskeleton rearrangement during immune interactions. Immunol Rev *189*, 84-97.

Sandberg, R., Neilson, J.R., Sarma, A., Sharp, P.A., and Burge, C.B. (2008). Proliferating cells express mRNAs with shortened 3' untranslated regions and fewer microRNA target sites. Science *320*, 1643-1647.

Savina, A., Vidal, M., and Colombo, M.I. (2002). The exosome pathway in K562 cells is regulated by Rab11. Journal of cell science *115*, 2505-2515.

Schmidt, M.J., West, S., and Norbury, C.J. (2011). The human cytoplasmic RNA terminal U-transferase ZCCHC11 targets histone mRNAs for degradation. RNA *17*, 39-44.

Segura, E., Amigorena, S., and Thery, C. (2005a). Mature dendritic cells secrete exosomes with strong ability to induce antigen-specific effector immune responses. Blood Cells Mol Dis *35*, 89-93.

Segura, E., Nicco, C., Lombard, B., Veron, P., Raposo, G., Batteux, F., Amigorena, S., and Thery, C. (2005b). ICAM-1 on exosomes from mature dendritic cells is critical for efficient naive T-cell priming. Blood *106*, 216-223.

Shaked, I., Meerson, A., Wolf, Y., Avni, R., Greenberg, D., Gilboa-Geffen, A., and Soreq, H. (2009). MicroRNA-132 potentiates cholinergic anti-inflammatory signaling by targeting acetylcholinesterase. Immunity *31*, 965-973.

Shen, B., and Goodman, H.M. (2004). Uridine addition after microRNA-directed cleavage. Science *306*, 997.

Simons, M., and Raposo, G. (2009). Exosomes--vesicular carriers for intercellular communication. Curr Opin Cell Biol *21*, 575-581.

Skog, J., Wurdinger, T., van Rijn, S., Meijer, D.H., Gainche, L., Sena-Esteves, M., Curry, W.T., Jr., Carter, B.S., Krichevsky, A.M., and Breakefield, X.O. (2008). Glioblastoma microvesicles transport RNA and proteins that promote tumour growth and provide diagnostic biomarkers. Nat Cell Biol *10*, 1470-1476.

Sonkoly, E., Stahle, M., and Pivarcsi, A. (2008). MicroRNAs and immunity: novel players in the regulation of normal immune function and inflammation. Semin Cancer Biol *18*, 131-140.

Steiner, D.F., Thomas, M.F., Hu, J.K., Yang, Z., Babiarz, J.E., Allen, C.D., Matloubian, M., Blelloch, R., and Ansel, K.M. (2011). MicroRNA-29 regulates T-box transcription factors and interferon-gamma production in helper T cells. Immunity *35*, 169-181.

Stinchcombe, J.C., Bossi, G., Booth, S., and Griffiths, G.M. (2001). The immunological synapse of CTL contains a secretory domain and membrane bridges. Immunity *15*, 751-761.

Stinchcombe, J.C., Majorovits, E., Bossi, G., Fuller, S., and Griffiths, G.M. (2006). Centrosome polarization delivers secretory granules to the immunological synapse. Nature *443*, 462-465.

Sun, B., and Zhang, Y. (2014). Overview of orchestration of CD4+ T cell subsets in immune responses. Adv Exp Med Biol *841*, 1-13.

Tabas-Madrid, D., Muniategui, A., Sanchez-Caballero, I., Martinez-Herrera, D.J., Sorzano, C.O., Rubio, A., and Pascual-Montano, A. (2014). Improving miRNA-mRNA interaction predictions. BMC Genomics *15 Suppl 10*, S2.

Tavazoie, S.F., Alarcon, C., Oskarsson, T., Padua, D., Wang, Q., Bos, P.D., Gerald, W.L., and Massague, J. (2008). Endogenous human microRNAs that suppress breast cancer metastasis. Nature *451*, 147-152.

Thery, C., Amigorena, S., Raposo, G., and Clayton, A. (2006). Isolation and characterization of exosomes from cell culture supernatants and biological fluids. Curr Protoc Cell Biol *Chapter 3*, Unit 3 22.

Thery, C., Ostrowski, M., and Segura, E. (2009). Membrane vesicles as conveyors of immune responses. Nat Rev Immunol *9*, 581-593.

Thomas, M.F., Abdul-Wajid, S., Panduro, M., Babiarz, J.E., Rajaram, M., Woodruff, P., Lanier, L.L., Heissmeyer, V., and Ansel, K.M. (2012). Eri1 regulates microRNA homeostasis and mouse lymphocyte development and antiviral function. Blood *120*, 130-142.

Thornton, J.E., Du, P., Jing, L., Sjekloca, L., Lin, S., Grossi, E., Sliz, P., Zon, L.I., and Gregory, R.I. (2015). Selective microRNA uridylation by Zcchc6 (TUT7) and Zcchc11 (TUT4). Nucleic Acids Res *42*, 11777-11791.

Tian, T., Wang, Y., Wang, H., Zhu, Z., and Xiao, Z. (2010). Visualizing of the cellular uptake and intracellular trafficking of exosomes by live-cell microscopy. J Cell Biochem *111*, 488-496.

Trajkovic, K., Hsu, C., Chiantia, S., Rajendran, L., Wenzel, D., Wieland, F., Schwille, P., Brugger, B., and Simons, M. (2008). Ceramide triggers budding of exosome vesicles into multivesicular endosomes. Science *319*, 1244-1247.

Valadi, H., Ekstrom, K., Bossios, A., Sjostrand, M., Lee, J.J., and Lotvall, J.O. (2007). Exosome-mediated transfer of mRNAs and microRNAs is a novel mechanism of genetic exchange between cells. Nat Cell Biol *9*, 654-659.

Valitutti, S., Dessing, M., Aktories, K., Gallati, H., and Lanzavecchia, A. (1995). Sustained signaling leading to T cell activation results from prolonged T cell receptor occupancy. Role of T cell actin cytoskeleton. J Exp Med *181*, 577-584.

Vanhaesebroeck, B., Guillermet-Guibert, J., Graupera, M., and Bilanges, B. (2010). The emerging mechanisms of isoform-specific PI3K signalling. Nature reviews Molecular cell biology *11*, 329-341.

Varma, R., Campi, G., Yokosuka, T., Saito, T., and Dustin, M.L. (2006). T cell receptor-proximal signals are sustained in peripheral microclusters and terminated in the central supramolecular activation cluster. Immunity *25*, 117-127.

Ventura, A., Young, A.G., Winslow, M.M., Lintault, L., Meissner, A., Erkeland, S.J., Newman, J., Bronson, R.T., Crowley, D., Stone, J.R., *et al.* (2008). Targeted deletion reveals essential and overlapping functions of the miR-17 through 92 family of miRNA clusters. Cell *132*, 875-886.

Vicente-Manzanares, M., and Sanchez-Madrid, F. (2004). Role of the cytoskeleton during leukocyte responses. Nat Rev Immunol *4*, 110-122.

Vidal, M.J., and Stahl, P.D. (1993). The small GTP-binding proteins Rab4 and ARF are associated with released exosomes during reticulocyte maturation. Eur J Cell Biol *60*, 261-267.

Villarroya-Beltri, C., Gutierrez-Vazquez, C., Sanchez-Cabo, F., Perez-Hernandez, D., Vazquez, J., Martin-Cofreces, N., Martinez-Herrera, D.J., Pascual-Montano, A., Mittelbrunn, M., and Sanchez-Madrid, F. (2013). Sumoylated hnRNPA2B1 controls the sorting of miRNAs into exosomes through binding to specific motifs. Nat Commun *4*, 2980.

Wightman, B., Ha, I., and Ruvkun, G. (1993). Posttranscriptional regulation of the heterochronic gene lin-14 by lin-4 mediates temporal pattern formation in C. elegans. Cell *75*, 855-862.

Wyman, S.K., Knouf, E.C., Parkin, R.K., Fritz, B.R., Lin, D.W., Dennis, L.M., Krouse, M.A., Webster, P.J., and Tewari, M. (2011). Post-transcriptional generation of miRNA variants by multiple nucleotidyl transferases contributes to miRNA transcriptome complexity. Genome Res *21*, 1450-1461.

Xiao, C., and Rajewsky, K. (2009). MicroRNA control in the immune system: basic principles. Cell *136*, 26-36.

Xiao, C., Srinivasan, L., Calado, D.P., Patterson, H.C., Zhang, B., Wang, J., Henderson, J.M., Kutok, J.L., and Rajewsky, K. (2008). Lymphoproliferative disease and autoimmunity in mice with increased miR-17-92 expression in lymphocytes. Nature immunology *9*, 405-414.

Xie, Y., Zhang, H., Li, W., Deng, Y., Munegowda, M.A., Chibbar, R., Qureshi, M., and Xiang, J. (2010). Dendritic cells recruit T cell exosomes via exosomal LFA-1 leading to inhibition of CD8+ CTL responses through downregulation of peptide/MHC class I and Fas ligand-mediated cytotoxicity. Journal of immunology *185*, 5268-5278.

Yanez-Mo, M., Barreiro, O., Gordon-Alonso, M., Sala-Valdes, M., and Sanchez-Madrid, F. (2009). Tetraspanin-enriched microdomains: a functional unit in cell plasma membranes. Trends Cell Biol *19*, 434-446.

Yang, W., Chendrimada, T.P., Wang, Q., Higuchi, M., Seeburg, P.H., Shiekhattar, R., and Nishikura, K. (2006). Modulation of microRNA processing and expression through RNA editing by ADAR deaminases. Nature structural & molecular biology *13*, 13-21.

Yoda, M., Cifuentes, D., Izumi, N., Sakaguchi, Y., Suzuki, T., Giraldez, A.J., and Tomari, Y. (2013). Poly(A)-specific ribonuclease mediates 3'-end trimming of Argonaute2-cleaved precursor microRNAs. Cell Rep *5*, 715-726.

Zamore, P.D., Tuschl, T., Sharp, P.A., and Bartel, D.P. (2000). RNAi: double-stranded RNA directs the ATP-dependent cleavage of mRNA at 21 to 23 nucleotide intervals. Cell *101*, 25-33.

Zernecke, A., Bidzhekov, K., Noels, H., Shagdarsuren, E., Gan, L., Denecke, B., Hristov, M., Koppel, T., Jahantigh, M.N., Lutgens, E., *et al.* (2009). Delivery of microRNA-126 by apoptotic bodies induces CXCL12-dependent vascular protection. Sci Signal *2*, ra81.

Zhang, Y., Liu, D., Chen, X., Li, J., Li, L., Bian, Z., Sun, F., Lu, J., Yin, Y., Cai, X., *et al.* (2010). Secreted monocytic miR-150 enhances targeted endothelial cell migration. Mol Cell *39*, 133-144.

Zhao, Y., Yu, Y., Zhai, J., Ramachandran, V., Dinh, T.T., Meyers, B.C., Mo, B., and Chen, X. (2012). The Arabidopsis nucleotidyl transferase HESO1 uridylates unmethylated small RNAs to trigger their degradation. Curr Biol *22*, 689-694.

ANNEXES

9 ANNEXES

Annex Table 9.1
Proteins identified in exosome extracts from T lymphoblasts
Proteins detected in exosomes lysates with at least 2 peptides indentified are presented.

Accession Number	Protein name	# Peptides
P08575	Leukocyte common antigen	72
P08133	Annexin A6	43
P06239	Proto-oncogene tyrosine-protein kinase LCK	38
P26038	Moesin	38
Q9H4M9	EH domain-containing protein 1	38
P14618	Pyruvate kinase isozymes M1/M2	37
B0I1T2	Myosin-Ig	36
P15311	Ezrin	32
P62736	Actin, aortic smooth muscle	32
Q00610	Clathrin heavy chain 1	27
P20701	Integrin alpha-L	24
P11142	Heat shock cognate 71 kDa protein	23
Q13885	Tubulin beta-2A chain	23
P00558	Phosphoglycerate kinase 1	22
P05107	Integrin beta-2	22
P07355	Annexin A2	22
P30443	HLA class I histocompatibility antigen, A-1 alpha chain	22
P46940	Ras GTPase-activating-like protein IQGAP1	22
P13612	Integrin alpha-4	21
P06733	Alpha-enolase	20
P27487	Dipeptidyl peptidase 4	20
P68104	Elongation factor 1-alpha 1	20
Q14254	Flotillin-2	20
Q14764	Major vault protein	20
Q71U36	Tubulin alpha-1A chain	20
O14745	Na(+)/H(+) exchange regulatory cofactor NHE-RF1	19
O75955	Flotillin-1	19
P04406	Glyceraldehyde-3-phosphate dehydrogenase	19
P08195	4F2 cell-surface antigen heavy chain	19
P13796	Plastin-2	19
P62873	Guanine nucleotide-binding protein G(I)/G(S)/G(T) subunit	19
P01892	HLA class I histocompatibility antigen, A-2 alpha chain	18
P04899	Guanine nucleotide-binding protein G(i), alpha-2 subunit	18

P05362	Intercellular adhesion molecule 1	18
O00299	Chloride intracellular channel protein 1	17
P02786	Transferrin receptor protein 1	16
P62834	Ras-related protein Rap-1A	16
O14672	Disintegrin and metalloproteinase domain-containing prot	15
P05023	Sodium/potassium-transporting ATPase subunit alpha-1	15
P16284	Platelet endothelial cell adhesion molecule	15
P31946	14-3-3 protein beta/alpha	15
P84077	ADP-ribosylation factor 1	15
Q13576	Ras GTPase-activating-like protein IQGAP2	15
Q15758	Neutral amino acid transporter B(0)	15
Q86UX7	Fermitin family homolog 3	15
Q96BY6	Dedicator of cytokinesis protein 10	15
P06729	T-cell surface antigen CE2	14
P20963	T-cell surface glycoprotein CE3 zeta chain	14
P52566	Rho GDP-dissociation inhibitor 2	14
Q86YV0	RAS protein activator like-3	14
P08758	Annexin A5	13
P10114	Ras-related protein Rap-2a	13
Q6UWD8	Transmembrane protein C16orf54	13
Q9H4E7	Differentially expressed in FDCP 6 homolog	13
Q9Y3P8	Signaling threshold-regulating transmembrane adapter 1	13
P27105	Erythrocyte band 7 integral membrane protein	12
P43007	Neutral amino acid transporter A	12
P60709	Actin, cytoplasmic 1	12
P61586	Transforming protein RhoA	12
P62136	Serine/threonine-protein phosphatase PP1-alpha catalytic	12
P63096	Guanine nucleotide-binding protein G(i), alpha-1 subunit	12
Q9H223	EH domain-containing protein 4	12
Q9Y490	Talin-1	12
O95466	Formin-like protein 1	11
P04075	Fructose-bisphosphate aldolase A	11
P05556	Integrin beta-1	11
P07766	T-cell surface glycoprotein CE3 epsilon chain	11
P16070	CE44 antigen	11
P26010	Integrin beta-7	11
P50995	Annexin A11	11
P62805	Histone H4	11
P62937	Peptidyl-prolyl cis-trans isomerase A	11
Q8WUM4	Programmed cell death 6-interacting protein	11

Q969P0	Immunoglobulin superfamily member 8	11
Q99828	Calcium and integrin-binding protein 1	11
Q9P265	Disco-interacting protein 2 homolog B	11
P01023	Alpha-2-macroglobulin	10
P04229	HLA class II histocompatibility antigen, DRB1-1 beta chain	10
P07737	Profilin-1	10
P08754	Guanine nucleotide-binding protein G(k) subunit alpha	10
P09525	Annexin A4	10
P09693	T-cell surface glycoprotein CE3 gamma chain	10
P21333	Filamin-A	10
P33778	Histone H2B type 1-B	10
P50395	Rab GDP dissociation inhibitor beta	10
P52907	F-actin-capping protein subunit alpha-1	10
P84095	Rho-related GTP-binding protein RhoG	10
Q8TDB8	Solute carrier family 2, facilitated glucose transporter	10
P01903	HLA class II histocompatibility antigen, DR alpha chain	9
P04083	Annexin A1	9
P04234	T-cell surface glycoprotein CE3 delta chain	9
P06127	T-cell surface glycoprotein CE5	9
P07195	L-lactate dehydrogenase B chain	9
P27701	CD82 antigen	9
P31146	Coronin-1A	9
P35579	Myosin-9	9
P42356	Phosphatidylinositol 4-kinase alpha	9
P61006	Ras-related protein Rab-8A	9
P62330	ADP-ribosylation factor 6	9
Q14761	Protein tyrosine phosphatase receptor type C-associated p	9
Q7L576	Cytoplasmic FMR1-interacting protein 1	9
Q9BXI6	TBC1 domain family member 10A	9
O94804	Serine/threonine-protein kinase 10	8
P01732	T-cell surface glycoprotein CD8 alpha chain	8
P01889	HLA class I histocompatibility antigen, B-7 alpha chain	8
P11215	Integrin alpha-M	8
P18462	HLA class I histocompatibility antigen, A-25 alpha chain	8
P21580	Tumor necrosis factor, alpha-induced protein 3	8
P23528	Cofilin-1	8
P28907	ADP-ribosyl cyclase 1	8
P42224	Signal transducer and activator of transcription 1-alpha	8
P51149	Ras-related protein Rab-7a	8
P54709	Sodium/potassium-transporting ATPase subunit beta-3	8

P60174	Triosephosphate isomerase	8
P60660	Myosin light polypeptide 6	8
P60953	Cell division control protein 42 homolog	8
P61158	Actin-related protein 3	8
P62258	14-3-3 protein epsilon	8
P63000	Ras-related C3 botulinum toxin substrate 1	8
P63104	14-3-3 protein zeta/delta	8
Q15286	Ras-related protein Rab-35	8
Q8IWA5	Choline transporter-like protein 2	8
Q96F07	Cytoplasmic FMR1-interacting protein 2	8
Q9NWQ8	Phosphoprotein associated with glycosphingolipid-enriched	8
O75083	WD repeat-containing protein 1	7
O95819	Mitogen-activated protein kinase kinase kinase kinase 4	7
P02768	Serum albumin	7
P06744	Glucose-6-phosphate isomerase	7
P08670	Vimentin	7
P11233	Ras-related protein Ral-A	7
P11836	B-lymphocyte antigen CE20	7
P15153	Ras-related C3 botulinum toxin substrate 2	7
P16150	Leukosialin	7
P23381	Tryptophanyl-tRNA synthetase, cytoplasmic	7
P54652	Heat shock-related 70 kDa protein 2	7
P61160	Actin-related protein 2	7
P62070	Ras-related protein R-Ras2	7
Q5JWF2	Guanine nucleotide-binding protein G(s) subunit alpha is	7
Q8IU68	Transmembrane channel-like protein 8	7
Q8N5I2	Arrestin domain-containing protein 1	7
O00161	Synaptosomal-associated protein 23	6
O00560	Syntenin-1	6
P01730	T-cell surface glycoprotein CE4	6
P01909	HLA class II histocompatibility antigen, DQ alpha 1 chain	6
P01918	HLA class II histocompatibility antigen, DQ(1) beta chain	6
P04440	HLA class II histocompatibility antigen, DP beta 1 chain	6
P09326	CE48 antigen	6
P11166	Solute carrier family 2, facilitated glucose transporter	6
P13761	HLA class II histocompatibility antigen, DRB1-7 beta chain	6
P35613	Basigin	6
P37802	Transgelin-2	6
P48960	CD97 antigen	6
P69905	Hemoglobin subunit alpha	6

P78371	T-complex protein 1 subunit beta	6
Q14156	Protein EFR3 homolog A	6
Q14242	P-selectin glycoprotein ligand 1	6
Q9Y4F9	Protein FAM65B	6
O15144	Actin-related protein 2/3 complex subunit 2	5
P00338	L-lactate dehydrogenase A chain	5
P01848	T-cell receptor alpha chain C region	5
P01850	T-cell receptor beta chain C region	5
P13639	Elongation factor 2	5
P23634	Plasma membrane calcium-transporting ATPase 4	5
P30203	T-cell differentiation antigen CD6	5
P30447	HLA class I histocompatibility antigen, A-23 alpha chain	5
P30461	HLA class I histocompatibility antigen, B-13 alpha chain	5
P32942	Intercellular adhesion molecule 3	5
P55160	Nck-associated protein 1-like	5
P61224	Ras-related protein Rap-1b	5
P61225	Ras-related protein Rap-2b	5
P62491	Ras-related protein Rab-11A	5
P62879	Guanine nucleotide-binding protein G(I)/G(S)/G(T) subunit	5
Q06830	Peroxiredoxin-1	5
Q13077	TNF receptor-associated factor 1	5
Q14344	Guanine nucleotide-binding protein subunit alpha-13	5
Q30134	HLA class II histocompatibility antigen, DRB1-8 beta chai	5
Q58FF7	Putative heat shock protein HSP 90-beta-3	5
Q7Z403	Transmembrane channel-like protein 6	5
Q8NG11	Tetraspanin-14	5
Q96QV6	Histone H2A type 1-A	5
Q9NUQ9	Protein FAM49B	5
P00734	Prothrombin	4
P00738	Haptoglobin	4
P01024	Complement C3	4
P05090	Apolipoprotein D	4
P07437	Tubulin beta chain	4
P09211	Glutathione S-transferase P	4
P12259	Coagulation factor V	4
P12814	Alpha-actinin-1	4
P13164	Interferon-induced transmembrane protein 1	4
P14222	Perforin-1	4
P15880	40S ribosomal protein S2	4
P16403	Histone H1.2	4

P18669	Phosphoglycerate mutase 1	4
P20073	Annexin A7	4
P20702	Integrin alpha-X	4
P22629	STRAV Streptavidin	4
P30685	HLA class I histocompatibility antigen, B-35 alpha chain	4
P31949	Protein S100-A11	4
P32455	Interferon-induced guanylate-binding protein 1	4
P50991	T-complex protein 1 subunit delta	4
P59768	Guanine nucleotide-binding protein G(I)/G(S)/G(O) subunit	4
P60033	CD81 antigen	4
P60842	Eukaryotic initiation factor 4A-I	4
P61073	C-X-C chemokine receptor type 4	4
P62158	Calmodulin	4
P62241	40S ribosomal protein S8	4
P62249	40S ribosomal protein S16	4
P62807	Histone H2B type 1-C/E/F/G/I	4
P62988	Ubiquitin	4
P68371	Tubulin beta-2C chain	4
Q01518	Adenylyl cyclase-associated protein 1	4
Q07020	60S ribosomal protein L18	4
Q10589	Bone marrow stromal antigen 2	4
Q12846	Syntaxin-4	4
Q13291	Signaling lymphocytic activation molecule	4
Q14699	Raftlin	4
Q15025	TNFAIP3-interacting protein 1	4
Q58FF8	Putative heat shock protein HSP 90-beta 2	4
Q9BYT8	Neurolysin, mitochondrial	4
Q9H3M7	Thioredoxin-interacting protein	4
Q9H4B7	Tubulin beta-1 chain	4
Q9HBH0	Rho-related GTP-binding protein RhoF	4
O00159	Myosin-Ic	3
O00231	26S proteasome non-ATPase regulatory subunit 11	3
O43143	Putative pre-mRNA-splicing factor ATP-dependent RNA heli	3
O75131	Copine-3	3
O75340	Programmed cell death protein 6	3
O75427	Leucine-rich repeat and calponin homology domain-contain	3
P01008	Antithrombin-III	3
P01112	GTPase HRas	3
P02765	Alpha-2-HS-glycoprotein	3

P04233	HLA class II histocompatibility antigen gamma chain	3
P04908	Histone H2A type 1-B/E	3
P06241	Proto-oncogene tyrosine-protein kinase Fyn	3
P07900	Heat shock protein HSP 90-alpha	3
P08238	Heat shock protein HSP 90-beta	3
P09972	Fructose-bisphosphate aldolase C	3
P11049	Leukocyte antigen CE37	3
P11171	Protein 4.1	3
P11234	Ras-related protein Ral-B	3
P16401	Histone H1.5	3
P18124	60S ribosomal protein L7	3
P19397	Leukocyte surface antigen CE53	3
P19440	Gamma-glutamyltranspeptidase 1	3
P20020	Plasma membrane calcium-transporting ATPase 1	3
P20036	HLA class II histocompatibility antigen, DP alpha 1 chain	3
P20039	HLA class II histocompatibility antigen, DRB1-11 beta chain	3
P21980	Protein-glutamine gamma-glutamyltransferase 2	3
P22749	Granulysin	3
P27348	14-3-3 protein theta	3
P29350	Tyrosine-protein phosphatase non-receptor type 6	3
P29965	CE40 ligand	3
P30460	HLA class I histocompatibility antigen, B-8 alpha chain	3
P30481	HLA class I histocompatibility antigen, B-44 alpha chain	3
P30740	Leukocyte elastase inhibitor	3
P36578	60S ribosomal protein L4	3
P39023	60S ribosomal protein L3	3
P41240	Tyrosine-protein kinase CSK	3
P46776	60S ribosomal protein L27a	3
P46781	40S ribosomal protein S9	3
P50914	60S ribosomal protein L14	3
P52333	Tyrosine-protein kinase JAK3	3
P57075	Ubiquitin-associated and SH3 domain-containing protein A	3
P61769	Beta-2-microglobulin	3
P62847	40S ribosomal protein S24	3
P78527	DNA-dependent protein kinase catalytic subunit	3
P80723	Brain acid soluble protein 1	3
P81605	Dermcidin	3
Q04917	14-3-3 protein eta	3
Q08431	Lactadherin	3
Q15833	Syntaxin-binding protein 2	3

Q58FG0	Putative heat shock protein HSP 90-alpha A5	3
Q86X29	Lipolysis-stimulated lipoprotein receptor	3
Q92930	Ras-related protein Rab-8B	3
Q96TA1	Niban-like protein 1	3
Q9C0H2	Protein tweety homolog 3	3
Q9H2G2	STE20-like serine/threonine-protein kinase	3
Q9H4G4	Golgi-associated plant pathogenesis-related protein 1	3
Q9H665	Transmembrane protein 149	3
Q9NR48	Probable histone-lysine N-methyltransferase ASH1L	3
Q9NRY6	Phospholipid scramblase 3	3
Q9NZA1	Chloride intracellular channel protein 5	3
Q9P289	Serine/threonine-protein kinase MST4	3
Q9UI08	Ena/VASP-like protein	3
O15162	Phospholipid scramblase 1	2
O15260	Surfeit locus protein 4	2
O43491	Band 4.1-like protein 2	2
O43561	Linker for activation of T-cells family member 1	2
O60361	Putative nucleoside diphosphate kinase	2
O60488	Long-chain-fatty-acid--CoA ligase 4	2
O60880	SH2 domain-containing protein 1A	2
O75044	SLIT-ROBO Rho GTPase-activating protein 2	2
O75531	Barrier-to-autointegration factor	2
P00491	Purine nucleoside phosphorylase	2
P00739	Haptoglobin-related protein	2
P01111	GTPase NRas	2
P01906	HLA class II histocompatibility antigen, DQ alpha 2 chain	2
P01911	HLA class II histocompatibility antigen, DRB1-15 beta chain	2
P01919	HLA class II histocompatibility antigen, DQ(W1.1) beta chain	2
P02771	Alpha-fetoprotein	2
P02788	Lactotransferrin	2
P02792	Ferritin light chain	2
P04080	Cystatin-B	2
P05109	Protein S100-A8	2
P05164	Myeloperoxidase	2
P05534	HLA class I histocompatibility antigen, A-24 alpha chain	2
P05537	HLA class II histocompatibility antigen, DQ(W3) beta chain	2
P05543	Thyroxine-binding globulin	2
P06396	Gelsolin	2
P06702	Protein S100-A9	2

P08648	Integrin alpha-5	2
P08697	Alpha-2-antiplasmin	2
P08962	CD63 antigen	2
P09382	Galectin-1	2
P09543	2',3'-cyclic-nucleotide 3'-phosphodiesterase	2
P10599	Thioredoxin	2
P11021	78 kDa glucose-regulated protein	2
P13987	CE59 glycoprotein	2
P14649	Myosin light chain 6B	2
P15144	Aminopeptidase N	2
P18433	Receptor-type tyrosine-protein phosphatase alpha	2
P19971	Thymidine phosphorylase	2
P20333	Tumor necrosis factor receptor superfamily member 1B	2
P20339	Ras-related protein Rab-5A	2
P23284	Peptidyl-prolyl cis-trans isomerase B	2
P25311	Zinc-alpha-2-glycoprotein	2
P25445	Tumor necrosis factor receptor superfamily member 6	2
P25787	Proteasome subunit alpha type-2	2
P29966	Myristoylated alanine-rich C-kinase substrate	2
P30153	Serine/threonine-protein phosphatase 2A 65 kDa regulatory	2
P30462	HLA class I histocompatibility antigen, B-14 alpha chain	2
P30501	HLA class I histocompatibility antigen, Cw-2 alpha chain	2
P30626	Sorcin	2
P31150	Rab GDP dissociation inhibitor alpha	2
P32119	Peroxiredoxin-2	2
P35241	Radixin	2
P40121	Macrophage-capping protein	2
P40227	T-complex protein 1 subunit zeta	2
P43403	Tyrosine-protein kinase ZAP-70	2
P46939	Utrophin	2
P47756	F-actin-capping protein subunit beta	2
P48643	T-complex protein 1 subunit epsilon	2
P49327	Fatty acid synthase	2
P50552	Vasodilator-stimulated phosphoprotein	2
P51148	Ras-related protein Rab-5C	2
P52565	Rho GDP-dissociation inhibitor 1	2
P53985	Monocarboxylate transporter 1	2
P53990	IST1 homolog	2
P59998	Actin-related protein 2/3 complex subunit 4	2

P61020	Ras-related protein Rab-5B	2
P61026	Ras-related protein Rab-10	2
P61978	Heterogeneous nuclear ribonucleoprotein K	2
P61981	14-3-3 protein gamma	2
P62424	60S ribosomal protein L7a	2
P68363	Tubulin alpha-1B chain	2
P68871	Hemoglobin subunit beta	2
Q02878	60S ribosomal protein L6	2
Q06323	Proteasome activator complex subunit 1	2
Q08722	Leukocyte surface antigen CE47	2
Q13200	26S proteasome non-ATPase regulatory subunit 2	2
Q13277	Syntaxin-3	2
Q14019	Coactosin-like protein	2
Q14160	Protein scribble homolog	2
Q14847	LIM and SH3 domain protein 1	2
Q15283	Ras GTPase-activating protein 2	2
Q15762	CE226 antigen	2
Q16695	Histone H3.1t	2
Q53GL0	Pleckstrin homology domain-containing family O member 1	2
Q58EX2	Protein sidekick-2	2
Q6P2Q9	Pre-mRNA-processing-splicing factor 8	2
Q71UI9	Histone H2A.V	2
Q86VP6	Cullin-associated NEDD8-dissociated protein 1	2
Q8N4C8	Misshapen-like kinase 1	2
Q8NF50	Dedicator of cytokinesis protein 8	2
Q8NHW5	60S acidic ribosomal protein P0-like	2
Q8WV92	MIT domain-containing protein 1	2
Q92542	Nicastrin	2
Q92598	Heat shock protein 105 kDa	2
Q95365	HLA class I histocompatibility antigen, B-38 alpha chain	2
Q96A08	Histone H2B type 1-A	2
Q96DU3	SLAM family member 6	2
Q9BSJ8	Extended synaptotagmin-1	2
Q9BYX7	Beta-actin-like protein 3	2
Q9BZ29	Dedicator of cytokinesis protein 9	2
Q9H400	Lck-interacting transmembrane adapter 1	2
Q9UJT0	Tubulin epsilon chain	2
Q9ULT0	Tetratricopeptide repeat protein 7A	2
Q9Y265	RuvB-like 1	2
Q9Y376	Calcium-binding protein 39	2

Q9Y3L5	Ras-related protein Rap-2c	2
Q9Y6W5	Wiskott-Aldrich syndrome protein family member 2	2
Q9Y6W8	Inducible T-cell costimulator	2

Annex Table 9.2
Microarray analysis of exosomal miRNAs *vs* the miRNAs of their respective donor cells. miRNAs differentially represented in exosomes compared with their respective parental cells are shown. In each file, the columns represent: ProbeID; logFC= log Fold Change; A: average expression of the miRNA across all samples; P-value from the moderated t-test; Adjpvalue from the moderated t-test.

SUMMARY

DEG	DCs Cells vs Ex	J Cells vs Ex	R Cells vs Ex	Cells_J vs R	J Ex vs R Cell
Up	140	148	21	54	88
Down	8	89	47	29	105

DCs Cells vs Exosomes

Probe	logFC	A	pvalue	adjpvalue
hsa-miR-335	-12.0756	-0.95529	6.63E-10	2.97E-07
hsa-miR-760	-4.36396	2.490711	0.002414	0.010181
hsa-miR-630	-4.2164	7.597597	0.008613	0.027434
hsa-miR-632	-3.61822	0.599001	0.002437	0.010181
hsa-miR-654-5p	-3.02642	3.7374	0.008465	0.027223
hsa-miR-671-5p	-2.96257	3.809781	0.012867	0.039667
hcmv-miR-US4	-2.94002	2.537085	0.001953	0.00873
kshv-miR-K12-3	-2.67215	7.030808	0.006267	0.021119
hsa-miR-505	1.99294	3.278082	0.006284	0.021119
hsa-miR-326	2.316675	0.911044	0.002123	0.009304
hsa-miR-769-5p	2.369604	2.928335	0.006441	0.021169
hsa-miR-199b-5p	2.369803	1.297736	0.003591	0.013838
hsa-miR-502-5p	2.395754	1.218676	0.002381	0.010136
hsa-miR-551b	2.443113	1.146242	0.005615	0.019609
hsa-miR-92a	2.647713	7.888559	0.005029	0.017985
hsa-miR-221*	2.666148	0.780369	0.006207	0.021119
hsa-miR-223*	2.697283	-0.20081	0.011054	0.034554
hsa-miR-892b	2.767039	3.400897	0.006488	0.021169

hsa-miR-186	2.804144	4.096928	0.005309	0.018836
kshv-miR-K12-12	2.821377	0.498928	0.013499	0.041329
hsa-miR-542-5p	2.870363	2.439135	0.013974	0.042493
hsa-let-7i*	2.941409	0.37316	0.006353	0.021169
hsa-miR-188-3p	2.949323	-1.11087	0.010288	0.032384
hsa-miR-155	3.042164	6.39405	0.01241	0.038523
hsa-miR-324-3p	3.050461	6.555508	0.008654	0.027434
hsa-miR-340*	3.102608	2.002909	0.001542	0.007331
hsa-miR-132*	3.282246	0.940431	0.000563	0.003267
hsa-miR-148a	3.437728	5.479736	0.003689	0.014092
hsa-miR-450a	3.505534	1.522633	0.00017	0.001621
hsa-miR-361-3p	3.54784	2.411733	0.001173	0.0057
hsa-miR-363	3.57258	3.132228	0.003887	0.014605
hsa-miR-501-3p	3.659003	0.677307	0.016548	0.049978
hsa-miR-25	3.722619	7.128739	0.000979	0.00503
hsa-miR-195	3.739732	1.98425	0.000665	0.003762
hsa-miR-132	3.766694	2.179877	0.00298	0.011789
hsa-miR-500*	3.811061	2.523807	0.000663	0.003762
hsa-miR-181b	3.823066	4.408795	0.00238	0.010136
hsa-miR-22*	3.829635	0.556572	0.001013	0.005145
hsa-miR-342-3p	3.997499	6.228904	0.005895	0.02027
hsa-miR-128	3.997814	4.50142	0.002732	0.011308
hsa-miR-221	4.040188	3.755918	0.000132	0.001552
hsa-miR-342-5p	4.047348	2.278087	0.002927	0.011681
hsa-miR-181a	4.048904	6.633956	0.002889	0.011681
hsa-miR-18b	4.087797	4.354533	0.004956	0.017864
hsa-miR-130b	4.090896	5.623911	0.001763	0.008101
hsa-miR-193b	4.11264	4.68102	0.000222	0.001807
hsa-miR-362-3p	4.139051	1.577961	8.65E-05	0.001248
hsa-miR-886-3p	4.176504	2.104636	0.000284	0.002116
hsa-miR-361-5p	4.231149	4.611954	0.000246	0.001931
hsa-miR-30a	4.246496	1.314469	0.000521	0.003137
hsa-miR-223	4.247999	6.524582	0.000203	0.001745
hsa-miR-331-3p	4.289376	5.767948	0.00018	0.001675
hsa-miR-564	4.296045	2.565284	0.003888	0.014605
hsa-miR-425	4.333441	6.216363	0.001159	0.005693
hsa-miR-100	4.336212	0.796681	0.002208	0.00958
hsa-miR-125b	4.337546	2.884451	0.001598	0.007521

hsa-miR-502-3p	4.51077	1.453375	0.001774	0.008101
hsa-miR-93	4.511776	6.651276	0.00026	0.002003
hsa-let-7b	4.51446	6.372928	0.001482	0.007122
hsa-miR-23b	4.522701	4.232274	7.08E-05	0.001173
hsa-miR-181c	4.538496	1.041504	0.004436	0.016255
hsa-miR-590-5p	4.542851	4.424362	0.000368	0.002456
hsa-miR-330-3p	4.559807	1.68355	0.000196	0.001745
hsa-miR-30c	4.625263	5.281099	8.18E-05	0.001219
hsa-miR-378	4.629269	5.655411	0.000717	0.00391
hsa-miR-345	4.649667	1.488388	0.005737	0.01988
hsa-miR-139-3p	4.669857	-0.254	0.005567	0.019594
hsa-miR-146a	4.71275	5.349883	0.00355	0.013799
hsa-miR-18a	4.808042	5.439979	0.002801	0.011487
hsa-miR-23a	4.814407	5.39411	0.000108	0.001354
hsa-miR-28-3p	4.858821	0.514537	0.004886	0.017755
hsa-miR-30b	4.864099	6.057354	9.40E-05	0.001273
hsa-miR-32	4.917479	2.183182	0.000677	0.00378
hsa-miR-301a	4.969014	4.364936	0.000913	0.004803
hsa-miR-22	4.986587	5.994069	0.000235	0.001872
hsa-miR-542-3p	5.00366	0.032834	0.004238	0.015786
hsa-miR-34b*	5.018456	0.240663	0.000489	0.003038
hsa-miR-103	5.063557	7.886716	0.0003	0.00217
hsa-miR-17	5.068094	7.850754	0.000216	0.001807
hsa-let-7c	5.082043	4.899644	0.00051	0.003123
hsa-miR-16	5.123376	9.236763	0.000446	0.002892
hsa-miR-20a	5.149536	8.596518	0.000153	0.001588
hsa-miR-15b	5.15992	7.80479	0.000129	0.001552
hsa-miR-27b	5.200296	4.645793	3.35E-05	0.000832
hsa-miR-532-3p	5.209571	0.658134	9.04E-06	0.000422
hsa-miR-107	5.249441	7.648953	0.000416	0.002737
hsa-miR-140-3p	5.254607	4.521609	0.000271	0.002052
hsa-let-7d	5.307949	6.646928	0.000168	0.001621
hsa-miR-28-5p	5.39533	3.456186	0.000536	0.003152
hsa-miR-152	5.397609	0.511274	0.003466	0.013592
hsa-miR-222	5.403254	2.034864	0.001794	0.008101
hsa-miR-24	5.407399	5.455675	6.17E-05	0.001103
hsa-miR-26b	5.443177	5.99802	0.000146	0.001581
hsa-miR-30e*	5.44797	3.212352	0.000201	0.001745

hsa-miR-532-5p	5.495909	1.678208	0.000331	0.002277
hsa-miR-146b-5p	5.501737	2.814973	1.02E-05	0.000422
hsa-miR-503	5.510063	-0.02112	0.000476	0.003
hsa-miR-339-3p	5.510554	0.977504	0.000319	0.002237
hsa-miR-424	5.541397	3.14083	0.000169	0.001621
hsa-let-7e	5.560933	0.518388	0.002088	0.009242
hsa-let-7a	5.581678	8.193576	0.000195	0.001745
hsa-miR-26a	5.588987	6.114013	0.000222	0.001807
hsa-miR-98	5.608458	4.161263	0.000156	0.001589
hsa-miR-338-3p	5.636554	0.827574	9.11E-07	0.000136
hsa-miR-500	5.644595	2.958047	2.74E-05	0.00072
hsa-miR-33a	5.660906	2.52445	0.006488	0.021169
hsa-miR-374b	5.666651	3.398956	0.000708	0.003905
hsa-miR-99a	5.749345	2.224874	7.88E-05	0.001214
hsa-miR-130a	5.77136	0.506265	0.004416	0.016255
hsa-let-7i	5.773538	6.904096	9.20E-05	0.001273
hsa-miR-19b	5.77444	8.995531	0.000526	0.003137
hsa-miR-30e	5.786303	5.906367	0.000728	0.003921
hsa-miR-19a	5.797445	7.72209	0.00032	0.002237
hsa-miR-21	5.806479	10.42407	9.92E-05	0.001304
hsa-miR-141	5.815741	1.303714	9.14E-06	0.000422
hsa-miR-29a	5.872355	7.206803	1.64E-05	0.000489
hsa-miR-362-5p	5.876292	0.840336	0.006545	0.021202
hsa-miR-140-5p	5.903781	4.627514	1.59E-05	0.000489
hsa-miR-34a	5.929041	2.422767	4.11E-05	0.000905
hsa-let-7f	5.969023	8.488932	0.000109	0.001354
hsa-miR-151-3p	5.971591	2.560655	1.39E-05	0.000479
hsa-miR-454	6.022069	2.023527	0.000907	0.004803
hsa-miR-29c	6.026364	7.039184	0.000143	0.001581
hsa-miR-494	6.063026	6.488467	0.001107	0.005496
hsa-miR-15a	6.081912	7.401147	6.72E-05	0.001155
hsa-miR-142-5p	6.166791	6.631964	0.000469	0.002996
hsa-miR-27a	6.170025	4.496759	4.25E-05	0.000905
hsa-miR-374a	6.239875	4.185961	0.000354	0.002398
hsa-miR-660	6.259716	2.08946	1.35E-06	0.000151
hsa-miR-193a-3p	6.29447	1.559961	0.00014	0.001581
hsa-miR-185	6.294521	3.543762	0.001794	0.008101
hsa-let-7g	6.326692	7.436612	6.13E-05	0.001103

hsa-miR-652	6.361945	2.061111	5.77E-05	0.001103
hsa-miR-151-5p	6.381351	3.967527	4.71E-06	0.000316
hsa-miR-20b	6.442932	6.744308	1.33E-05	0.000479
hsa-miR-744	6.58519	1.344977	0.002917	0.011681
hsa-miR-29b	6.65758	7.15443	2.58E-05	0.00072
ebv-miR-BART19-3p	6.724201	2.68927	0.000961	0.004997
hsa-miR-106b	6.986247	7.155615	0.000149	0.001581
hsa-miR-378*	7.057995	2.117641	2.00E-06	0.000179
hsa-miR-324-5p	7.062603	4.037968	1.04E-05	0.000422
hsa-miR-101	7.302425	4.280864	0.000301	0.00217
hsa-miR-210	7.347209	6.236888	4.79E-05	0.000974
hsa-miR-340	7.440852	0.979883	0.00105	0.005274
hsa-miR-21*	7.575147	2.993364	4.95E-06	0.000316
hsa-miR-17*	7.673531	3.830187	7.85E-05	0.001214
hsa-miR-142-3p	7.77528	9.278608	3.54E-05	0.000832
hsa-miR-148b	7.881156	2.971673	6.91E-07	0.000136

J77 Cells vs Exosomes

Probe	logFC	A	pvalue	adjpvalue
hsa-miR-422a	-6.715	2.179435	3.12E-05	0.000887
hsa-miR-193a-5p	-6.3524	1.586369	0.00088	0.003846
hsa-miR-936	-6.34831	-0.09782	3.05E-05	0.000887
hsa-miR-193b*	-6.18078	1.850504	0.000833	0.003699
hsa-miR-198	-5.83439	1.648131	0.000146	0.00152
kshv-miR-K12-3	-5.65175	7.030808	1.27E-06	0.000285
hsa-miR-451	-5.62282	4.004414	1.16E-06	0.000285
hsa-miR-921	-5.54841	0.242427	0.009487	0.022088
hsa-miR-654-5p	-5.52022	3.7374	1.02E-05	0.000887
hsv1-miR-H1	-5.44706	1.665387	0.002902	0.009332
hsa-miR-510	-5.31121	-0.97687	0.000936	0.003878
hsa-miR-483-5p	-5.2542	4.840386	2.94E-05	0.000887
hsa-miR-150*	-5.00425	3.911789	0.001286	0.005044
hsa-miR-452	-4.95942	-0.72503	0.024306	0.046629
kshv-miR-K12-7	-4.93412	-0.97239	0.000302	0.002177
hsa-miR-125b-1*	-4.91826	0.987357	0.011424	0.025281
hcmv-miR-US25-2-5p	-4.91436	1.669543	0.007643	0.018568
hsa-miR-373*	-4.90393	-0.19265	4.20E-05	0.000887
hsa-miR-149*	-4.89735	0.431632	0.000503	0.002882

hsa-miR-200a*	-4.86985	0.015043	0.000148	0.00152
hsa-miR-513a-5p	-4.80981	4.377892	0.000536	0.002886
hsa-miR-575	-4.69112	7.827253	0.010111	0.022941
hsa-miR-125a-3p	-4.68497	5.0213	0.006589	0.016926
hsa-miR-632	-4.68246	0.599001	4.56E-05	0.000887
hsa-miR-1224-5p	-4.60459	3.435022	0.000643	0.003201
hsa-miR-490-5p	-4.5977	0.099988	3.71E-05	0.000887
hsa-miR-188-5p	-4.56884	5.340045	0.000454	0.002635
hcmv-miR-US4	-4.52692	2.537085	5.88E-06	0.000657
hsa-miR-370	-4.51006	-0.16016	0.004572	0.012935
hsa-miR-765	-4.50633	2.7042	0.000709	0.003335
hsa-miR-1226*	-4.43468	1.97751	0.000432	0.002538
hsa-miR-610	-4.41785	1.635868	0.000291	0.002165
hsa-miR-877	-4.35834	1.275374	0.00648	0.016744
hsa-miR-424*	-4.29388	1.055555	0.022776	0.044265
hsa-miR-887	-4.26695	2.018044	3.79E-05	0.000887
hsa-miR-584	-4.22102	2.201837	1.83E-05	0.000887
hsa-miR-760	-4.2105	2.490711	0.000609	0.003131
hsa-miR-601	-4.19247	2.468441	0.000343	0.002325
hsa-miR-125b-2*	-4.1664	1.64737	0.000193	0.001797
hsa-miR-513b	-4.16116	2.783108	0.000662	0.003215
hsa-miR-662	-4.11234	1.737444	1.76E-05	0.000887
hsa-miR-28-3p	-4.07604	0.514537	0.003719	0.011309
hsa-miR-518e*	-4.04984	-0.51745	0.005424	0.014695
hsa-miR-99b*	-3.95424	0.815586	0.021807	0.042753
hsa-miR-638	-3.86994	7.327502	0.003751	0.011329
hsa-miR-671-5p	-3.80161	3.809781	0.000526	0.002886
hsa-miR-520e	-3.79614	1.563527	0.000365	0.002417
hiv1-miR-H1	-3.73346	1.944811	0.01152	0.025367
hsa-miR-617	-3.71381	2.197965	0.002662	0.008681
ebv-miR-BART19-3p	-3.63361	2.68927	0.01338	0.028893
hsa-miR-513c	-3.63153	2.107752	0.000296	0.002165
hsa-miR-10b*	-3.62337	0.814464	0.018978	0.037872
hsa-miR-135a*	-3.61625	3.760621	0.006236	0.016397
hsa-miR-1225-5p	-3.61307	7.167043	0.005731	0.015249
hsa-miR-498	-3.59555	0.968832	0.00063	0.003198
hsa-miR-630	-3.56148	7.597597	0.006429	0.016708
ebv-miR-BART14	-3.54465	0.22025	0.002663	0.008681

hsa-miR-200b*	-3.45914	-0.89685	0.015848	0.032495
hsa-miR-557	-3.4179	1.865727	0.025226	0.048188
hsa-miR-520b	-3.41197	1.73105	0.009982	0.022882
hsa-miR-134	-3.39363	3.710506	0.015404	0.031878
hsa-miR-453	-3.34113	-0.74515	0.00702	0.01752
hsa-miR-518c*	-3.3333	0.851379	0.006668	0.017033
ebv-miR-BART7	-3.32684	0.742811	0.001303	0.005066
hsa-miR-491-5p	-3.22655	-0.50783	0.005329	0.014614
hsa-miR-382	-3.18177	0.340161	0.007013	0.01752
hsa-miR-583	-3.15857	0.711317	0.007094	0.01752
hsa-miR-339-3p	-3.1552	0.977504	0.004192	0.012248
hsa-miR-874	-3.09928	4.698323	0.011357	0.025257
hsa-miR-516b	-2.93605	-0.63473	0.021161	0.041853
hsa-miR-518f	-2.93233	-0.30978	0.008215	0.019637
hsa-miR-622	-2.87693	1.614827	0.004448	0.012779
kshv-miR-K12-8	-2.84093	-0.29682	0.013107	0.02844
hsa-miR-513a-3p	-2.8323	0.780434	0.008369	0.0199
hcmv-miR-UL36	-2.77984	0.320012	0.007068	0.01752
hsa-miR-141*	-2.67343	-0.79115	0.00508	0.014016
hsa-miR-492	-2.65829	0.457549	0.007766	0.018763
hsa-miR-129-5p	-2.58269	-0.11327	0.010559	0.023718
hsa-miR-30c-2*	-2.56741	0.321023	0.002161	0.007545
hsa-miR-486-5p	-2.49626	1.749489	0.004809	0.013351
hsa-miR-631	-2.46885	1.865422	0.003972	0.01179
hsa-miR-184	-2.38128	0.20812	0.015306	0.031821
hsa-miR-145	-2.26583	0.960143	0.016825	0.034341
hsa-miR-769-3p	-2.15956	1.088625	0.009031	0.021359
hsa-miR-628-5p	-2.15472	1.069156	0.014778	0.031158
hsa-miR-10b	-1.85925	0.51196	0.003138	0.009949
ebv-miR-BHRF1-1	-1.75942	2.97448	0.018517	0.037117
hsa-miR-518d-3p	-1.7254	0.079174	0.019962	0.039657
hsa-let-7d*	-1.33814	1.82913	0.015195	0.03174
hsa-miR-505	1.485509	3.278082	0.009931	0.022882
hsa-miR-197	1.659617	5.203971	0.009392	0.021981
hsa-miR-93*	1.667247	0.672559	0.007946	0.019096
hsa-miR-502-5p	1.745284	1.218676	0.004673	0.013073
hsa-miR-548d-5p	1.748357	1.145468	0.02275	0.044265
hsa-miR-548c-5p	1.776163	1.382284	0.026223	0.049669

hsa-miR-199b-5p	1.785141	1.297736	0.005524	0.014875
hsa-miR-221*	1.794714	0.780369	0.01714	0.034826
hsa-miR-770-5p	1.794742	3.077351	0.023943	0.046131
hsa-miR-484	1.808492	3.818109	0.001349	0.005198
hsa-miR-151-3p	1.841954	2.560655	0.021369	0.042079
hsa-miR-186	1.922338	4.096928	0.013644	0.029321
hsa-miR-744*	1.946595	1.917892	0.015768	0.032482
hsa-miR-361-3p	2.008106	2.411733	0.011953	0.026063
hsa-miR-22	2.042326	5.994069	0.023102	0.044703
hsa-miR-92a	2.083366	7.888559	0.005799	0.015339
hsa-miR-23a	2.086582	5.39411	0.010916	0.024398
hsa-miR-449a	2.09259	0.810515	0.010404	0.023487
hsa-miR-548a-5p	2.100562	0.428327	0.017947	0.036136
hsa-miR-192	2.205406	3.142452	0.003307	0.010336
hsa-miR-450a	2.207824	1.522633	0.001286	0.005044
hsa-miR-148a*	2.266968	-0.79829	0.014911	0.031292
hsa-miR-624*	2.270253	0.807887	0.006798	0.017264
hsa-miR-324-3p	2.391106	6.555508	0.010082	0.022941
hsa-miR-378	2.39641	5.655411	0.013806	0.029527
hsa-miR-146b-5p	2.519216	2.814973	0.001545	0.005754
hsa-miR-219-5p	2.532555	2.050207	0.000836	0.003699
hsa-miR-221	2.577099	3.755918	0.000937	0.003878
hsa-miR-16-2*	2.59845	2.100713	0.000579	0.003043
hsa-miR-340*	2.606594	2.002909	0.001114	0.004446
hsa-miR-29c*	2.621287	2.767852	0.003062	0.009777
hsa-miR-195	2.636029	1.98425	0.001836	0.006618
hsa-miR-25	2.650268	7.128739	0.002428	0.008221
hsa-miR-550*	2.655955	1.665154	0.000368	0.002417
hsa-miR-15b*	2.702458	1.203659	0.001039	0.004185
hsa-miR-23b	2.704576	4.232274	0.000915	0.003862
hsa-miR-15a*	2.745492	1.058576	0.000142	0.00152
hsa-miR-24	2.767254	5.455675	0.002601	0.008613
hsa-miR-193b	2.789989	4.68102	0.000916	0.003862
hsa-miR-660	2.806678	2.08946	0.000402	0.002538
hsa-miR-181d	2.808829	2.529472	0.006989	0.01752
hsa-miR-194	2.82154	1.459043	0.009807	0.022714
hsa-miR-188-3p	2.82359	-1.11087	0.003489	0.010755
hsa-miR-128	2.835244	4.50142	0.006274	0.0164

hsa-miR-150	2.835626	2.916366	0.004341	0.012602
hsa-miR-132	2.844915	2.179877	0.004555	0.012935
hsa-miR-342-3p	2.861857	6.228904	0.011776	0.025803
hsa-miR-106a*	2.868669	0.350731	0.001451	0.005497
hsa-miR-196a	2.878518	1.814899	0.001013	0.004118
hsa-miR-532-5p	2.892581	1.678208	0.007341	0.01793
hsa-miR-103	2.917134	7.886716	0.00384	0.01152
hsa-miR-27b	2.97002	4.645793	0.000709	0.003335
hsa-miR-130b	2.973298	5.623911	0.003601	0.011025
hsa-miR-769-5p	2.984919	2.928335	0.000225	0.001861
hsa-miR-625	3.009816	3.063671	0.00333	0.010336
hsa-miR-222	3.0175	2.034864	0.017418	0.035231
hsa-miR-361-5p	3.035242	4.611954	0.000645	0.003201
hsa-miR-152	3.047342	0.511274	0.026205	0.049669
hsa-miR-378*	3.093929	2.117641	0.000652	0.003201
hsa-miR-181b	3.122786	4.408795	0.00214	0.007532
hsa-miR-425	3.225857	6.216363	0.002065	0.007327
hsa-miR-140-3p	3.235695	4.521609	0.002237	0.007692
hsa-miR-27a	3.239678	4.496759	0.001633	0.006034
hsa-let-7a	3.256363	8.193576	0.00251	0.008437
hsa-miR-193a-3p	3.290883	1.559961	0.004108	0.012082
hsa-miR-148b	3.300032	2.971673	0.000426	0.002538
hsa-miR-200c	3.341582	0.940946	0.014212	0.030251
hsa-miR-331-3p	3.358338	5.767948	0.000229	0.001861
hsa-miR-138-2*	3.418646	0.455684	0.014614	0.03096
hsa-miR-151-5p	3.44851	3.967527	0.000221	0.001861
hsa-miR-33b	3.48818	-0.47633	0.00468	0.013073
hsa-miR-181a	3.524479	6.633956	0.001649	0.006042
hsa-miR-532-3p	3.562321	0.658134	4.55E-05	0.000887
hsa-miR-30c	3.577445	5.281099	0.000118	0.00152
hsa-miR-29a	3.588112	7.206803	0.000219	0.001861
hsa-miR-141	3.594151	1.303714	0.000118	0.00152
hsa-miR-140-5p	3.626306	4.627514	0.000204	0.001805
hsa-miR-210	3.645846	6.236888	0.00268	0.008681
hsa-miR-301b	3.646298	2.355695	0.005414	0.014695
hsa-miR-362-3p	3.658112	1.577961	3.56E-05	0.000887
hsa-miR-21	3.673982	10.42407	0.000781	0.003561
hsa-miR-183	3.694076	0.456838	0.009295	0.021869

hsa-miR-148a	3.696211	5.479736	0.000415	0.002538
hsa-miR-181c	3.712684	1.041504	0.003983	0.01179
hsa-miR-7-1*	3.727289	2.961363	9.90E-05	0.00152
hsa-miR-30e*	3.735669	3.212352	0.000768	0.003541
hsa-miR-30e	3.800534	5.906367	0.003269	0.010292
hsa-miR-26a	3.807022	6.114013	0.000886	0.003846
hsa-miR-652	3.820726	2.061111	0.000745	0.003469
hsa-miR-30d*	3.832491	0.469122	0.000101	0.00152
hsa-miR-363	3.855702	3.132228	0.00043	0.002538
hsa-miR-107	3.893979	7.648953	0.000808	0.003646
hsa-miR-93	3.911997	6.651276	0.000134	0.00152
hsa-miR-182	3.976464	-0.51534	0.00015	0.00152
hsa-miR-30b	3.992347	6.057354	7.83E-05	0.001399
hsa-miR-574-3p	4.002783	3.407865	0.000206	0.001805
hsa-miR-191	4.008188	0.402267	2.95E-05	0.000887
hsa-miR-181a*	4.032505	3.458474	0.000376	0.002437
hsa-miR-503	4.038662	-0.02112	0.001007	0.004118
hsa-miR-16	4.043719	9.236763	0.000524	0.002886
hsa-miR-20b	4.099877	6.744308	0.000127	0.00152
hsa-miR-424	4.143597	3.14083	0.000321	0.002279
hsa-miR-17	4.149988	7.850754	0.000185	0.001797
hsa-let-7i	4.152481	6.904096	0.000252	0.001934
hsa-miR-20a	4.17425	8.596518	0.000143	0.00152
hsa-miR-590-5p	4.203424	4.424362	0.000108	0.00152
hsa-miR-26b	4.227011	5.99802	0.000201	0.001805
hsa-miR-454	4.246079	2.023527	0.002426	0.008221
hsa-miR-19b-1*	4.248059	1.633824	0.000129	0.00152
hsa-miR-28-5p	4.275852	3.456186	0.000607	0.003131
hsa-miR-20a*	4.281869	2.511058	0.000328	0.002288
hsa-miR-301a	4.289713	4.364936	0.00052	0.002886
hsa-let-7d	4.364109	6.646928	0.000139	0.00152
hsa-miR-185	4.440188	3.543762	0.00446	0.012779
hsa-miR-98	4.455491	4.161263	0.000175	0.001743
hsa-miR-9*	4.469793	3.224868	0.007202	0.017689
hsa-miR-542-3p	4.48736	0.032834	0.002009	0.007184
hsa-miR-106b	4.531011	7.155615	0.000912	0.003862
hsa-miR-29c	4.573217	7.039184	0.000241	0.001889
hsa-miR-15b	4.577173	7.80479	5.24E-05	0.000976

hsa-miR-18b	4.588286	4.354533	0.000422	0.002538
hsa-miR-324-5p	4.602037	4.037968	8.14E-05	0.0014
hsa-miR-19b	4.619041	8.995531	0.000553	0.002942
hsa-miR-7	4.665231	4.889295	0.00142	0.005423
hsa-let-7g	4.706648	7.436612	0.000127	0.00152
hsa-miR-374b	4.719566	3.398956	0.000536	0.002886
hsa-miR-9	4.724144	2.372944	3.29E-06	0.00049
hsa-miR-15a	4.733328	7.401147	9.17E-05	0.001518
hsa-let-7f	4.790065	8.488932	0.000112	0.00152
hsa-miR-19a	4.790195	7.72209	0.000255	0.001934
hsa-miR-744	4.79439	1.344977	0.005649	0.015121
hsa-miR-101	4.823534	4.280864	0.001467	0.00551
hsa-miR-431*	4.91777	0.776972	0.000238	0.001889
hsa-miR-18a	4.973288	5.439979	0.000409	0.002538
hsa-miR-21*	5.062058	2.993364	3.24E-05	0.000887
hsa-miR-96	5.094901	2.095749	2.30E-05	0.000887
hsa-miR-142-5p	5.157389	6.631964	0.00034	0.002325
ebv-miR-BART12	5.23419	3.375875	0.002235	0.007692
hsa-miR-374a	5.387318	4.185961	0.000193	0.001797
hsa-miR-362-5p	5.447151	0.840336	0.00258	0.008608
hsa-miR-29b	5.500428	7.15443	1.99E-05	0.000887
hsa-miR-340	5.607931	0.979883	0.00172	0.00625
hsa-miR-17*	5.764045	3.830187	0.000147	0.00152
hsa-miR-32	5.800386	2.183182	2.15E-05	0.000887
hsa-miR-142-3p	6.134129	9.278608	4.28E-05	0.000887
hsa-miR-153	6.172829	-1.22659	3.16E-05	0.000887
hsa-miR-33a	6.241604	2.52445	0.000693	0.003333

Raji Cells vs Exosomes

Probe	logFC	A	pvalue	adjpvalue
hsa-miR-451	-7.46927	4.004414	4.78E-08	2.14E-05
hsa-miR-575	-6.58693	7.827253	0.001028	0.014611
hsa-miR-125b-1*	-6.48942	0.987357	0.001925	0.021057
hsa-miR-198	-6.12724	1.648131	9.36E-05	0.00499
hsa-miR-125a-3p	-5.72874	5.0213	0.001694	0.019927
hsa-miR-658	-5.01178	1.359686	0.005389	0.039489
hsa-miR-27a	-5.00499	4.496759	3.94E-05	0.00352

hsa-miR-936	-4.86763	-0.09782	0.000346	0.011895
hsa-miR-654-5p	-4.85215	3.7374	3.69E-05	0.00352
hsa-miR-126	-4.82742	2.733188	3.69E-05	0.00352
hsa-miR-513a-5p	-4.47072	4.377892	0.000961	0.014318
hsa-miR-149*	-4.46787	0.431632	0.001046	0.014611
hsa-miR-10b*	-4.34616	0.814464	0.006873	0.045854
hsa-miR-760	-4.32058	2.490711	0.000494	0.012257
hsa-miR-422a	-4.25136	2.179435	0.00161	0.019927
hsa-miR-483-5p	-4.24282	4.840386	0.000214	0.008701
hsa-miR-518c*	-4.06732	0.851379	0.001745	0.020005
hsa-miR-513b	-3.99957	2.783108	0.000906	0.013965
hsa-miR-122	-3.85855	0.04668	0.000759	0.013965
hsa-miR-610	-3.85027	1.635868	0.000901	0.013965
hsa-miR-632	-3.82026	0.599001	0.00029	0.01082
hsa-miR-513a-3p	-3.81307	0.780434	0.001107	0.015001
hsa-miR-141*	-3.7537	-0.79115	0.000413	0.012257
hsa-miR-492	-3.75195	0.457549	0.000693	0.013965
hsa-miR-1225-5p	-3.69434	7.167043	0.004976	0.037363
kshv-miR-K12-3	-3.64391	7.030808	0.000106	0.00499
hsa-miR-184	-3.38111	0.20812	0.001667	0.019927
hcmv-miR-US4	-3.35232	2.537085	0.000112	0.00499
hsa-miR-373*	-3.33226	-0.19265	0.001192	0.015676
hsa-miR-200a*	-3.32871	0.015043	0.003054	0.027862
hsa-miR-23a	-3.29621	5.39411	0.000445	0.012257
hsa-miR-498	-3.26805	0.968832	0.001328	0.016956
hsa-miR-513c	-3.23952	2.107752	0.00076	0.013965
hsa-miR-30c-2*	-3.08061	0.321023	0.000533	0.012545
hsa-miR-502-3p	-3.0742	1.453375	0.005509	0.039716
hsa-miR-150	-3.06376	2.916366	0.00257	0.025345
hsa-miR-500*	-3.0016	2.523807	0.000787	0.013965
hsa-miR-671-5p	-3.00104	3.809781	0.003119	0.027885
hsa-miR-584	-2.96508	2.201837	0.000467	0.012257
hsa-miR-939	-2.94603	6.200593	0.006347	0.043649
hsa-miR-542-5p	-2.93123	2.439135	0.003274	0.02814
hsa-miR-181c*	-2.87241	0.687299	0.00413	0.033563
hsa-miR-223	-2.56602	6.524582	0.002026	0.021057
hsa-miR-662	-2.27539	1.737444	0.002797	0.026046
hsa-miR-199b-5p	-2.07536	1.297736	0.001992	0.021057

hsa-miR-10b	-1.95659	0.51196	0.002197	0.022322
hsa-miR-338-3p	-1.84395	0.827574	0.003339	0.028164
hsa-miR-885-5p	1.712088	1.928617	0.00478	0.037245
hsa-miR-769-5p	1.912402	2.928335	0.006327	0.043649
hsa-miR-219-5p	2.173338	2.050207	0.002608	0.025345
hsa-miR-378*	2.225296	2.117641	0.00677	0.045851
hsa-miR-197	2.36303	5.203971	0.000835	0.013965
hsa-miR-590-5p	2.573758	4.424362	0.005015	0.037363
hsa-miR-191	2.738933	0.402267	0.000861	0.013965
ebv-miR-BART11-5p	2.771278	-1.02908	0.003634	0.030078
hsa-miR-9	2.870101	2.372944	0.00039	0.012257
hsa-miR-324-5p	2.923193	4.037968	0.003218	0.02814
ebv-miR-BART19-5p	3.174379	-1.09169	0.004833	0.037245
hsa-miR-29b	3.229791	7.15443	0.001998	0.021057
hsa-miR-193a-3p	3.278232	1.559961	0.004214	0.033636
hsa-miR-17*	3.576346	3.830187	0.005743	0.040749
ebv-miR-BHRF1-2*	3.581587	0.52684	0.000104	0.00499
hsa-miR-142-3p	3.728955	9.278608	0.002726	0.025929
hsa-miR-32	3.958077	2.183182	0.000675	0.013965
hsa-miR-744*	4.145577	1.917892	5.66E-05	0.004218
hsa-miR-431*	4.309403	0.776972	0.000717	0.013965
hsa-miR-574-3p	4.854247	3.407865	3.45E-05	0.00352

Annex Table 9.3. Targets of TUT4.
(A) Mono-uridylated (nont_3p_U) and oligo-uridylated (nont_3p_oligoU) miRNAs that are significantly less abundant in TUT4-deficient CD4 T cells. Species that are identified both for mono- or oligo-uridylation appear in bold. **(B)** miRNAs significantly less abundant in both the mono- and oligo-uridylated form in TUT4-deficient CD4 T cells.

A: Complete list of TUT4 targets

ID	log_2 Fold Change	Adjusted p value
mmu-let-7c-2-5p_nont_3p_U	-1.167309726	0.02574908
mmu-let-7f-2-5p_nont_3p_U	-1.781355148	0.00021568
mmu-let-7g-5p_nont_3p_U	-1.7925212	1.83E-06
mmu-let-7i-5p_nont_3p_U	-0.657803428	3.39E-10
mmu-mir-101b-3p_nont_3p_U	-0.731672466	3.49E-11
mmu-mir-106a-5p_nont_3p_U	-1.521703894	0.00966257
mmu-mir-106b-5p_nont_3p_U	-1.36618412	0.03823983
mmu-mir-130b-3p_nont_3p_U	-0.757508609	0.00027401
mmu-mir-132-3p_nont_3p_U	-0.914747694	0.00186816
mmu-mir-140-3p_nont_3p_U	-1.06746012	3.68E-49
mmu-mir-140-3p_nont_3p_oligoU	-1.497566549	1.54E-05
mmu-mir-140-5p_nont_3p_U	-1.323650233	0.03457858
mmu-mir-142-3p_nont_3p_U	-1.162625018	8.25E-38
mmu-mir-142-5p_nont_3p_U	-1.119266718	8.07E-14
mmu-mir-142-5p_nont_3p_oligoU	-1.087649295	1.06E-06
mmu-mir-146a-5p_nont_3p_U	-0.575549883	0.03457858
mmu-mir-146a-5p_nont_3p_oligoU	-1.135284176	0.00021568
mmu-mir-148b-3p_nont_3p_oligoU	-0.580199386	8.66E-05
mmu-mir-150-5p_nont_3p_U	-0.823708066	0.00024956
mmu-mir-150-5p_nont_3p_oligoU	-0.893117924	0.02977229
mmu-mir-155-5p_nont_3p_U	-1.38292442	1.83E-07
mmu-mir-15a-5p_nont_3p_U	-0.950540696	0.00134439
mmu-mir-15b-3p_nont_3p_U	-1.228413995	0.02928478
mmu-mir-17-3p_nont_3p_U	-1.241786	0.01677079
mmu-mir-17-5p_nont_3p_U	-1.315542467	0.01670394
mmu-mir-181a-2-5p_nont_3p_U	-0.858754426	2.30E-41
mmu-mir-181a-2-5p_nont_3p_oligoU	-1.172783199	9.61E-09
mmu-mir-192-5p_nont_3p_oligoU	-1.025718311	0.00167943
mmu-mir-19a-3p_nont_3p_U	-1.083384538	0.01310334
mmu-mir-19b-2-3p_nont_3p_U	-1.229718913	2.41E-14
mmu-mir-203-3p_nont_3p_U	-1.191205403	4.78E-05
mmu-mir-211-5p_nont_3p_U	-1.253870647	0.02616096
mmu-mir-21a-5p_nont_3p_U	-0.810856854	0.01264793
mmu-mir-25-3p_nont_3p_U	-0.737184914	8.09E-19

mmu-mir-25-3p_nont_3p_oligoU	-1.70606826	9.38E-07
mmu-mir-26a-2-5p_nont_3p_U	-0.939689388	2.36E-12
mmu-mir-26a-2-5p_nont_3p_oligoU	-1.696846625	1.58E-20
mmu-mir-26b-5p_nont_3p_U	-1.032433347	1.66E-21
mmu-mir-26b-5p_nont_3p_oligoU	-1.850375815	1.23E-06
mmu-mir-27b-3p_nont_3p_oligoU	-1.160756428	7.65E-13
mmu-mir-28a-5p_nont_3p_U	-1.867289555	0.0015607
mmu-mir-29a-3p_nont_3p_U	-0.833912905	3.35E-10
mmu-mir-30a-5p_nont_3p_U	-1.156514422	0.01370107
mmu-mir-30c-1-5p_nont_3p_U	-1.552391836	1.77E-11
mmu-mir-30d-5p_nont_3p_U	-1.168617517	3.57E-12
mmu-mir-30d-5p_nont_3p_oligoU	-1.851773274	0.00012624
mmu-mir-30e-5p_nont_3p_U	-0.840940373	5.17E-12
mmu-mir-30e-5p_nont_3p_oligoU	-2.356737519	0.00017378
mmu-mir-322-5p_nont_3p_U	-1.185099797	1.83E-06
mmu-mir-378a-3p_nont_3p_oligoU	-0.759430267	0.00835518
mmu-mir-378c-5p_nont_3p_U	-1.083600463	1.04E-07
mmu-mir-421-3p_nont_3p_U	-1.016570589	1.58E-06
mmu-mir-425-5p_nont_3p_U	-1.238368606	3.98E-08
mmu-mir-92a-1-3p_nont_3p_U	-0.881862797	2.50E-15
mmu-mir-92a-1-3p_nont_3p_oligoU	-1.436571358	3.72E-27
mmu-mir-92a-2-3p_nont_3p_U	-0.723421579	2.32E-07
mmu-mir-92a-2-3p_nont_3p_oligoU	-1.14678676	2.32E-09
mmu-mir-93-5p_nont_3p_U	-1.046286403	1.71E-12
mmu-mir-93-5p_nont_3p_oligoU	-1.858286979	3.79E-09
mmu-mir-98-5p_nont_3p_U	-1.168208826	0.01642043

B: Short list of TUT4 targets

mmu-mir-140-3p
mmu-mir-142-5p
mmu-mir-146a-5p
mmu-mir-150-5p
mmu-mir-181a-2-5p
mmu-mir-25-3p
mmu-mir-26a-2-5p
mmu-mir-26b-5p
mmu-mir-30d-5p
mmu-mir-30e-5p
mmu-mir-92a-1-3p
mmu-mir-92a-2-3p
mmu-mir-93-5p

Annex Table 9.4. TUT4 targets are downregulated after T cell activation.
miRNAs whose abundance in the oligo-uridylated form is reduced after T cell activation; species that were also identified as TUT4 targets in TUT4-deficient mice are shown in ***bold italics***.

miR	Log2 FC	adj p value
mmu-mir-150-5p	-6.497	5.18E-12
mmu-mir-150-3p	-6.02	4.09E-10
mmu-mir-181a-2-5p	-5.749	6.71E-09
mmu-mir-142-5p	-5.38	1.31E-07
mmu-mir-140-3p	-5.361	1.11E-07
mmu-mir-191-5p	-5.032	1.08E-06
mmu-mir-328-3p	-4.993	1.39E-06
mmu-mir-423-3p	-4.711	8.05E-06
mmu-let-7i-5p	-4.174	1.06E-09
mmu-mir-151-3p	-3.62	6.85E-10
mmu-mir-92b-3p	-3.598	1.69E-06
mmu-mir-25-3p	-3.177	5.62E-14
mmu-mir-26a-2-5p	-3.113	1.49E-24
mmu-mir-146a-5p	-3.09	2.30E-06
mmu-mir-92a-1-3p	-2.955	1.58E-34
mmu-mir-378a-3p	-2.687	1.67E-16
mmu-mir-27b-3p	-2.583	9.74E-05
mmu-mir-93-5p	-2.542	0.00804452
mmu-mir-92a-2-3p	-2.048	8.78E-20
mmu-mir-30e-3p	-1.984	0.00304615
mmu-mir-103-2-3p	-1.46	3.68E-08

PUBLICATIONS

10 PUBLICATIONS

10.1 Publications related to this Thesis work:

- Mittelbrunn M*, **Gutiérrez-Vázquez C***, Villarroya-Beltri C, González S,Sánchez-Cabo F, González MÁ, Bernad A, Sánchez-Madrid F. Unidirectional transfer of microRNA-loaded exosomes from T cells to antigen-presenting cells. (2011) **Nature Communications**. 2:282. doi: 10.1038/ncomms1285.

- **Gutiérrez-Vázquez C***, Villarroya-Beltri C*, Mittelbrunn M, Sánchez-Madrid F. Transfer of extracellular vesicles during immune cell-cell interactions. (2013) **Immunological Reviews**. 251(1):125-42. doi: 10.1111/imr.12013.

- Perez-Hernandez D, **Gutiérrez-Vázquez C**, Jorge I, Lopez-Martin S, Ursa A, Sanchez-Madrid F, Vazquez J, Yanez-Mo M. (2013) The intracellular interactome of tetraspanin-enriched microdomains reveals their function as sorting machineries to exosomes. **Journal of Biological Chemistry**. 2013 Apr 26;288(17).

- Villarroya-Beltri C*, **Gutiérrez-Vázquez C***, Mittelbrunn M, Sanchez-Madrid F. Analysis of microRNA and protein Transfer by exosomes during immune synapse. **Methods in Molecular Biology** 2013;1024:41-51.

- Villarroya-Beltri C, **Gutiérrez-Vázquez C**, Sanchez-Cabo F, Perez-Hernandez D, Vazquez J, Martin-Cofreces N, Martinez-Herrera D, Pascual-Montano A, Mittelbrunn M, Sanchez-Madrid F. Sumoylated hnRNPA2B1 controls the sorting of miRNAs into exosomes through binding to specific motifs **Nature Communications**. 2013;4:2980.

- Villarroya-Beltri C, Baixauli F, **Gutiérrez-Vázquez C**, Sánchez-Madrid F, Mittelbrunn M. Sorting it out: regulation of exosome loading. **Semin Cancer Biol**. 2014 Oct;28:3-13.

- Fernández-Messina L, **Gutiérrez-Vázquez C**, Rivas-García E, Sánchez-Madrid F, de la Fuente H. Immunomodulatory role of microRNAs transferred by extracellular vesicles. **Biol Cell**. 2015 Mar;107(3):61-77. doi: 10.1111/boc.201400081. Epub 2015 Feb 12.

- **Gutiérrez-Vázquez C**, Enright AJ, Rodríguez-Galán A, Collier P, Jones MR, Benes V, Mizgerd JP, Mittelbrunn M and Sánchez-Madrid F. 3'uridylation controls mature miRNA turnover during T cell activation. Submitted for publication.

- **Gutiérrez-Vázquez C**, Mittelbrunn M, Fernández-Alfara M, Ramírez-Huesca M, Martínez del Hoyo G, Martinez-Herrera DJ, Pascual-Montano A and Sánchez-Madrid F. MicroRNAs as fine tuners of T cell activation. Manuscript in preparation.

10.2 Publications unrelated to this Thesis work:

- Martín P, Gómez M, Lamana A, Matesanz Marín A, Cortés JR, Ramírez-Huesca M, Barreiro O, López-Romero P, **Gutiérrez-Vázquez C**, de la Fuente H, Cruz-Adalia A, Sánchez-Madrid F. (2010) The leukocyte activation antigen CD69 limits allergic asthma and skin contact hypersensitivity. Journal of Allergy and Clinical Immunology. 126(2):355-65, 365.e1-3. doi: 10.1016/j.jaci.2010.05.010.

- Calabia-Linares C, Robles-Valero J, de la Fuente H, Perez-Martinez M, Martín-Cofreces N, Alfonso-Pérez M, **Gutiérrez-Vázquez C**, Mittelbrunn M, Ibiza S, Urbano-Olmos FR, Aguado-Ballano C, Sánchez-Sorzano CO, Sanchez-Madrid F, Veiga E. (2011) Endosomal clathrin drives actin accumulation at the immunological synapse. Journal of Cell Science. 124(Pt 5):820-30. doi: 10.1242/jcs.078832.